Electronic Supplementary Material (ESI) for Polymer Chemistry.
This journal is © The Royal Society of Chemistry 2022

# Electronic Supporting Information (ESI)

# Thermal Response and Thermochromism of Methyl Red-Based Copolymer Systems - Coupled Responsiveness in Critical Solution Behaviour and Optical Absorption Properties

Thorben Jaik[1]; Betty Ciubini[2]; Francesca Frascella[2]; Ulrich Jonas[1*]

[1] Department Chemistry - Biology, University of Siegen, Adolf-Reichwein-Strasse 2, D-57076, Siegen, Germany

[2] Department of Applied Science and Technology, Politecnico di Torino, Corso Duca degli Abruzzi 24, IT-10129, Torino, Italy

*Corresponding author: Prof. Dr. Ulrich Jonas, jonas@chemie.uni-siegen.de

This document contains experimental details like syntheses and sample preparations, additional optical analysis data, graphs from the van't Hoff analyses, etc.

*Experimentals:*

Materials and equipment:

All solvents used were of Milli-Q®, spectroscopic or HPLC-grade. Absolute ethanol was purchased from VWR Chemicals. Tetrahydrofurane was dried and distilled over potassium. Trifluoroacetic acid was purchased from Carl Roth (Germany) in PEPTIPURE® ≥99,9% quality. Sulfuric acid (≥95%, Fisher Chemical), hydrochloric acid (37%, Anal. Reag. Gr., Fisher Chemical), acetic acid (Anal. Reag. Gr., ChemSolute), methyl red (Alfa Aesar), carbonyldiimidazole (97%, Alfa Aesar), *N*-(2-hydroxyethyl)acrylamide (97%, Sigma Aldrich), 4-aminobenzoic acid (Merck) and 3-aminobenzoic acid (98%, Merck) were used as received. 1,8-Diazabicyclo[5.4.0]undec-7-ene was dried over calciumchloride (anhydrous, technical, Bernd Kraft) and distilled *in vacuo*. *N*-Isopropylacrylamide was recrystallised from n-hexane. Azobisisobutyronitrile was recrystallised from methanol. 4-Benzophenoneacrylamide was synthesised according to literature.[1] 4-(3-

Triethoxysilyl)propoxybenzophenone was synthesised by Mr. Daniel John according to literature.[2]

UV-vis measurements were performed on a Thermo Scientific™ Evolution™ 220 UV-Vis-spectrophotometer. If not stated otherwise, the measurements were done with 100 nm/min and a resolution of 1 nm.

NMR-measurements were performed on either a Bruker AV 400 or a Jeol EZC 500. Detailed assignments of peaks are given in the ESI in the corresponding spectra.

GPC/SEC was measured on a PSS GRAM linM column (Polymer Standards Service GmbH, Mainz, Germany) in dimethylacetamide with LiBr (0.1 g/L) at 60 °C with PMMA-standards as reference.

*Synthesis of methyl red imidazolide:*

Methyl red (1 mol eq.) was dissolved in tetrahydrofuran (0.1 mmol/L), carbonyldiimidazole (1.8 mol eq.) was added and the solution was stirred until no more gas evolution occurred, typically overnight or for three hours at 45 °C. The solution was used without purification for further syntheses. (Adapted from literature[3-5])

*Synthesis of 2-(prop-2-enamido)ethyl-2-[(1E)-2-[4-(dimethylamino)phenyl]diazen-1-yl]benzoate (o-methyl red ester of N-(2-hydroxyethyl)acrylamide, o-MREAm):*

To a solution of methyl red imidazolide in tetrahydrofuran (0.1 mmol/L), *N*-(2-hydroxyethyl)acrylamide (2 mol eq.) and 1,8-diazabicyclo[5.4.0]undec-7-ene (1.5 mol eq.) were added. The reaction mixture was stirred overnight, before the reaction was stopped by addition of acetic acid. The solvent was removed azeotropically with toluene and the remaining solid extracted with water. The product was purified via column chromatography on neutral AlOx in ethyl acetate, followed by column chromatography on silica in diethylether. The yield was 90%.

δH(400 MHz; $CDCl_3$) 7.82 (d, J = 9.3 Hz, 2H; Ph-*H*), 7.74 (dd, J = 7.9, 1.1 Hz, 1H; Ph-*H*), 7.56 (qd, J = 7.9, 1.6 Hz, 2H; Ph-*H*), 7.39 (ddd, J = 7.6, 6.7, 1.9 Hz, 1H; Ph-*H*), 6.72 (d, J = 9.3 Hz, 2H; Ph-*H*), 6.12 (dd, J = 17.0, 1.5 Hz, 1H; CHC*H*H(trans)), 5.85 (s, br, 1H; CON*H*), 5.63 (dd, J = 17.0, 10.4 Hz, 1H; C*H*CHH), 5.43 (dd, J = 10.4, 1.5 Hz, 1H; CHCH*H*(cis)), 4.39 (t, J = 5.0 Hz, 2H; COOC$H_2$), 3.59 (q, J = 5.3 Hz, 2H; CONHC$H_2$), 3.07 (s, 6H; $N(Me)_2$).

δC(101 MHz; $CDCl_3$) δ 168.61 (COO), 165.49 (CONH), 152.99 (Ph), 152.54 (Ph), 143.54 (Ph), 132.08 (Ph), 130.59 ($COCHCH_2$), 129.70 (Ph), 128.50 (Ph), 127.72 (Ph), 126.36 ($COCHCH_2$), 125.35 (Ph), 119.50 (Ph), 111.70 (Ph), 64.35 ($COOCH_2$), 40.35 ($N(Me)_2$), 38.79 ($CONHCH_2$).

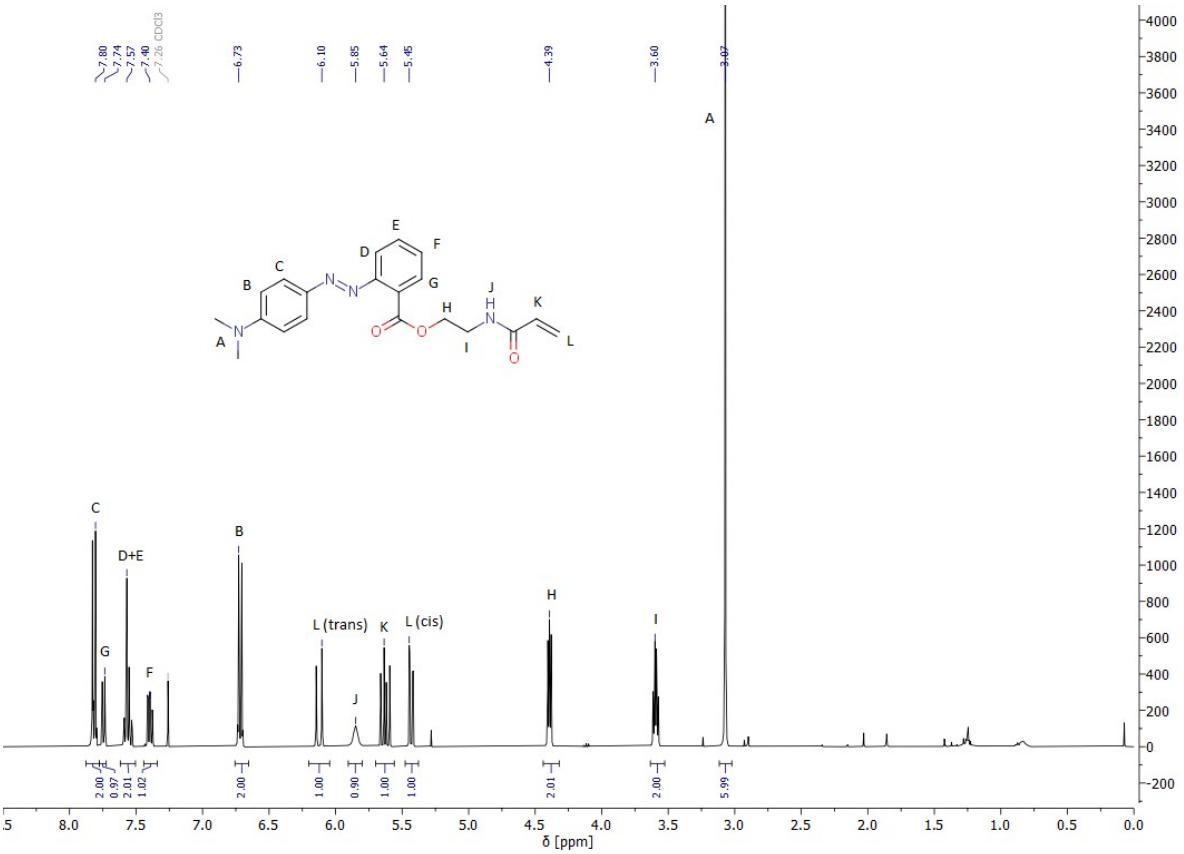


*Figure S 1: [1]H-NMR spectrum (400 MHz) in $CDCl_3$ of 2-(prop-2-enamido)ethyl-2-[(1E)-2-[4-(dimethylamino)phenyl]diazen-1-yl]benzoate (o-methyl red ester of N-(2-hydroxyethyl)acrylamide, o-MREAm).*

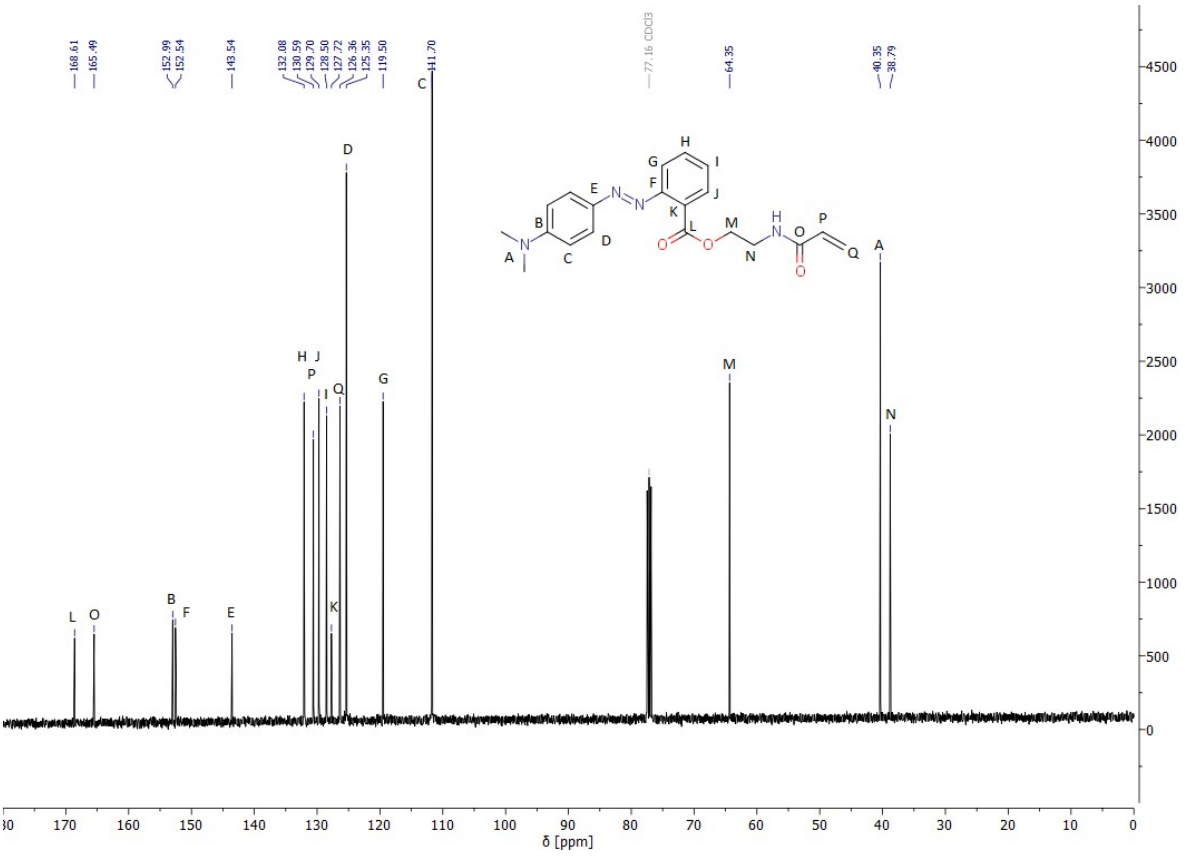


*Figure S 2: $^{13}$C-NMR spectrum (133 MHz) in $CDCl_3$ of 2-(prop-2-enamido)ethyl-2-[(1E)-2-[4-(dimethylamino)phenyl]diazen-1-yl]benzoate (o-methyl red ester of N-(2-hydroxyethyl)acrylamide, o-MREAm).*

*Synthesis of 4-[(1E)-2-[4-(dimethylamino)phenyl]diazen-1-yl]benzoic acid (p-methyl red, p-MR):*

4-Aminobenzoic acid (1412 mg, $1.0*10^{-2}$ mol) was dispersed in concentrated hydrochloric acid (4.5 mL) and cooled to 0 °C. An aqueous solution of sodium nitrite (713 mg, $1.0*10^{-2}$ mol) was added dropwise to the slurry over the course of 40 minutes and the resulting turbid mixture was stirred at 0 °C for another 40 minutes. Five minutes after the cooling was removed, it was added to a solution of N,N-dimethylanilin (1.5 mL, $1.2*10^{-2}$ mol) in water (100 mL, pH6). After 2.5 hours, the red precipitate was filtered off. The filtrate was neutralised with a saturated solution of $NaHCO_3$ and the precipitate filtered again. The solids were combined, washed with copious amounts of water and heated under reflux in $H_2O$:EtOH (1:1, 60 mL) for several hours, before cooling to room temperature and filtration. The yield was 2219 mg or 80%. This procedure was adapted from literature,[6] additionally reporting yield and NMR data.

δH(400 MHz; DMSO-d$^6$) 8.07 (d, J = 8.6 Hz, 2H; Ph-*H*), 7.83 (d, J = 8.6 Hz, 2H; Ph-*H*), 7.82 (d, J = 9.1 Hz, 2H; Ph-*H*), 6.83 (d, J = 9.4 Hz, 2H; Ph-*H*), 3.07 (s, 6H; $N(Me)_2$).

δC(101 MHz, DMSO-$d^6$) 167.15 (COOH), 155.30 (Ph), 153.21 (Ph), 142.90 (Ph), 131.10 (Ph), 130.73 (Ph)S, 125.50 (Ph), 121.96 (Ph), 111.81 (Ph), 40.06 ($N(Me)_2$).

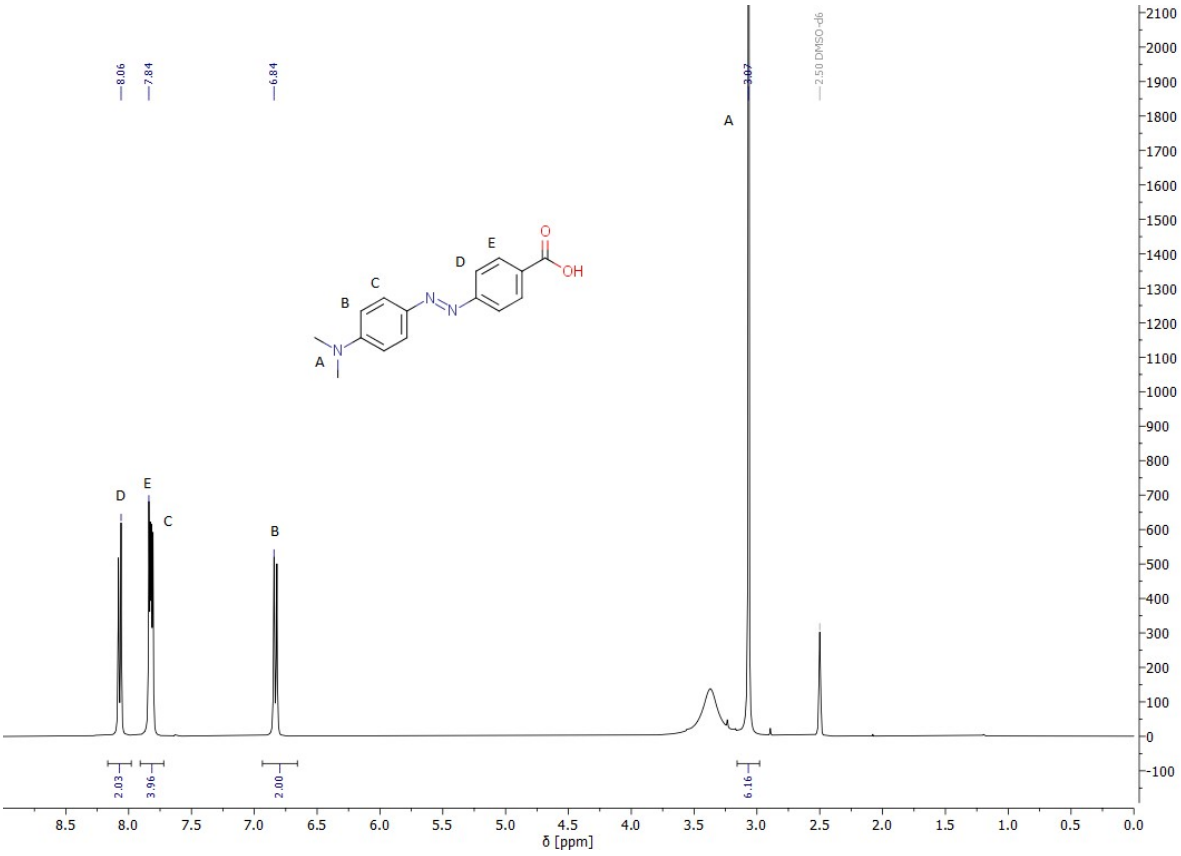


*Figure S 3: $^1$H-NMR spectrum (400 MHz) in DMSO-$d^6$ of 4-[(1E)-2-[4-(dimethylamino)phenyl]diazen-1-yl]benzoic acid (p-methyl red, p-MR.*

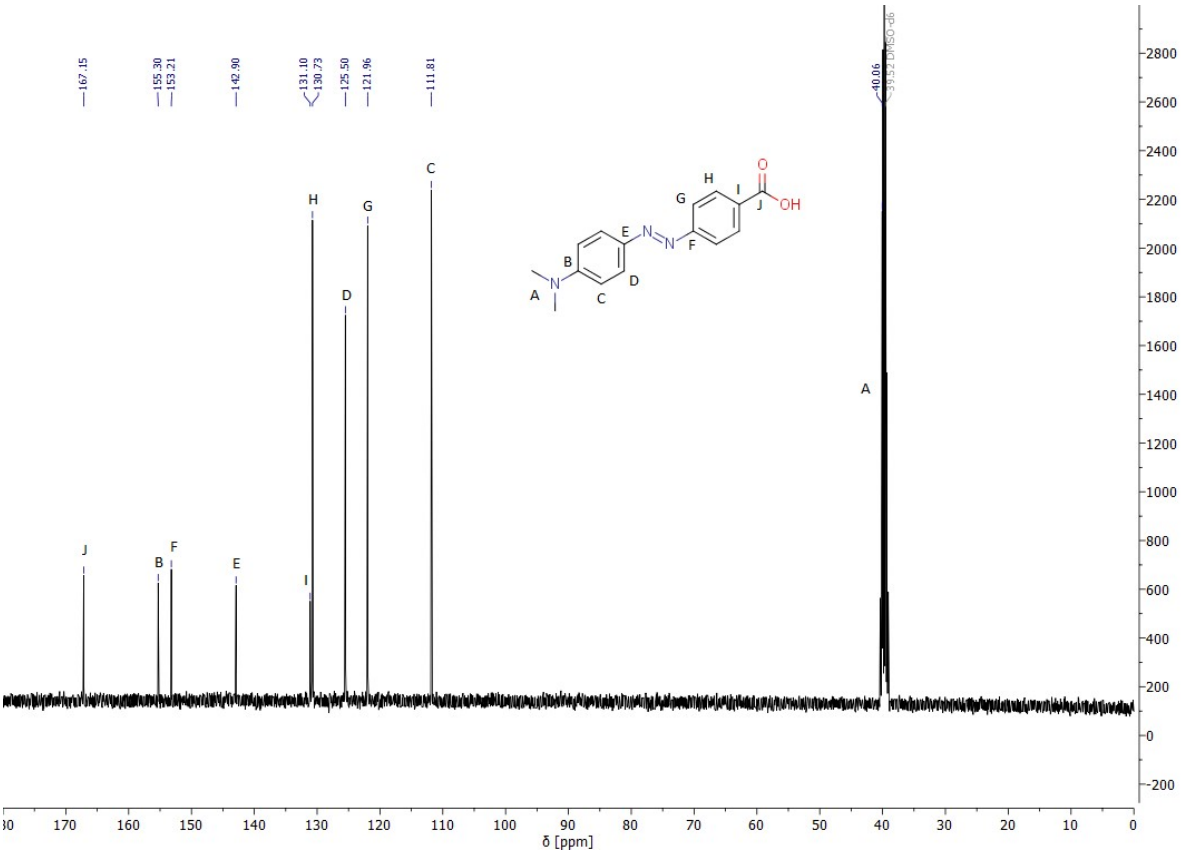


*Figure S 4: $^{13}$C-NMR spectrum (133 MHz) in DMSO-d$^6$ of 4-[(1E)-2-[4-(dimethylamino)phenyl]diazen-1-yl]benzoic acid (p-methyl red, p-MR.*

*Synthesis of 2-(prop-2-enamido)ethyl-4-[(1E)-2-[4-(dimethylamino)phenyl]diazen-1-yl]benzoate (p-methyl red ester of N-(2-hydroxyethyl)acrylamide, p-MREAm):*

p-Methyl red (202 mg, 7.5*10$^{-4}$ mol) and carbonyldiimidazole (184 mg, 1.1*10$^{-3}$ mol) were dispersed in tetrahydrofuran (8 mL) and stirred at room temperature for 19 hours. *N*-(2-Hydroxyethyl)acrylamide (0.14 mL, 1.4*10$^{-3}$ mol) and 1,8-diazabicyclo[5.4.0]undec-7-en (0.17 mL, 1.1*10$^{-3}$ mol) were added. The solution was stirred for 1 hour, before the reaction was stopped by addition of acetic acid (5 mL). The organic solvent was removed *in vacuo* and the residue dispersed in water before it was extracted with dichloromethane. The organic phase was washed with brine. The product was purified *via* column chromatography on silica in diethylether. The yield was 252 mg or 92%.

δH(400 MHz; $CDCl_3$) 8.13 (d, J = 8.8 Hz, 2H; Ph-*H*), 7.90 (d, J = 9.2 Hz, 2H; Ph-*H*), 7.86 (d, J = 8.8 Hz, 2H; Ph-*H*), 6.75 (d, J = 9.4 Hz, 2H; Ph-*H*), 6.31 (dd, J = 17.1, 1.5 Hz, 1H; CHC*H*H(trans)), 6.13 (dd, J = 17.1, 10.2 Hz, 1H; C*H*CHH; overlapped 1H;

CON*H*), 5.66 (dd, J = 10.2, 1.5 Hz, 1H; CHCH*H*(cis)), 4.48 (t, J = 5.2 Hz, 2H; COOC$H_2$), 3.76 (q, J = 5.4 Hz, 2H; CONHC$H_2$), 3.11 (s, 6H; N(Me)$_2$).

δC(101 MHz, $CDCl_3$) 166.63 (COO), 165.84 (CONH), 156.35 (Ph), 153.09 (Ph), 143.81 (Ph), 130.79 (Ph), 130.71 (CO*C*HCH$_2$), 129.67 (Ph), 127.01 (COCH*C*H$_2$), 125.72 (Ph), 122.18 (Ph), 111.58 (Ph), 63.97 (COO*C*H$_2$), 40.41 (N(Me)$_2$), 39.22 (CONH*C*H$_2$).

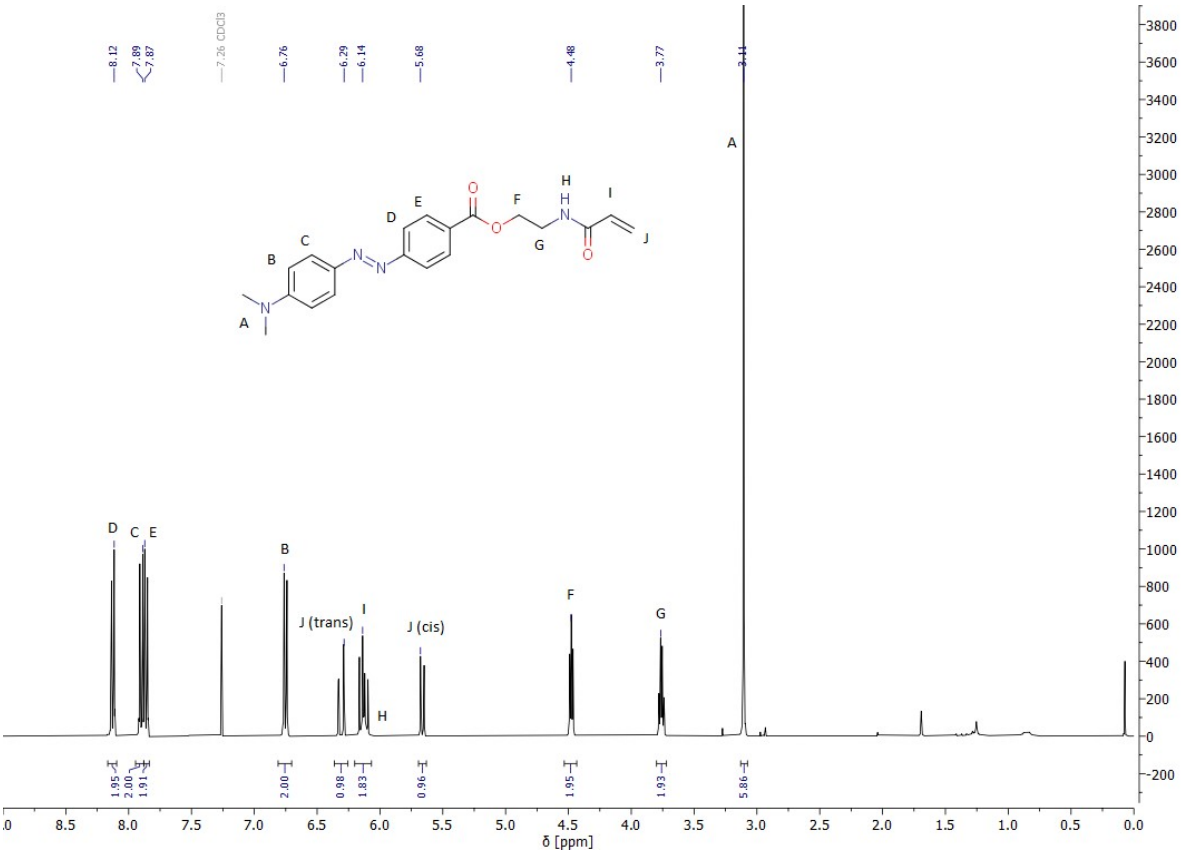


*Figure S 5: $^1$H-NMR spectrum (400 MHz) in $CDCl_3$ of 2-(prop-2-enamido)ethyl-4-[(1E)-2-[4-(dimethylamino)phenyl]diazen-1-yl]benzoate (p-methyl red ester of N-(2-hydroxyethyl)acrylamide, p-MREAm).*

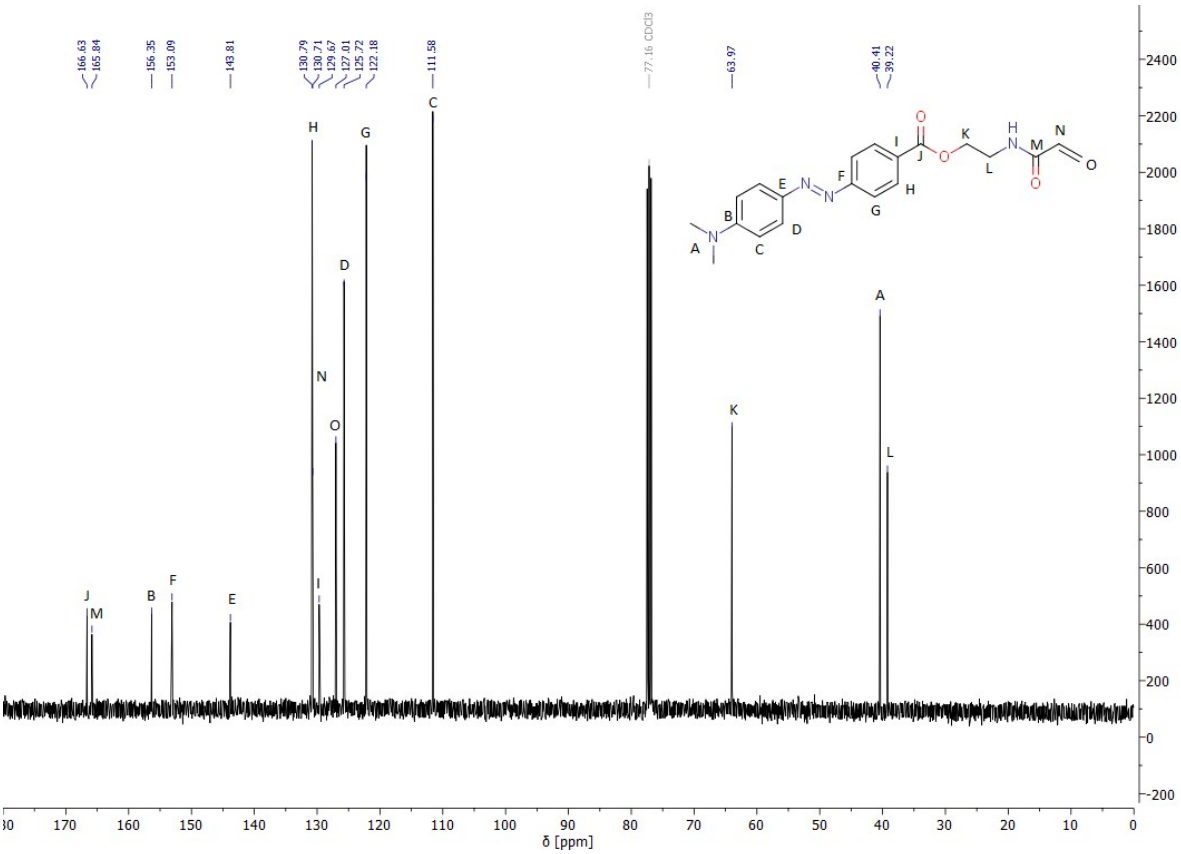


*Figure S 6: $^{13}$C-NMR spectrum (133 MHz) in $CDCl_3$ of 2-(prop-2-enamido)ethyl-4-[(1E)-2-[4-(dimethylamino)phenyl]diazen-1-yl]benzoate (p-methyl red ester of N-(2-hydroxyethyl)acrylamide, p-MREAm).*

*Synthesis of 3-[(1E)-2-[4-(dimethylamino)phenyl]diazen-1-yl]benzoic acid (m-methyl red, m-MR):*

3-Aminobenzoic acid (141 mg, 1.0*10$^{-3}$ mol) was dispersed in concentrated hydrochloric acid (0.45 mL) and cooled to 0 °C. A cooled aqueous solution of sodium nitrite (71.5 mg, 1.0*10$^{-3}$ mol in 1 mL) was added dropwise to the slurry over the course of 40 minutes. The resulting turbid mixture was stirred at 0 °C for 50 minutes and at room temperature for another 20 minutes. It was added to a solution of *N,N*-dimethylanilin (0.15 mL, 1.2*10$^{-3}$ mol) in water (10 mL, pH5). After 20 hours, the solution was neutralised with aq. NaOH (1M) and then extracted with dichloromethane until the aqueous phase was colourless. The organic phase was dried over magnesium sulfate and the solvent evaporated. The product was purified *via* column chromatography on silica in diethylether. The yield was 136 mg or 49%.

δH(500 MHz; DMSO-d$^6$) 8.29 (t, J = 1.8 Hz, 2H; Ph-*H*), 8.00 (ddt, J = 10.5, 7.7, 1.2 Hz, 2H; Ph-*H*), 7.83 (d, J = 9.2 Hz, 2H; Ph-*H*), 7.65 (t, J = 7.8 Hz, 1H; Ph-*H*), 6.83 (d, J = 9.3 Hz, 2H; Ph-*H*), 3.06 (s, 6H; N(Me)$_2$).

δC(126 MHz, DMSO-$d^6$) 166.99 (COO), 152.79 (Ph), 152.48 (Ph), 142.47 (Ph), 131.95 (Ph), 129.90 (Ph), 129.61 (Ph), 126.64 (Ph), 125.02 (Ph), 121.58 (Ph), 111.56 (Ph), 39.82 ($N(Me)_2$).

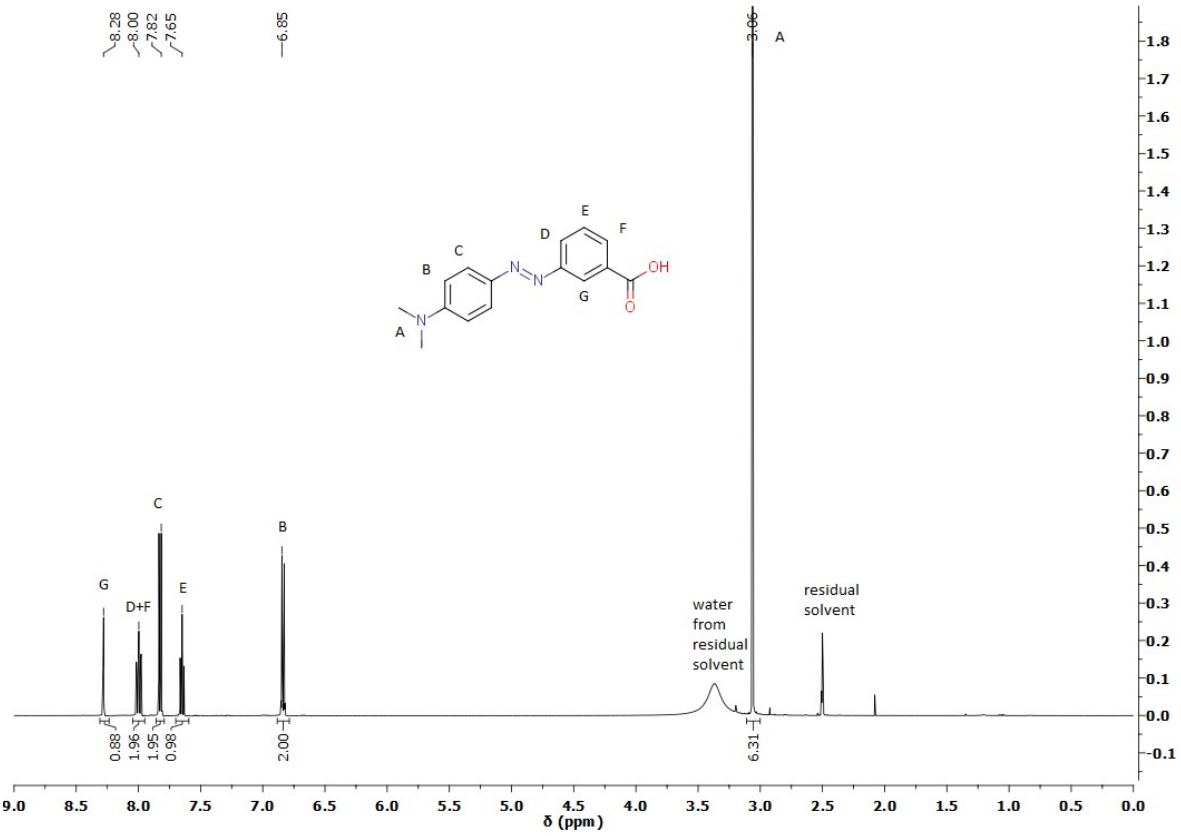


*Figure S 7: $^1$H-NMR spectrum (500 MHz) in DMSO-$d^6$ of 3-[(1E)-2-[4-(dimethylamino)phenyl]diazen-1-yl]benzoic acid (m-methyl red, m-MR).*

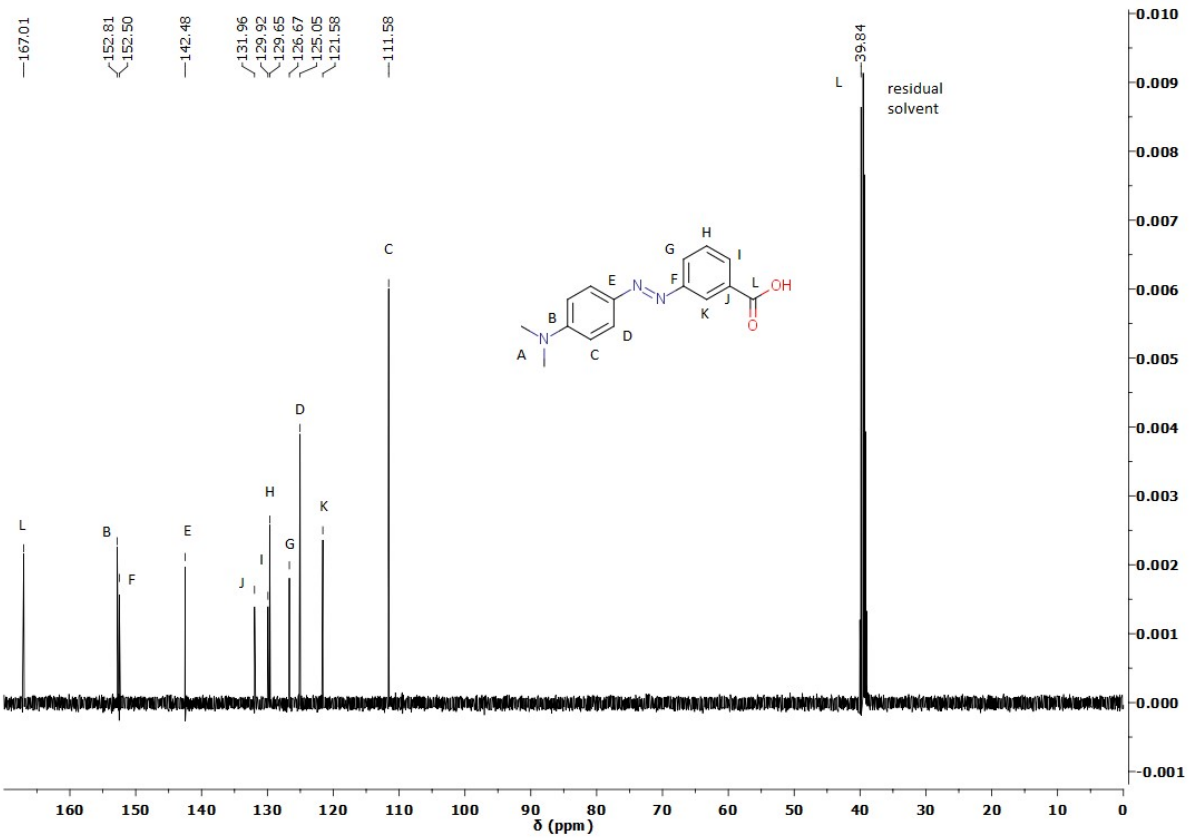


*Figure S 8: $^{13}$C-NMR spectrum (126 MHz) in DMSO-d$^6$ of 3-[(1E)-2-[4-(dimethylamino)phenyl]diazen-1-yl]benzoic acid (m-methyl red, m-MR).*

*Synthesis of 2-(prop-2-enamido)ethyl-3-[(1E)-2-[4-(dimethylamino)phenyl]diazen-1-yl]benzoate (m-methyl red ester of N-(2-hydroxyethyl)acrylamide, m-MREAm):*

m-Methyl red (201 mg, 7.5*10$^{-4}$ mol) and carbonyldiimidazole (185 mg, 1.1*10$^{-3}$ mol) were dissolved in tetrahydrofuran (8 mL) and stirred at room temperature for 19 hours. *N*-(2-Hydroxyethyl)acrylamide (0.14 mL, 1.4*10$^{-3}$ mol) and five minutes later 1,8-diazabicyclo[5.4.0]undec-7en (0.17 mL, 1.1*10$^{-3}$ mol) were added. The reaction mixture was stirred for three hours before the reaction was stopped via addition of acetic acid (5 mL).

The solvent was distilled of *in vacuo*, the leftover slurry dissolved in dichloromethane and the organic phase extracted with water. The product was then purified by column chromatography on silica in diethylether. The yield was 247 mg or 90%.

δH(500 MHz, DMSO-d$^6$) 8.39 (t, J = 5.6 Hz, 1H; Ph-*H*), 8.31 (t, J = 1.6 Hz, 1H; Ph-*H*), 8.03 (ddd, J = 3.6, 1.9, 1.2 Hz, 1H; Ph-*H*), 8.02 (dq, J = 1.9, 1.2 Hz, 1H; Ph-*H*), 7.83 (d, J = 9.3 Hz, 2H; Ph-*H*), 7.67 (t, J = 7.8 Hz, 1H; Ph-*H*), 6.85 (d, J = 9.4 Hz, 2H; Ph-*H*), 6.25 (dd, J = 17.1, 10.2 Hz, 1H; CHC*H*H(trans)), 6.11 (dd, J = 17.1, 2.2 Hz, 1H;

C*H*CHH), 5.60 (dd, J = 10.2, 2.2 Hz, 1H; CHCH*H*(cis)), 4.36 (t, J = 5.5 Hz, 2H; COOC$H_2$), 3.56 (q, J = 5.8 Hz, 2H; CONHC$H_2$), 3.07 (s, 6H; N(Me)$_2$).

δC(126 MHz, DMSO-d$^6$) 165.47 (COO), 165.02 (CONH), 152.88 (Ph), 152.54 (Ph), 142.46 (Ph), 131.57 (CO*C*HCH$_2$), 130.86 (Ph), 129.90 (Ph), 129.76 (Ph), 126.49 (Ph), 125.46 (COCH*C*H$_2$), 125.11 (Ph), 122.15 (Ph), 111.59 (Ph), 63.79 (COO*C*H$_2$), 39. (N(Me)$_2$), 37.79 (CONH*C*H$_2$).

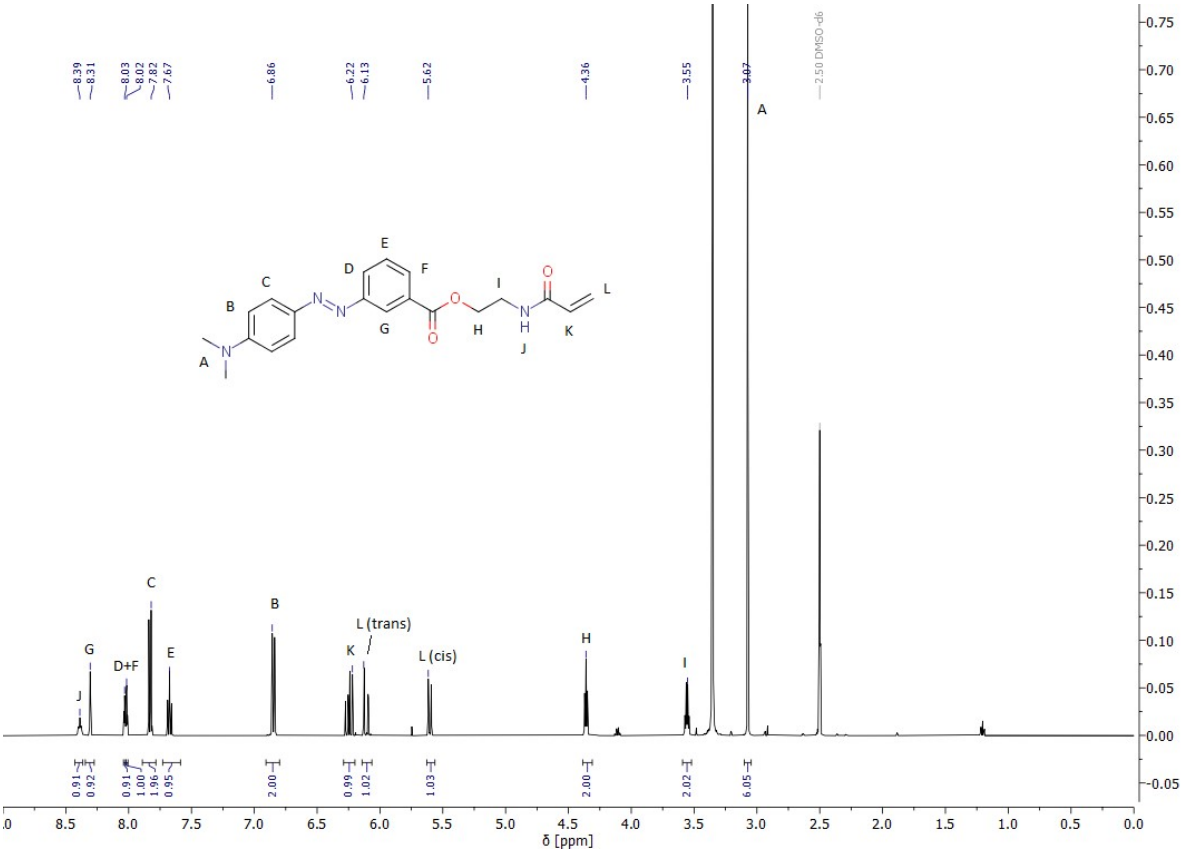


*Figure S 9: $^1$H-NMR spectrum (500 MHz) in DMSO-d$^6$ of 2-(prop-2-enamido)ethyl-3-[(1E)-2-[4-(dimethylamino)phenyl]diazen-1-yl]benzoate (m-methyl red ester of N-(2-hydroxyethyl)acrylamide, m-MREAm).*

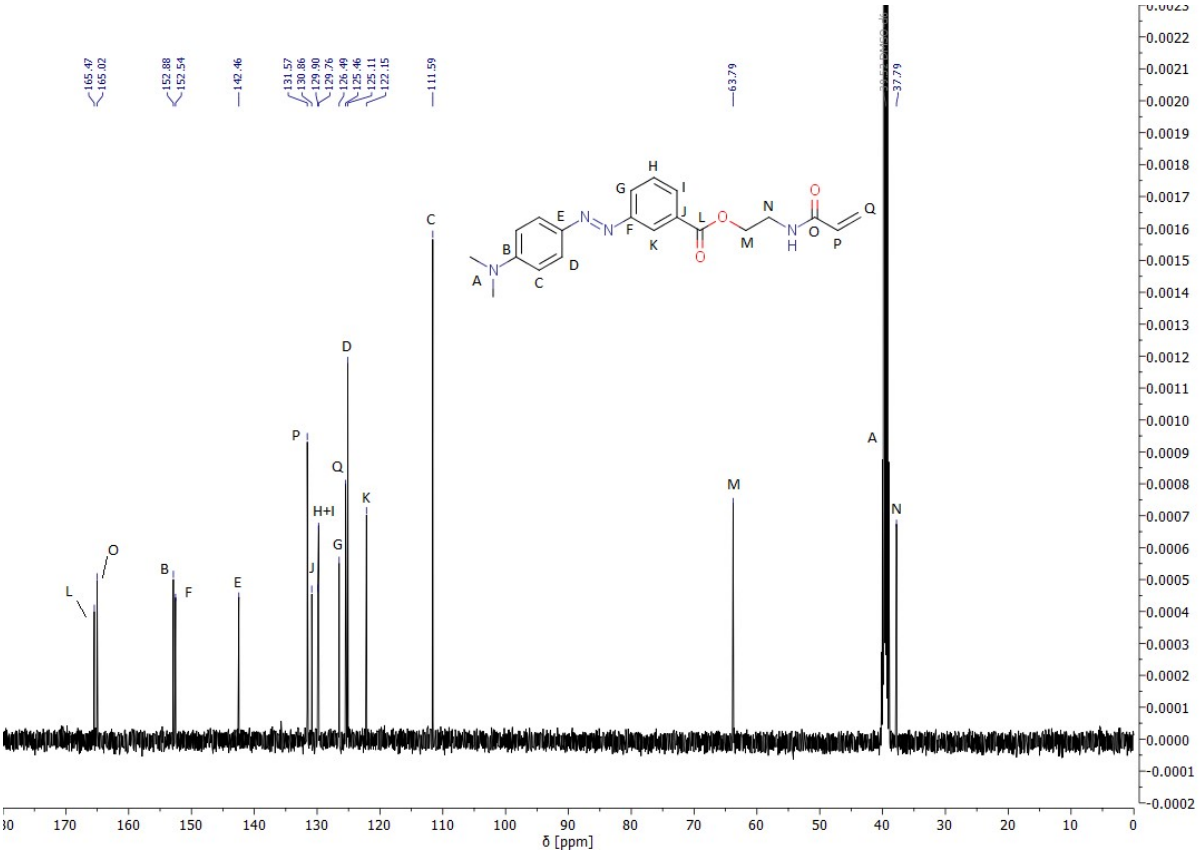


*Figure S 10: $^{13}$C-NMR spectrum (133 MHz) in DMSO-d$^6$ of 2-(prop-2-enamido)ethyl-3-[(1E)-2-[4-(dimethylamino)phenyl]diazen-1-yl]benzoate (m-methyl red ester of N-(2-hydroxyethyl)acrylamide, m-MREAm).*

*Copolymerisations with o-MREAm:*

The different copolymers were obtained by radical polymerisation. The monomers (0.6 mol/L) and azobisisobutyronitrile were dissolved in 1,4-dioxane or methanol. The solutions were purged with nitrogen for 30 minutes and heated in an oil bath at 75 °C for 1,4-dioxane or 60 °C for methanol for 24 to 63 hours. The polymers were then precipitated up to three times in a non-solvent. The details are summarised in Table S 1.

P1 (poly(HEAm-co-o-MREAm-co-BPAAm)): δH(500 MHz, MeOD) 8.5-6.5 (br, aromatic H), 4.57 (COOC$H_2$), 4.38 (Ar-CONHC$H_2$), 3.66 ($CH_2CH_2$OH), 3.51-3.12 (CONHC$H_2$), 2.4-1.25 (backbone)

P2 (poly(NiPAAm-co-HEAm-co-o-MREAm-co-BPAAm)): δH(500 MHz, $D_2O$) 8.0-6.5 (br, aromatic H), 4.41 (COOC$H_2$), 3.91 (NHC$H$($CH_3$)$_2$), 3.68 ($CH_2CH_2$OH), 3.36 (CONHC$H_2$), 2.3-1.25 (backbone), 1.16 (NHCH($CH_3$)$_2$)

P2b (poly(NiPAAm-co-HEAm-co-o-MREAm-co-BPAAm)): δH(400 MHz, MeOD) 8.0-6.75 (br, aromatic H), 4.38 (COOC$H_2$), 3.96 (NHC$H$($CH_3$)$_2$), 3.65 ($CH_2CH_2$OH), 3.12 (N(Me)$_2$), 2.3-1.25 (backbone), 1.16 (NHCH(C$H_3$)$_2$)

P3 (poly(HEAm-co-MAA-co-o-MREAm-co-BPAAm)): δH(400 MHz, $D_2O$) 8.5-6.5 (br, aromatic H), 4.42 (COOC$H_2$), 3.66 ($CH_2CH_2$OH), 3.34 (CONHC$H_2$), 2.4-1.25 (backbone), 1.00 (backbone-C$H_3$)

P4 (poly(NiPAAm-co-MAA-co-o-MREAm-co-BPAAm)): δH(500 MHz, MeOD) 8.0-6.5 (br, aromatic H), 4.58 (COOC$H_2$), 4.38 (Ar-CONHC$H_2$), 3.91 (NHC$H$($CH_3$)$_2$), 3.12 (N(Me)$_2$), 2.3-1.25 (backbone), 1.16 (NHCH(C$H_3$)$_2$)

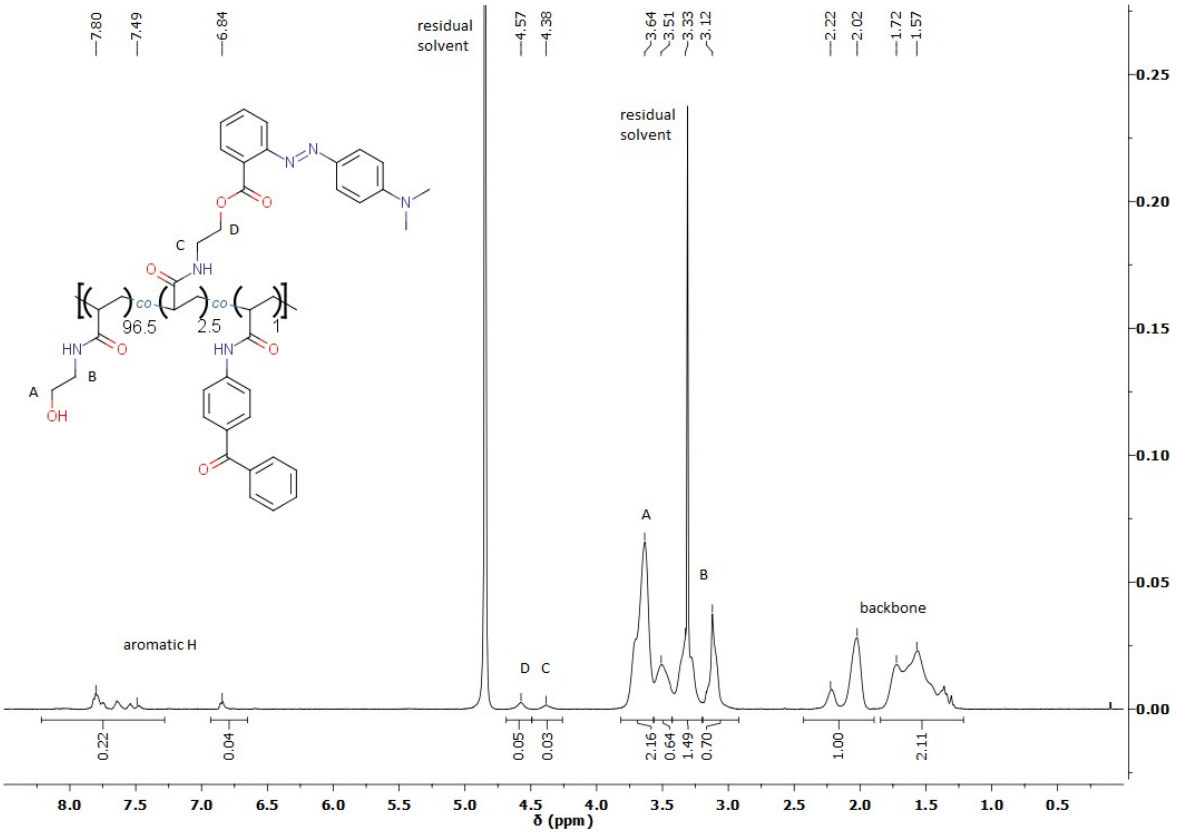


*Figure S 11: [1]H-NMR spectrum (500 MHz) in MeOD of a poly(HEAm-co-o-MREAm-co-BPAAm) copolymer (P1) (feed: HEAm:o-MREAm:BPAAm 96.5:2.5:1).*

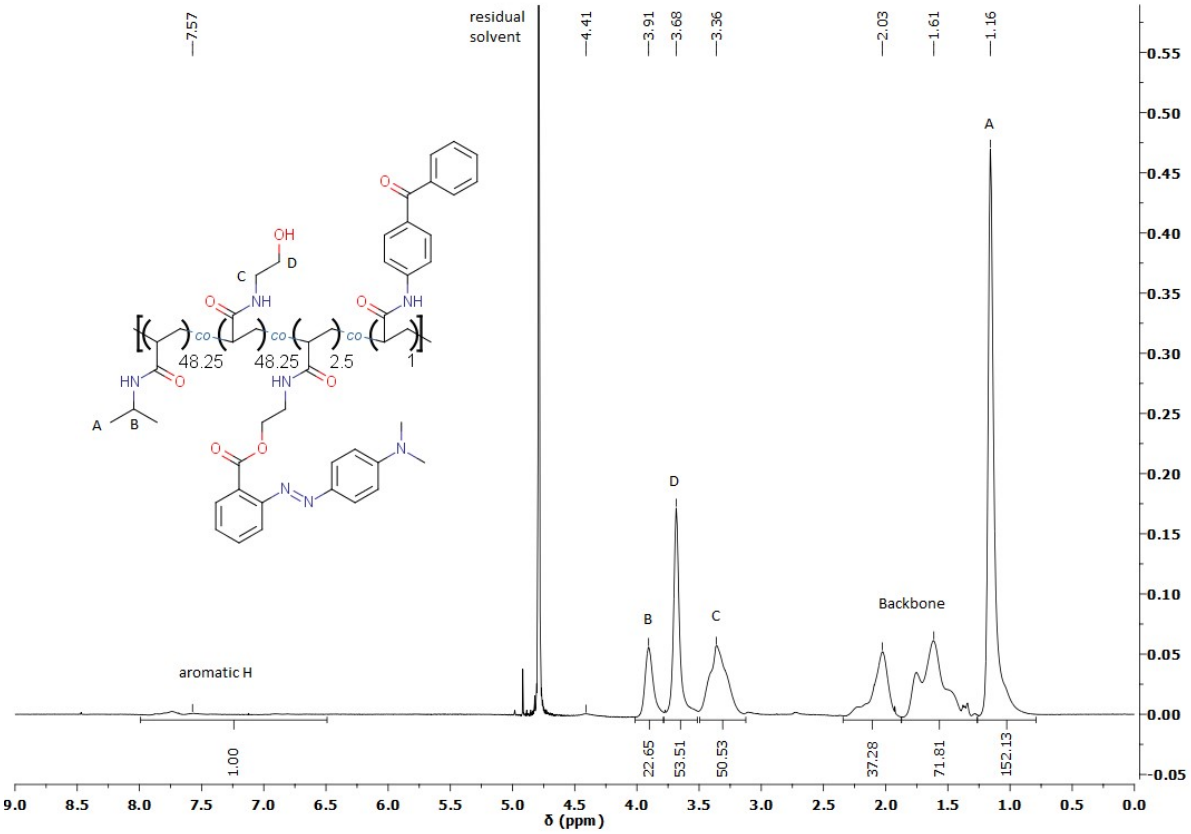


*Figure S 12: [1]H-NMR spectrum (500 MHz) in $D_2O$ of a poly(NiPAAm-co-HEAm-co-o-MREAm-co-BPAAm) copolymer (P2) (feed: NiPAAm:HEAm:o-MREAm:BPAAm 48.25:48.25:2.5:1).*

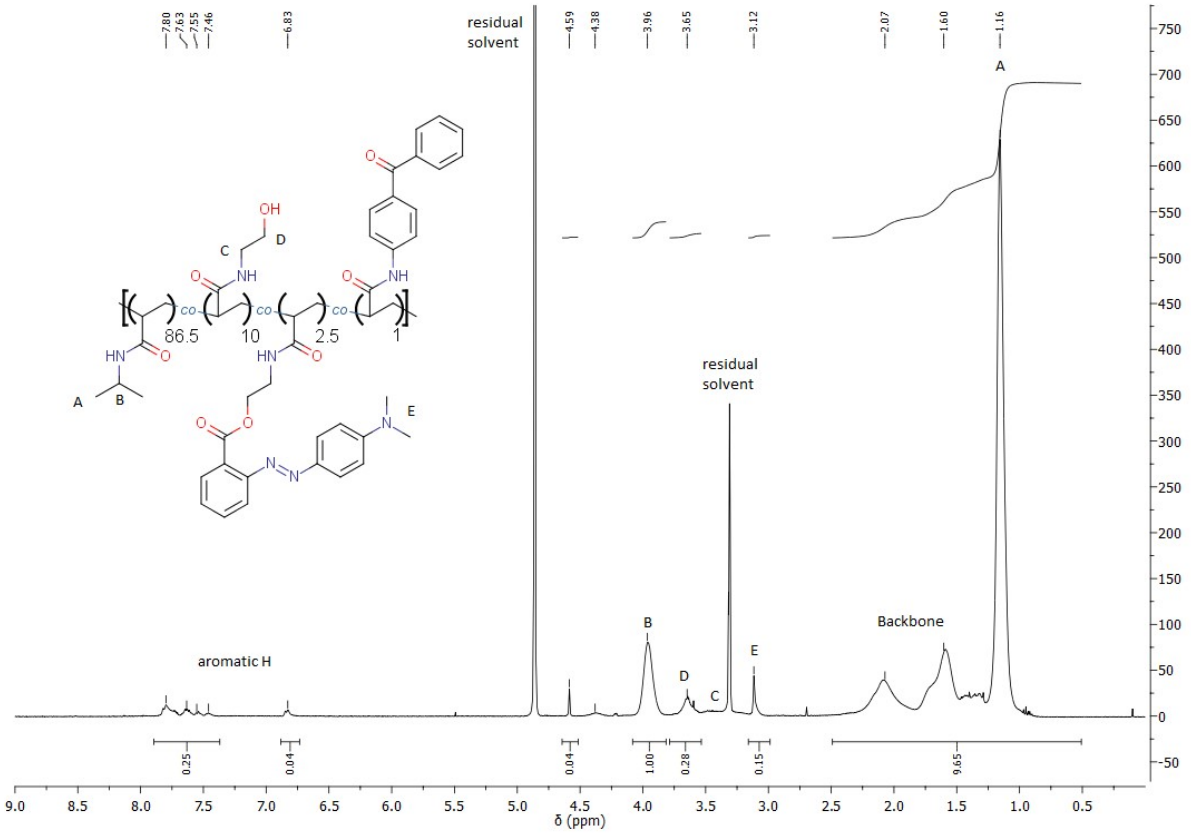


*Figure S 13: [1]H-NMR spectrum (400 MHz) in MeOD of a poly(NiPAAm-co-HEAm-co-o-MREAm-co-BPAAm) copolymer (P2b) (feed: NiPAAm:HEAm:o-MREAm:BPAAm 87.2:9.2:2.6:1).*

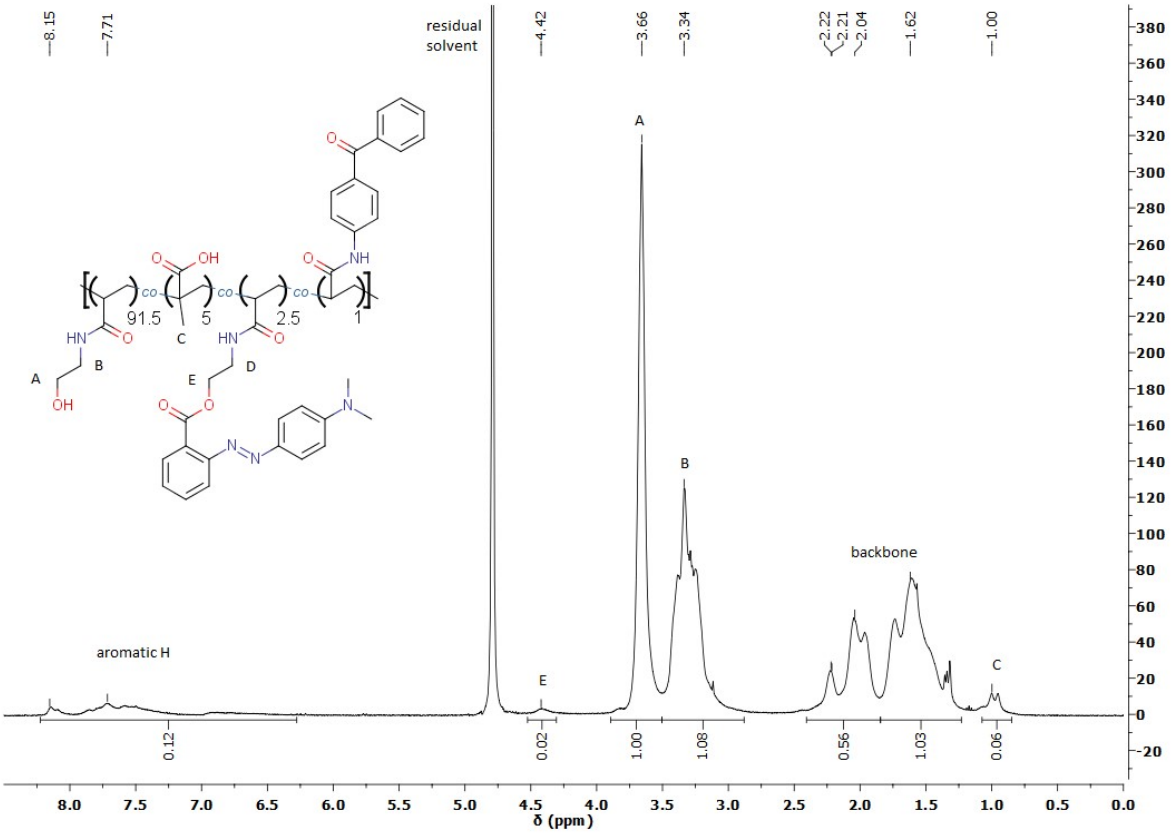


*Figure S 14: [1]H-NMR spectrum (400 MHz) in $D_2O$ of a poly(HEAm-co-MAA-co-o-MREAm-co-BPAAm) copolymer (P3) (feed: HEAm:MAA:o-MREAm:BPAAm 91.5:5:2.5:1).*

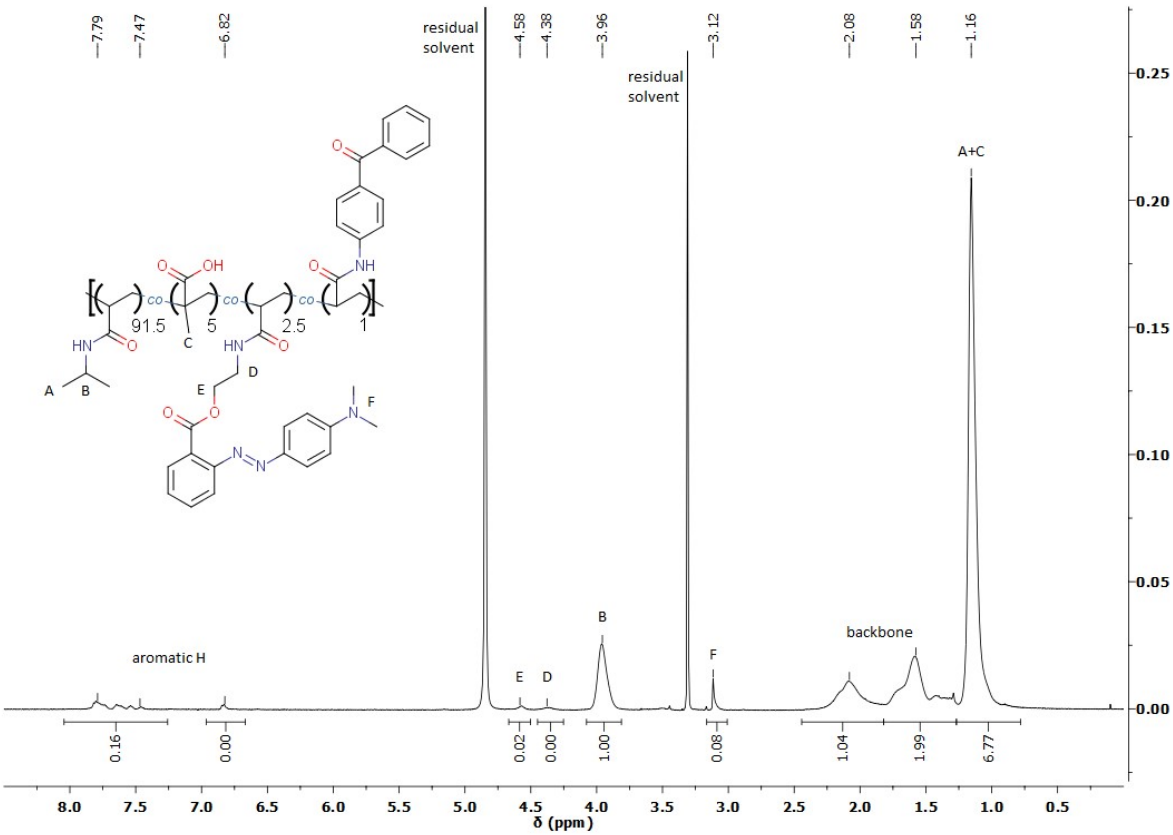


*Figure S 15: [1]H-NMR spectrum (500 MHz) in MeOD of a poly(NiPAAm-co-MAA-co-o-MREAm-co-BPAAm) copolymer (P4) (feed: NiPAAm:MAA:o-MREAm:BPAAm 91.8:4.9:2.3:1).*

*Table S 1: Feed composition in mol% and reaction parameters for the different copolymersations.*

| Polymer | NiPAAm [%] | HEAm [%] | MAA [%] | MREAm [%] | BPAAm [%] | AIBN [%] | T [°C] | Time [h] | Solvent | Non-solvent |
|---|---|---|---|---|---|---|---|---|---|---|
| **1** | 0 | 96.5 | 0 | 2.5 | 1 | 2 | 60 | 24 | Methanol | Ethyl acetate |
| **2** | 48.25 | 48.25 | 0 | 2.5 | 1 | 2 | 60 | 48 | Methanol | Diethylether |
| **2b** | 87.2 | 9.2 | 0 | 2.6 | 1 | 2 | 60 | 26 | 1,4-Dioxane | Diethylether |
| **3** | 0 | 91.5 | 5 | 2.5 | 1 | 2.1 | 60 | 63 | Methanol | Acetone |
| **4** | 91.8 | 0 | 4.9 | 2.3 | 1 | 1.9 | 75 | 24 | 1,4-Dioxane | Diethylether |

*Film preparation:*

The glass slides used in photocrosslinking experiments were cleaned with fresh Carothers' acid (sulfuric acid:hydrogen peroxide, 3:1) and rinsed thoroughly with water. The slides were dried under a nitrogen stream. They were submerged in an ethanolic solution of benzophenone silane (1 mmol/L) for 24 hours before they were rinsed thrice with absolute ethanol and finally dried under a nitrogen stream.

Polymers were drop-casted on the glass slides from methanolic solution (1 w%, 200 µL on 2.4cmx2.4cm slides). Photocrosslinking was performed at 302 nm with an energy of 20.3 J/cm². The polymer films of P1 and P2 were annealed at 170 °C prior to photocrosslinking. All films were washed with water until the supernatant remained colourless before thermochromicity measurements.

*General reference graphs and UV-vis data for thermochromic changes of different systems:*

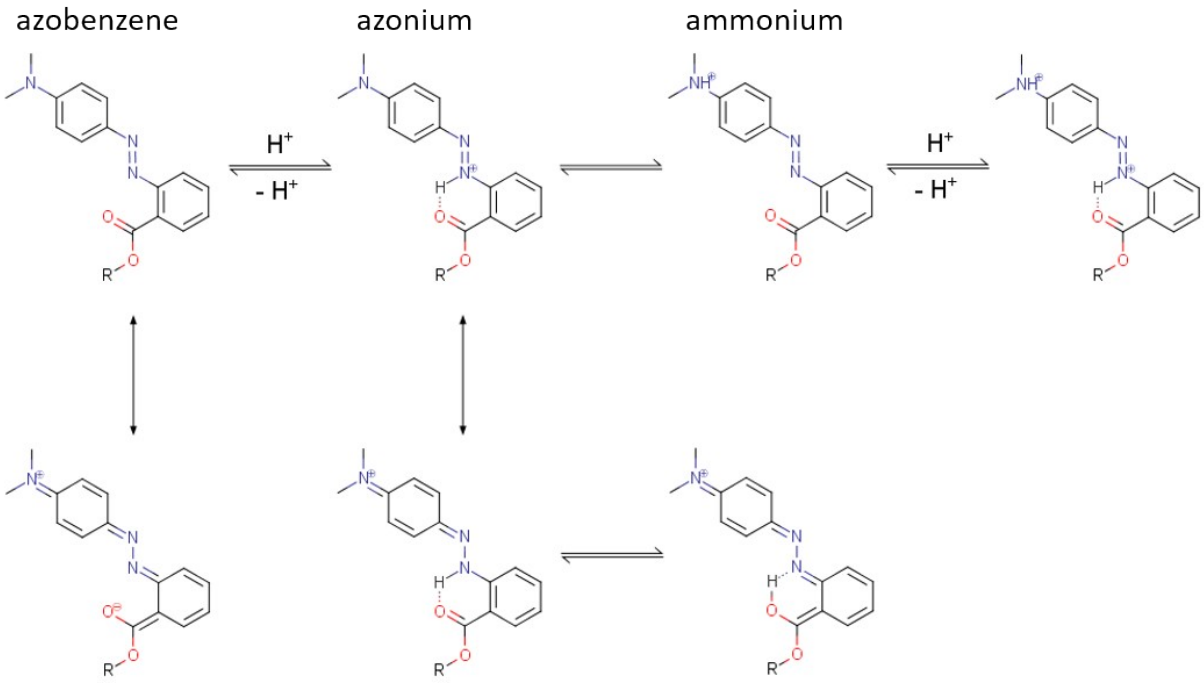


*Scheme S 1: Protonation equilibrium of a methyl red derivative showing the azonium, ammonium and diprotonated forms and important mesomeric structures.*

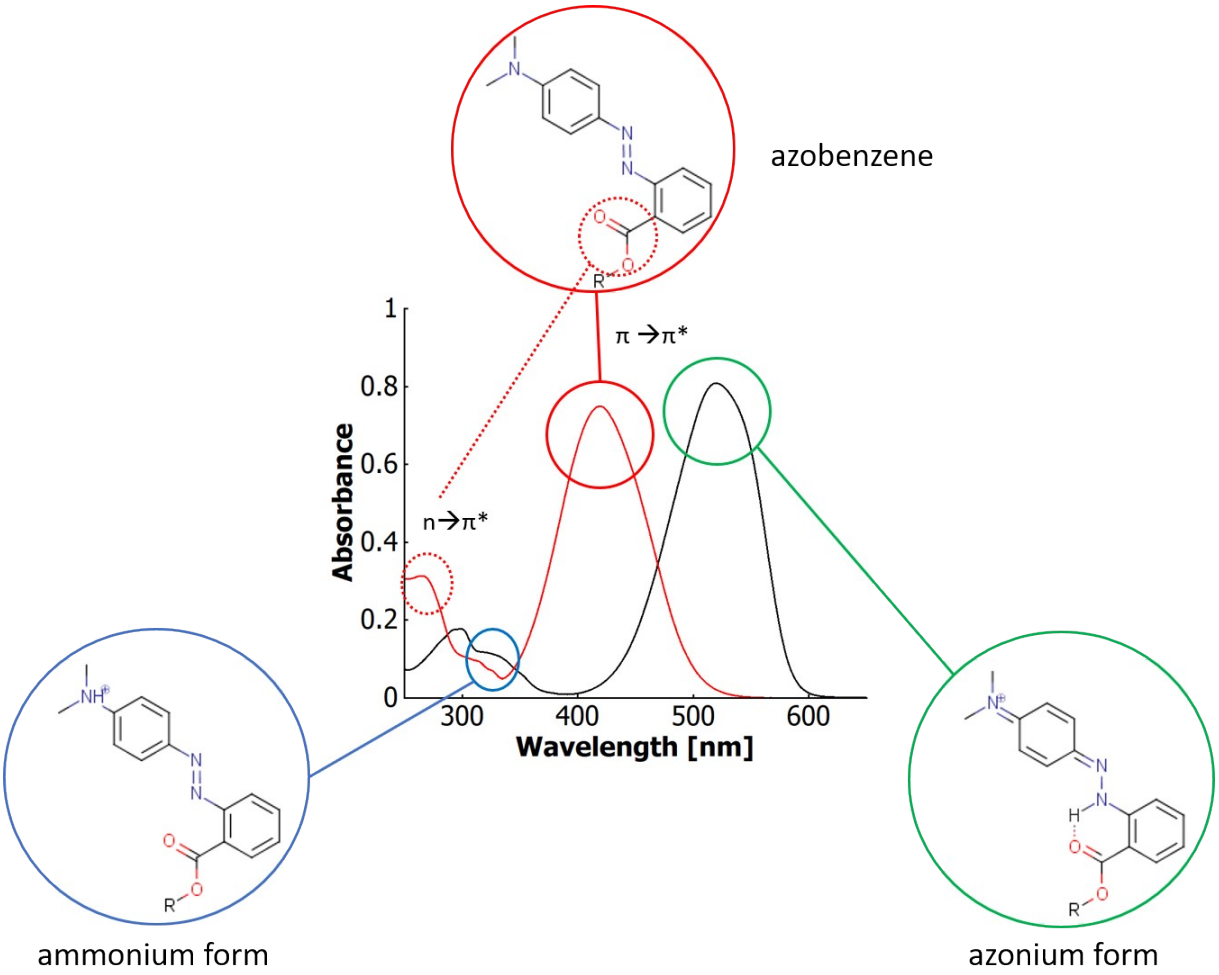


*Figure S 16: UV-vis spectra of the neutral and protonated form of a methyl red ester of N-(2-hydroxyethyl)acrylamide with the important absorption bands colour marked with the related structure (bands assigned according to literature [7-9]).*

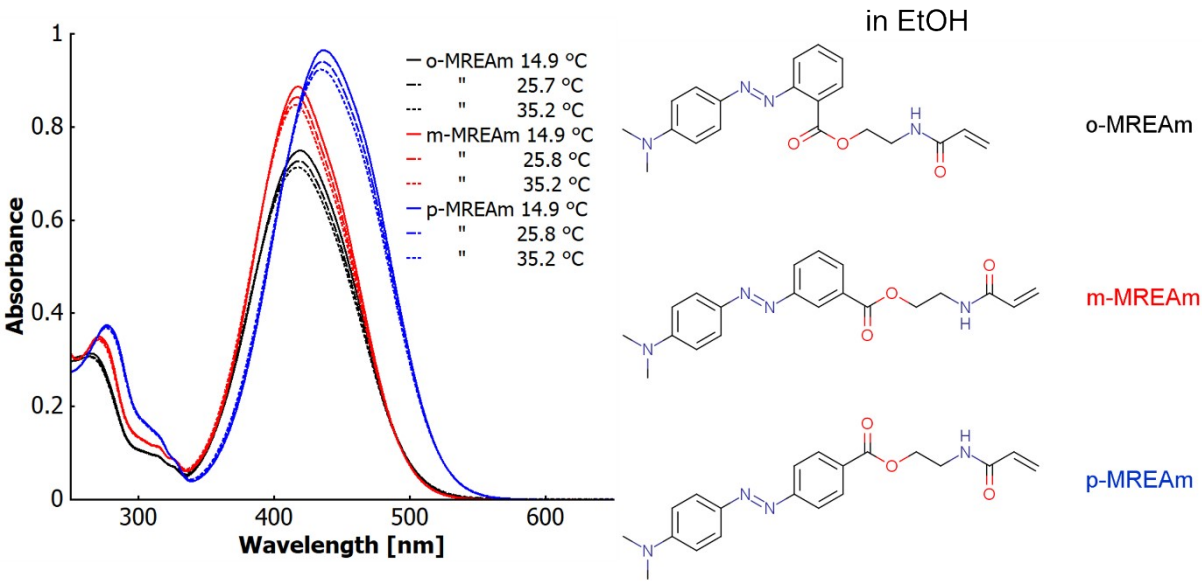


*Figure S 17: UV-vis spectra of ortho-, meta- and para-methyl red ester of N-(2-hydroxyethyl)acrylamide ($2.7*10^{-5}$ mol $L^{-1}$) at different temperatures in neat ethanol with structures.*

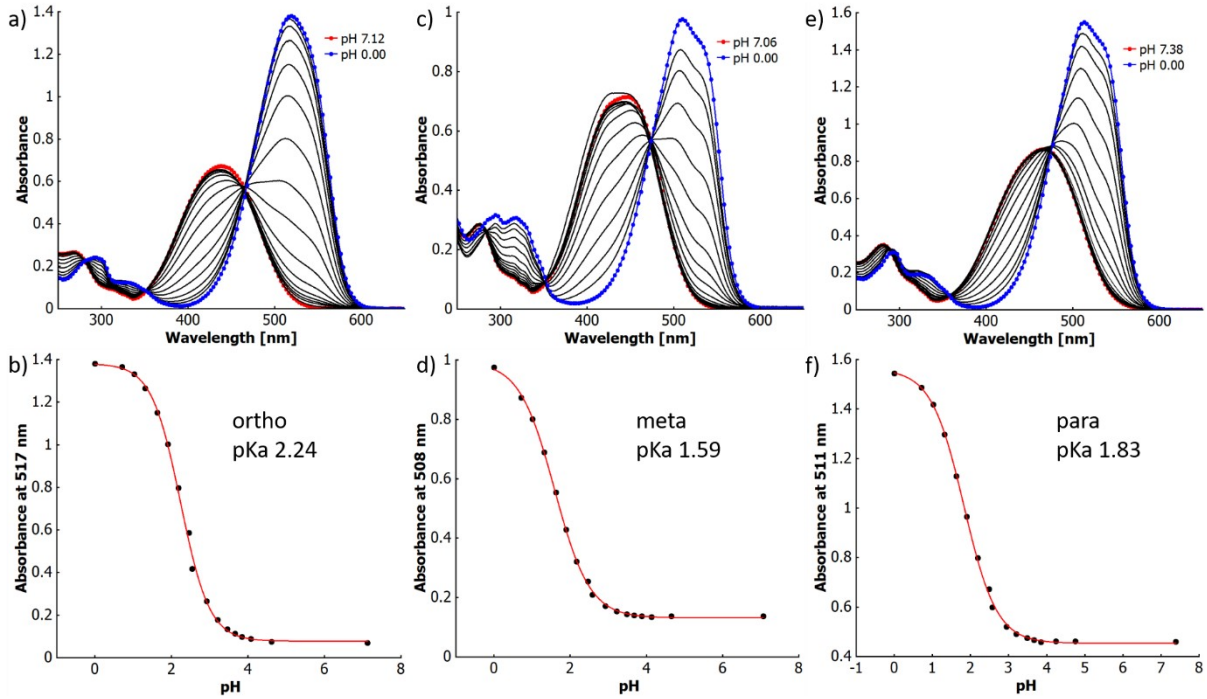


*Figure S 18: UV-vis spectra in $H_2O$:EtOH ($X_{EtOH}$=0.31) at different pH values at 20 °C for a) o-MREAm, c) m-MREAm and e) p-MREAm (all 2.7*10$^{-5}$ mol L$^{-1}$); and absorption at maximum of the azonium vs. pH for b) o-MREAm (517 nm), d) m-MREAm (508 nm) and f) p-MREAm (511 nm).*

*Table S 2: pKa values of the constitutional isomers of methyl red and their esters of 2-hydroxylethyl acrylamide.*

| | o-MR[7] | m-MR[10] | p-MR[11] | o-MREAm | m-MREAm | p-MREAm |
|---|---|---|---|---|---|---|
| **pKa free acid** | 4.85 | 4.94 | 4.93 | -[a] | -[a] | -[a] |
| **pKa azonium** | 2.38 | 1.99 | 2.08 | 2.24 | 1.54 | 1.83 |

*[a] this value is not available, as the free acid is substituted by an ester functionality*

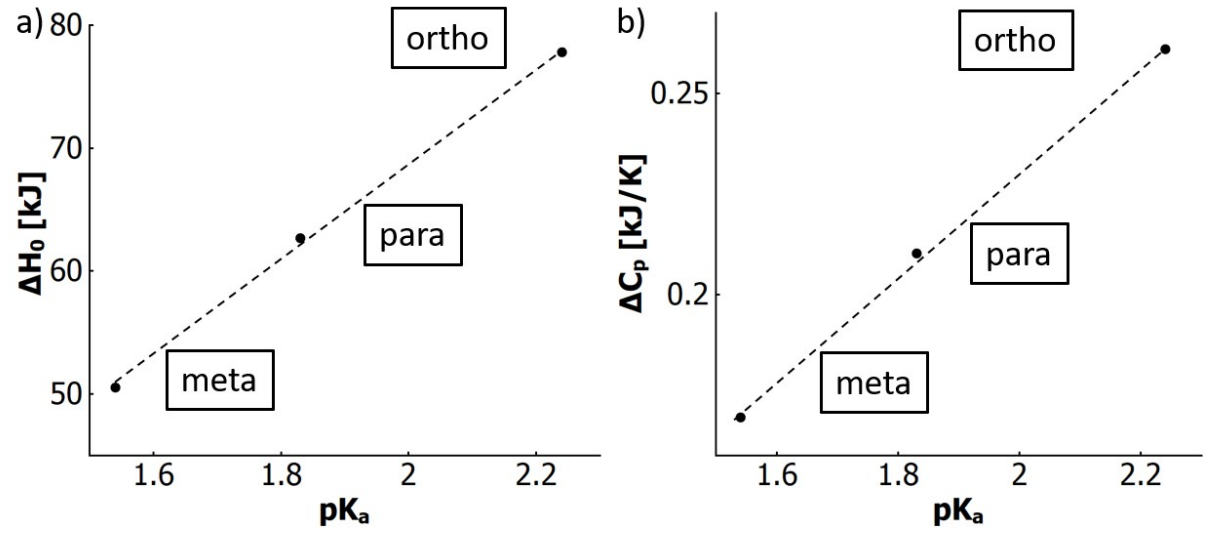


*Figure S 19: Correlation of thermochromicity parameters a) $H_0$ and b) $C_p$ and $pK_a$ for the constitutional isomers of the methyl red ester of N-(2-hydroxyethyl)acrylamide in $H_2O$:EtOH ($X_{EtOH}$=0.31). The black line serves as a guide to the eye.*

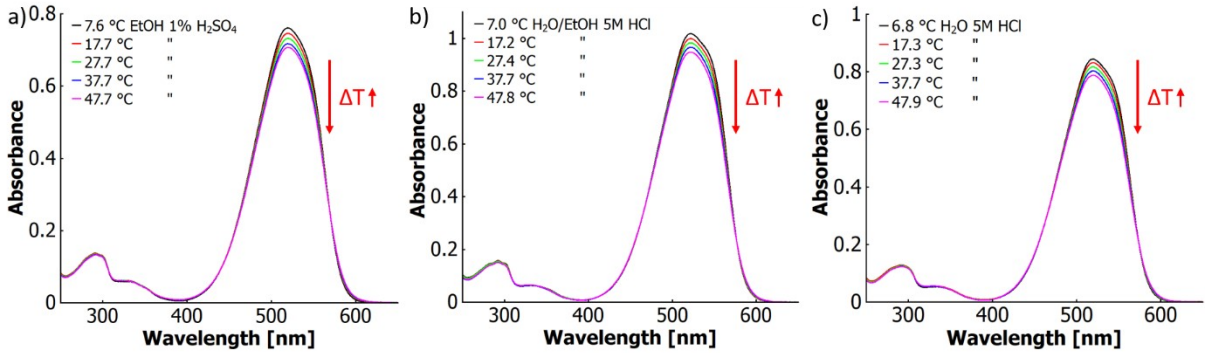


*Figure S 20: UV-vis spectra of o-MREAm ($1.4*10^{-5}$ mol) at different temperatures in a) ethanol saturated with HCl; b) $H_2O$:EtOH ($X_{EtOH}$=0.31) with 5M HCl and c) $H_2O$ with 5M HCl to determine thermo-solvatochromism of the azonium ion.*

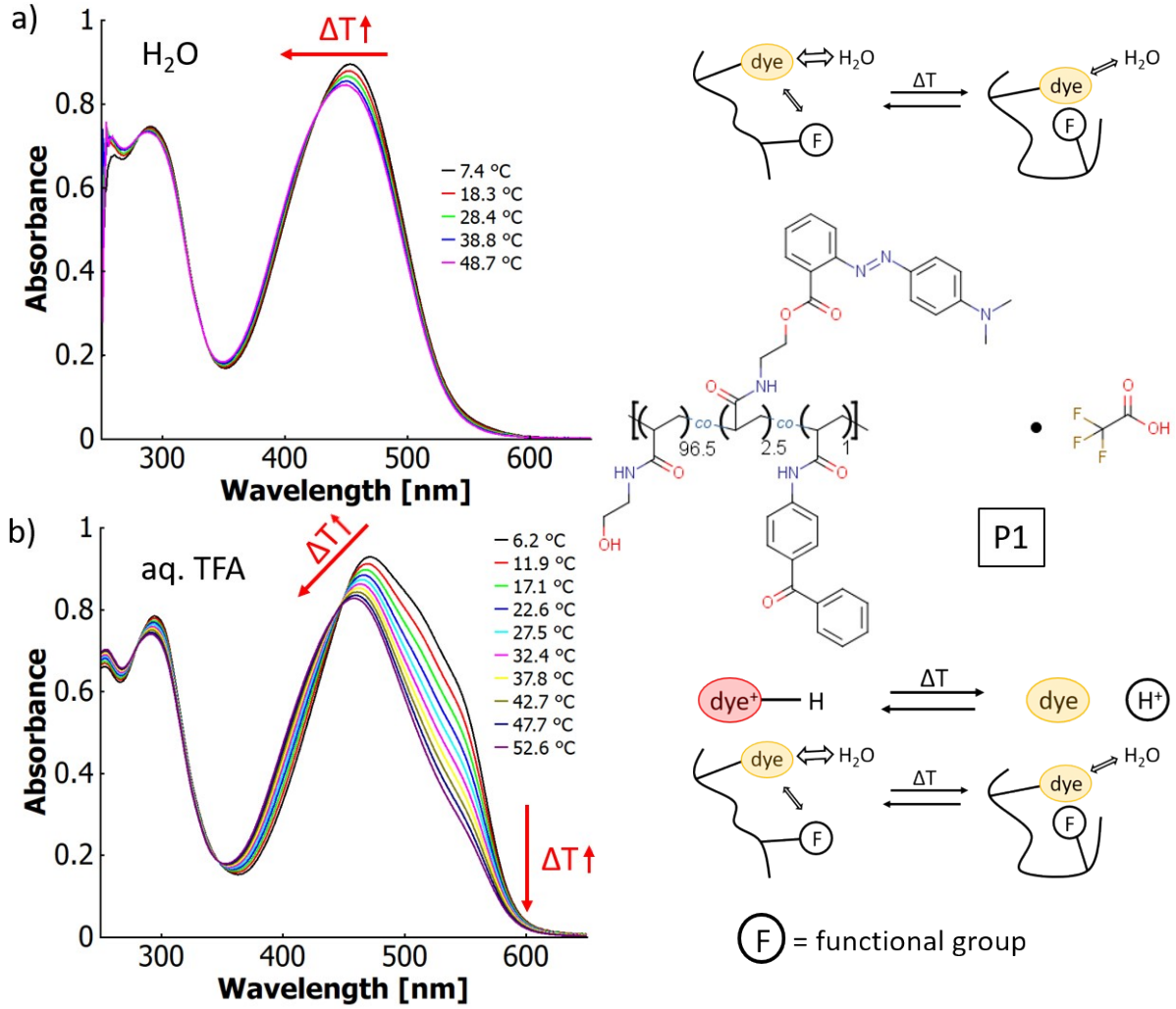


*Figure S 21: UV-vis spectra of a poly(HEAm-co-o-MREAm-co-BPAAm) copolymer (P1) at different temperatures with structure of the copolymer a) 0.03 w% in pure water and b) 0.03 w% in aqueous trifluoroacetic acid (0.001 v/v%), with the thermo-peri-halochromic mechanism sketched on the right side.*

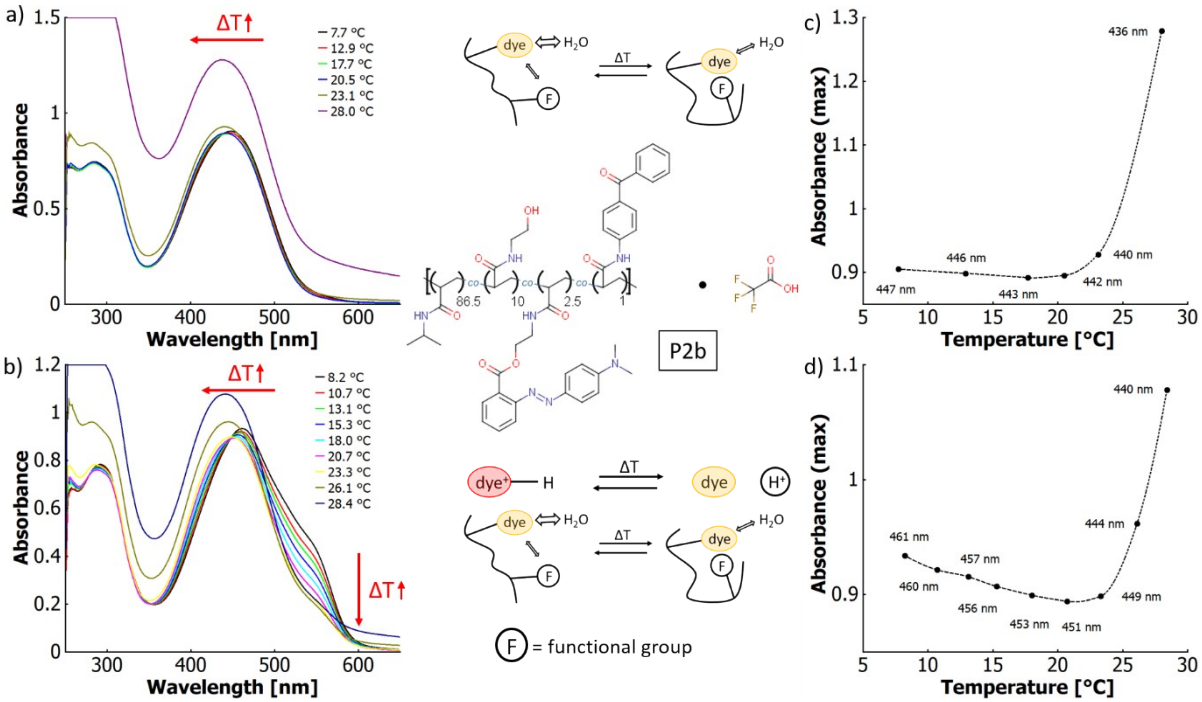


*Figure S 22: UV-vis spectra of a poly(NiPAAm-co-HEAm-co-o-MREAm-co-BPAAm) copolymer (P2b) 0.03 w% in a) pure water and b) aqueous trifluoroacetic acid (0.001 v/v%) at different temperatures (direction of shifts in absorbance upon heating marked with red arrows); absorbance at maximum (wavelength indicated in graph) vs temperature for c) pure water and d) aqueous trifluoroacetic acid (0.001 v/v%). The lines are generated by a non-rounded Akima interpolation and only serve as guide to the eye. The structure of the copolymer (acid optional) and cartoons of the ongoing thermochromic processes are shown in the middle section.*

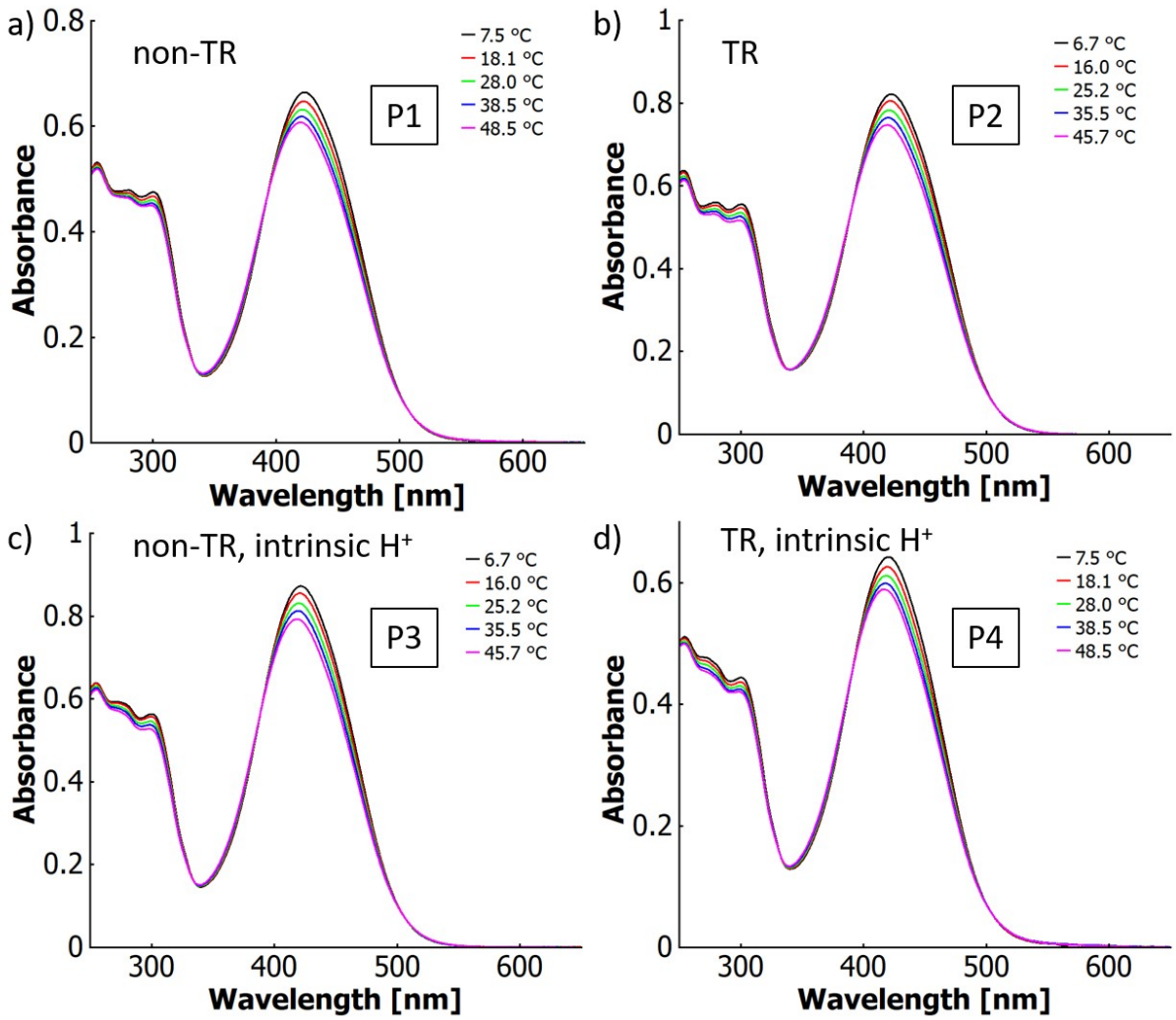


*Figure S 23: UV-vis spectra in neat ethanol of four dye-containing copolymers at different temperatures ("TR" = thermoresponsive, "intrinsic $H^+$" = -COOH substituents in the polymer); a) (P1) poly(HEAm-co-o-MREAm-co-BPAAm); b) (P2) poly(NiPAAm-co-HEAm-co-o-MREAm-co-BPAAm); c) (P3) poly(HEAm-co-MAA-co-o-MREAm-co-BPAAm) and d) (P4) poly(NiPAAm-co-MAA-co-o-MREAm-co-BPAAm) (all 0.2 g/L, TR denotes thermoresponsive).*

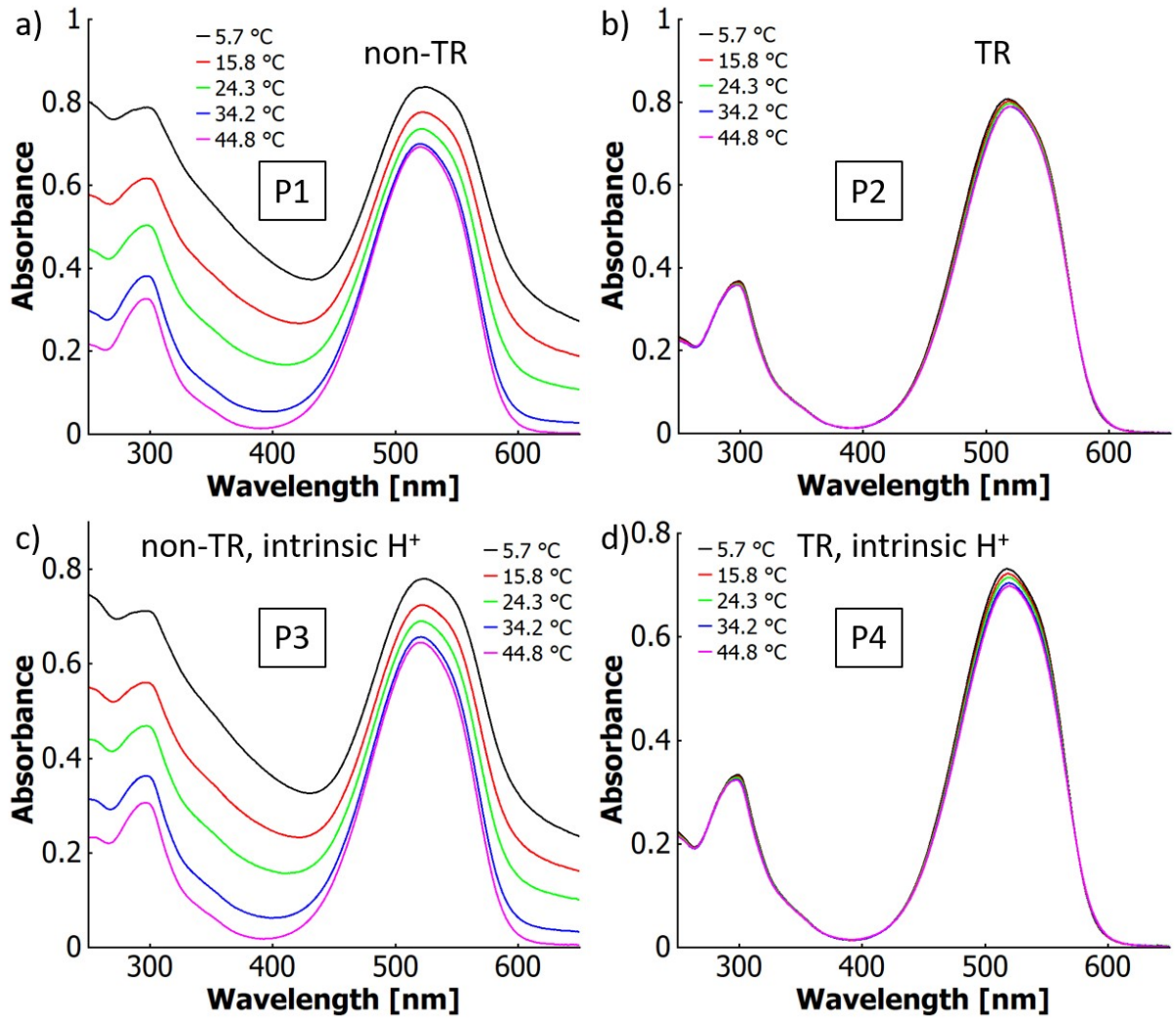


*Figure S 24: UV-vis spectra in ethanolic sulfuric acid (1 v/v%) of four dye-containing copolymers at different temperatures ("TR" = thermoresponsive, "intrinsic $H^+$" = -COOH substituents in the polymer); a) (P1) poly(HEAm-co-o-MREAm-co-BPAAm); b) (P2) poly(NiPAAm-co-HEAm-co-o-MREAm-co-BPAAm); c) (P3) poly(HEAm-co-MAA-co-o-MREAm-co-BPAAm) and d) (P4) poly(NiPAAm-co-MAA-co-o-MREAm-co-BPAAm) (all 0.1 g/L).*

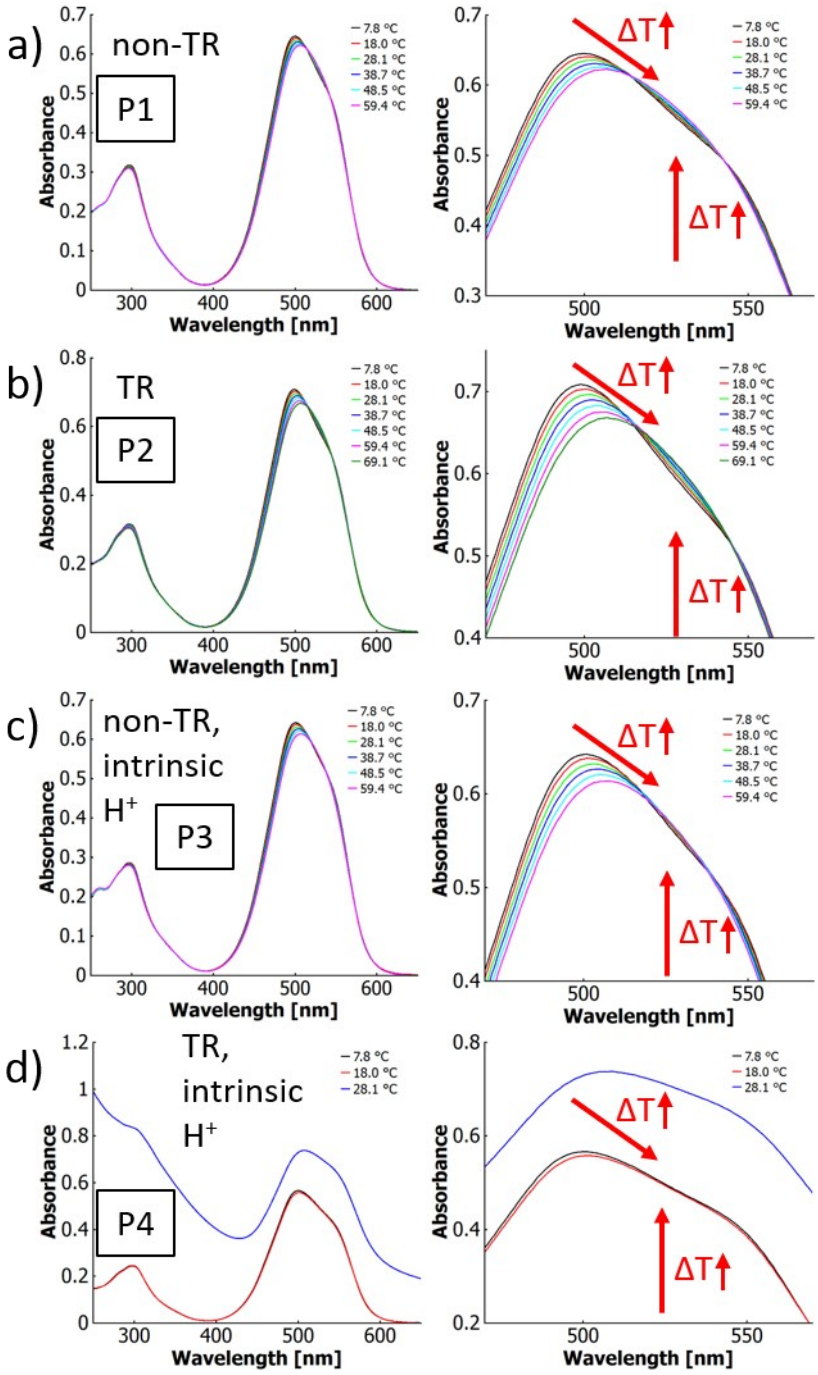


*Figure S 25: UV-vis spectra in aqueous hydrochloric acid (1 M) of four dye-containing copolymers at different temperatures ("TR" = thermoresponsive, "intrinsic $H^+$" = -COOH substituents in the polymer); a) (P1) poly(HEAm-co-o-MREAm-co-BPAAm); b) (P2) poly(NiPAAm-co-HEAm-co-o-MREAm-co-BPAAm); c) (P3) poly(HEAm-co-MAA-co-o-MREAm-co-BPAAm) and d) (P4) poly(NiPAAm-co-MAA-co-o-MREAm-co-BPAAm) (all 0.1 g/L).*

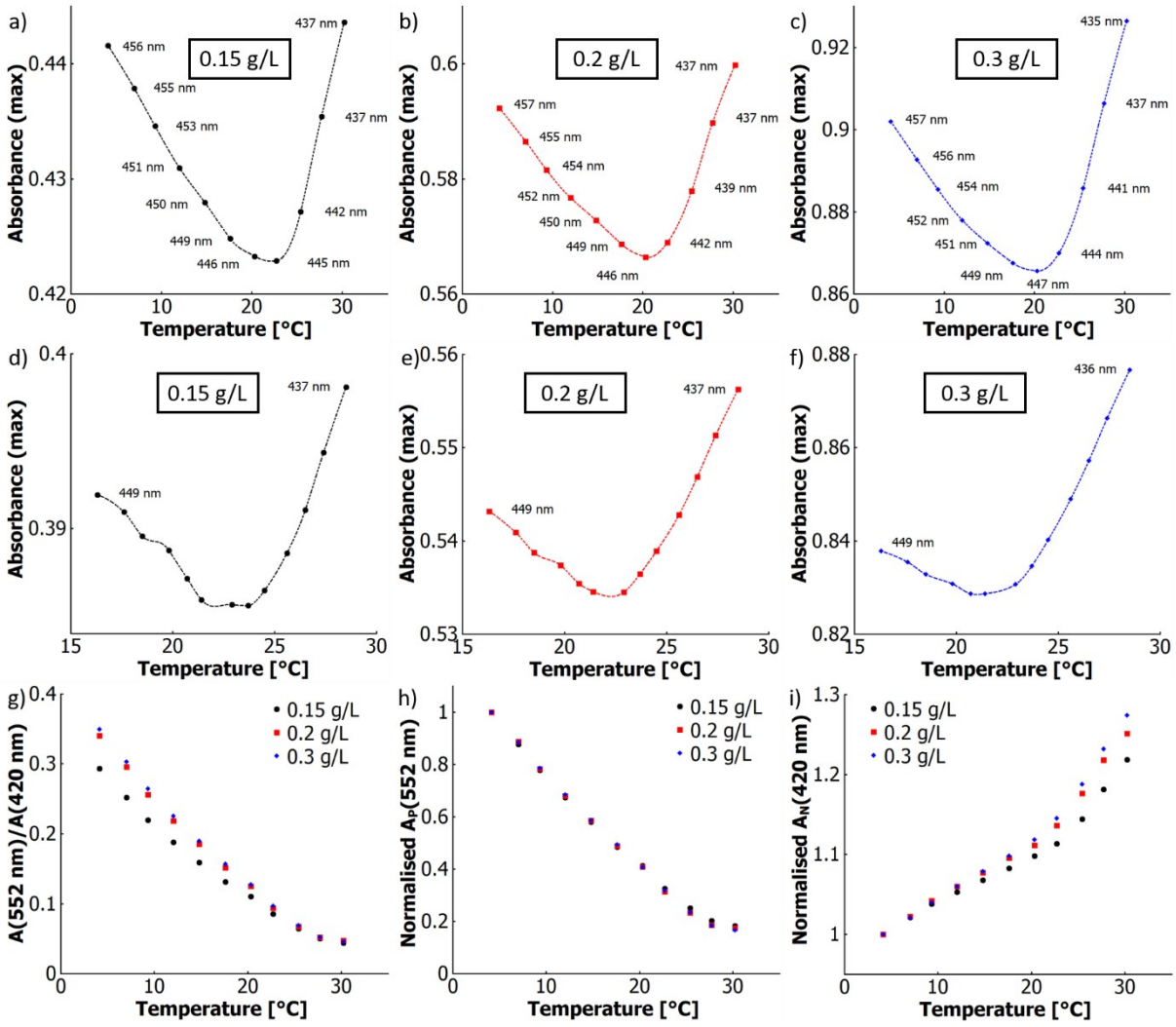


*Figure S 26: Absorbance at maximum vs temperature for the poly(NiPAAm-co-MAA-co-o-MREAm-co-BPAAm) copolymer P4 at a) and d) 0.15 g/L, b) and e) 0.2 g/L and c) and f) 0.3 g/L; g) ratio of absorbance at 552 nm and at 420 nm vs temperature, h) normalised absorbance at 552 nm vs temperature (normalised by dividing all values by the value at the lowest temperature) and i) normalised absorbance at 420 nm vs temperature (normalised by dividing all values by the value at the lowest temperature) for the same concentrations. The lines are generated by a non-rounded Akima interpolation and only serve as guide to the eye*

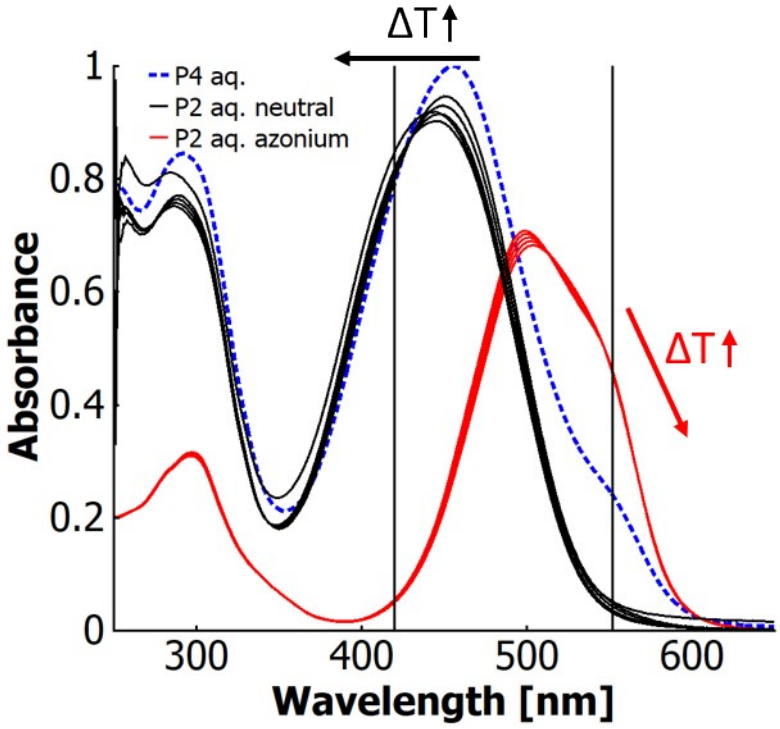


*Figure S 27: UV-vis spectra at different temperatures of the poly(NiPAAm-co-HEAm-co-o-MREAm-co-BPAAm) copolymer P2 in water (black) and in aqueous HCl (1M), as well as of the poly(NiPAAm-co-MAA-co-o-MREAm-co-BPAAm) P4 in water (blue). The wavelengths relevant and read were marked by vertical black lines.*

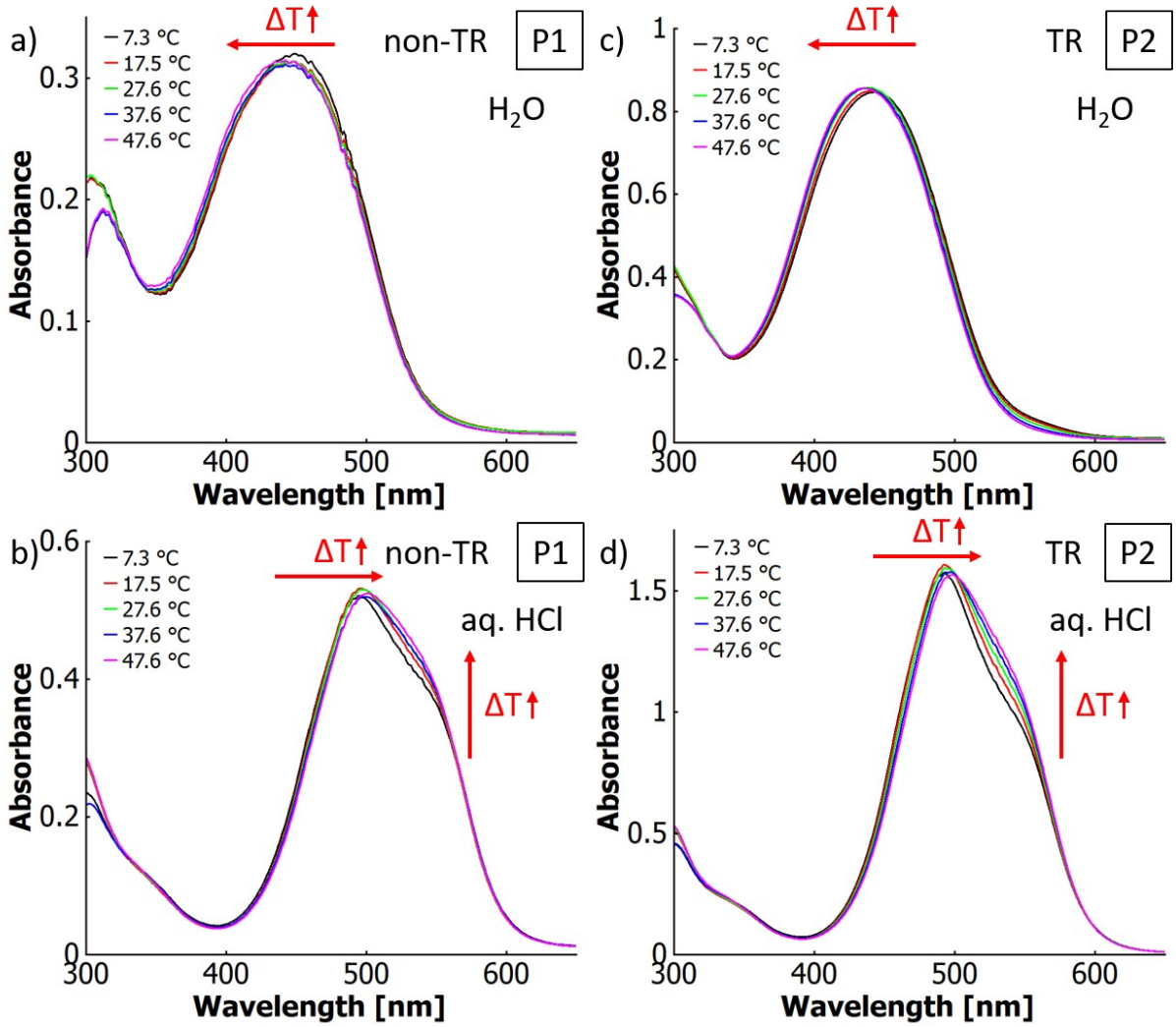


*Figure S 28: UV-vis spectra of photocrosslinked, swollen films at different temperatures of poly(HEAm-co-o-MREAm-co-BPAAm) P1 in a) water and b) aqueous HCl (1M), and of poly(NiPAAm-co-HEAm-co-o-MREAm-co-BPAAm) P2 in c) water and d) aqueous HCl (1M) ("TR" = thermoresponsive).*

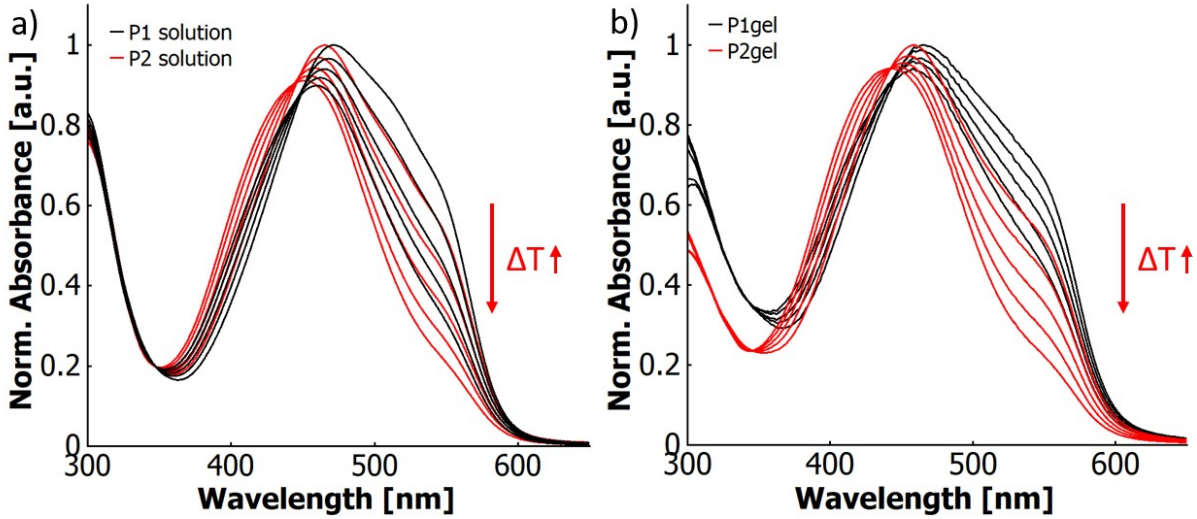


*Figure S 29: Normalised UV-vis spectra of poly(HEAm-co-MREAm-co-BPAAm) P1 (black spectra) and poly(NiPAAm-co-HEAm-co-MREAm-co-BPAAm) P2 (red spectra) at different temperatures (ca. 10-50 °C) a) dissolved in aqueous TFA (0.001 v/v%) and b) as a hydrogel film swollen in aqueous TFA (0.01 v/v%). Note the 10x higher acid concentration for the partially protonated films compared to the polymers in solution.*

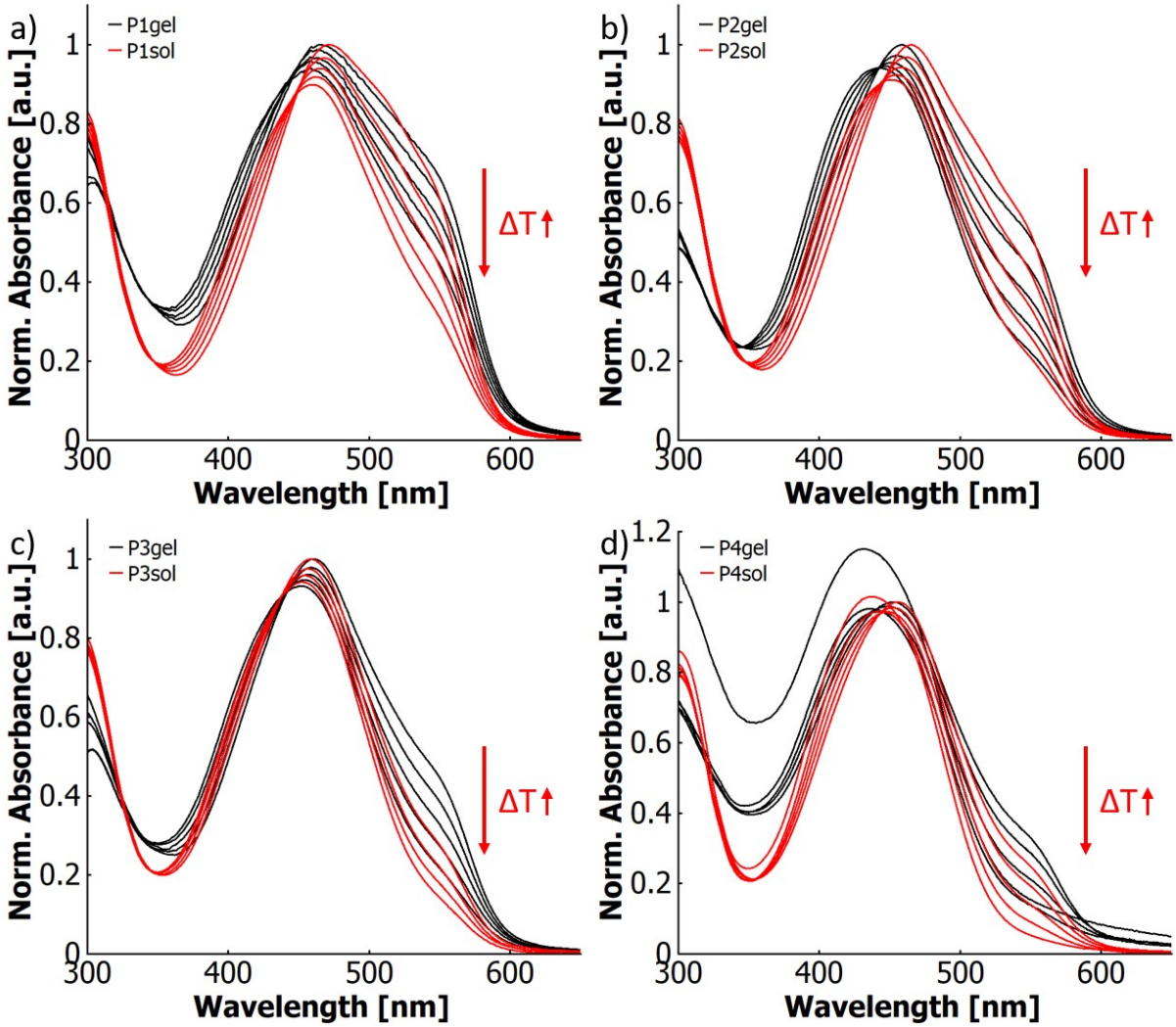


*Figure S 30: Normalised UV-vis spectra of a) poly(HEAm-co-MREAm-co-BPAAm) P1, b) poly(NiPAAm-co-HEAm-co-MREAm-co-BPAAm) P2, c) poly(HEAm-co-MAA-co-MREAm-co-BPAAm) P3 and d) poly(NiPAAm-co-MAA-co-MREAm-co-BPAAm) P4 at different temperatures (ca. 10-50 °C). The black spectra show the polymers as a hydrogel film swollen in aqueous TFA (0.01 v/v%) (P1 and P2) or water (P3 and P4), while the red spectra show the polymers dissolved in aqueous TFA (0.001 v/v%, P1 and P2) or water (P3 and P4). Note the 10x higher acid concentration for the partially protonated films compared to the polymers in solution for P1 and P2.*

*Difference and derivative spectra:*

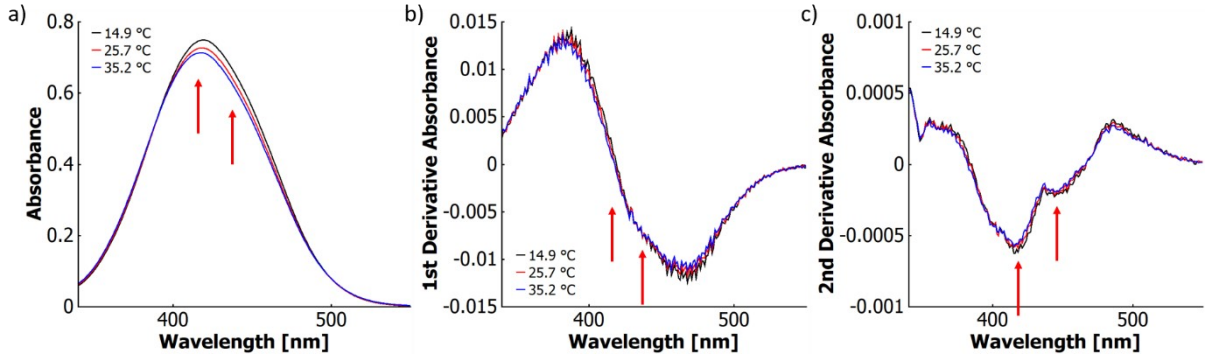


*Figure S 31: a) UV-vis spectra, b) 1st derivative of the UV-vis spectra and c) smoothed (Savitzky-Golay,[12] 25 points) 2nd derivative of the UV-vis spectra of o-MREAm (2.7*10$^{-5}$ mol/L) in ethanol at different temperatures to determine the wavelength of the vibronic sub-band maxima (marked with red arrows).*

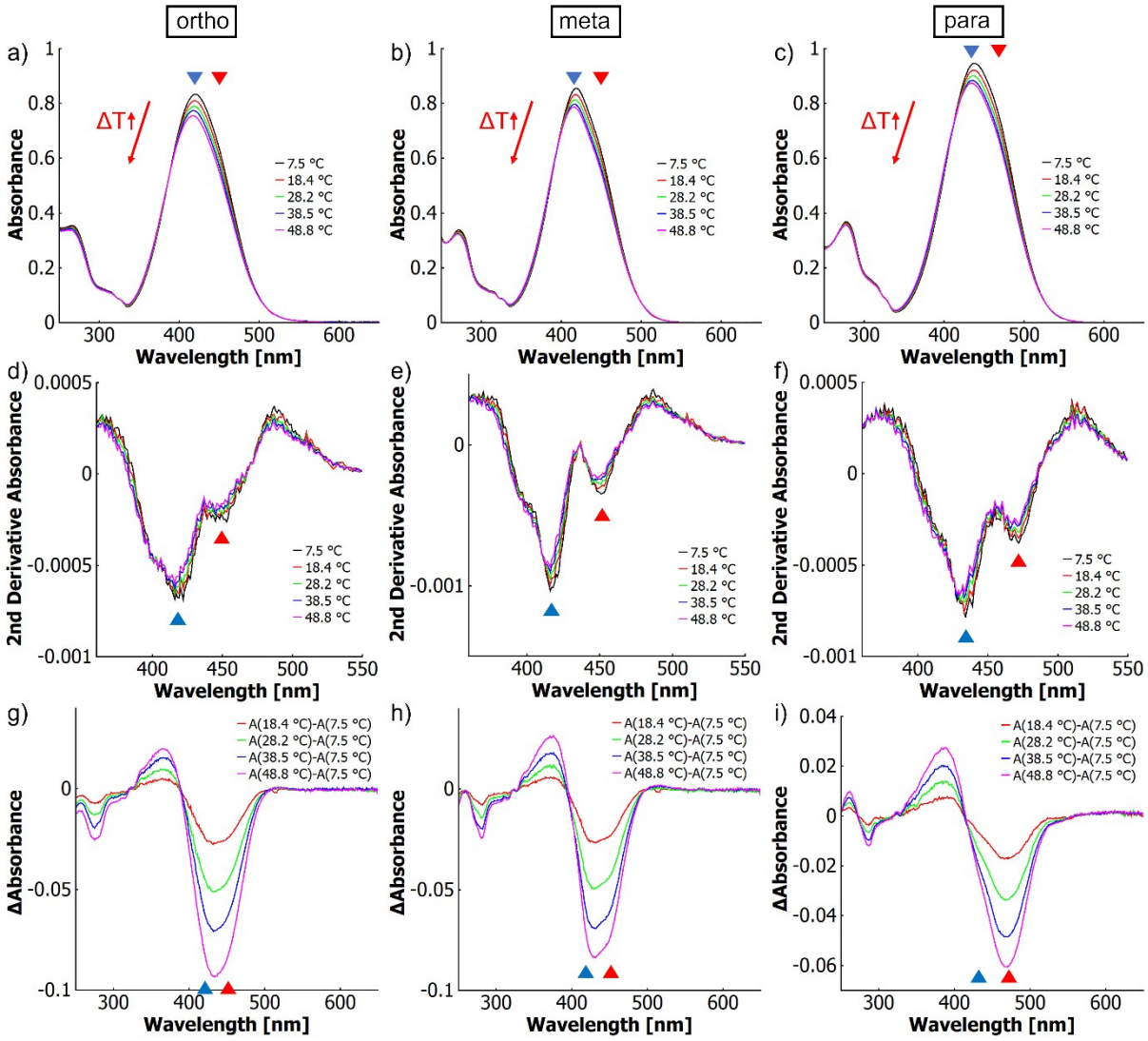


*Figure S 32: a)-c) UV-vis spectra, d)-f) derivative spectra and g)-i) difference spectra showing thermo-solvatochromism of ortho-, meta- and para-methyl red esters of N-(2-hydroxyethyl)acrylamide (2.7*10$^{-5}$ mol L$^{-1}$) at different temperatures in ethanol. Triangles mark the wavelength positions of vibronic sub-bands in the respective graphs (red: 0-0 transition; blue: 0-1 transition).*

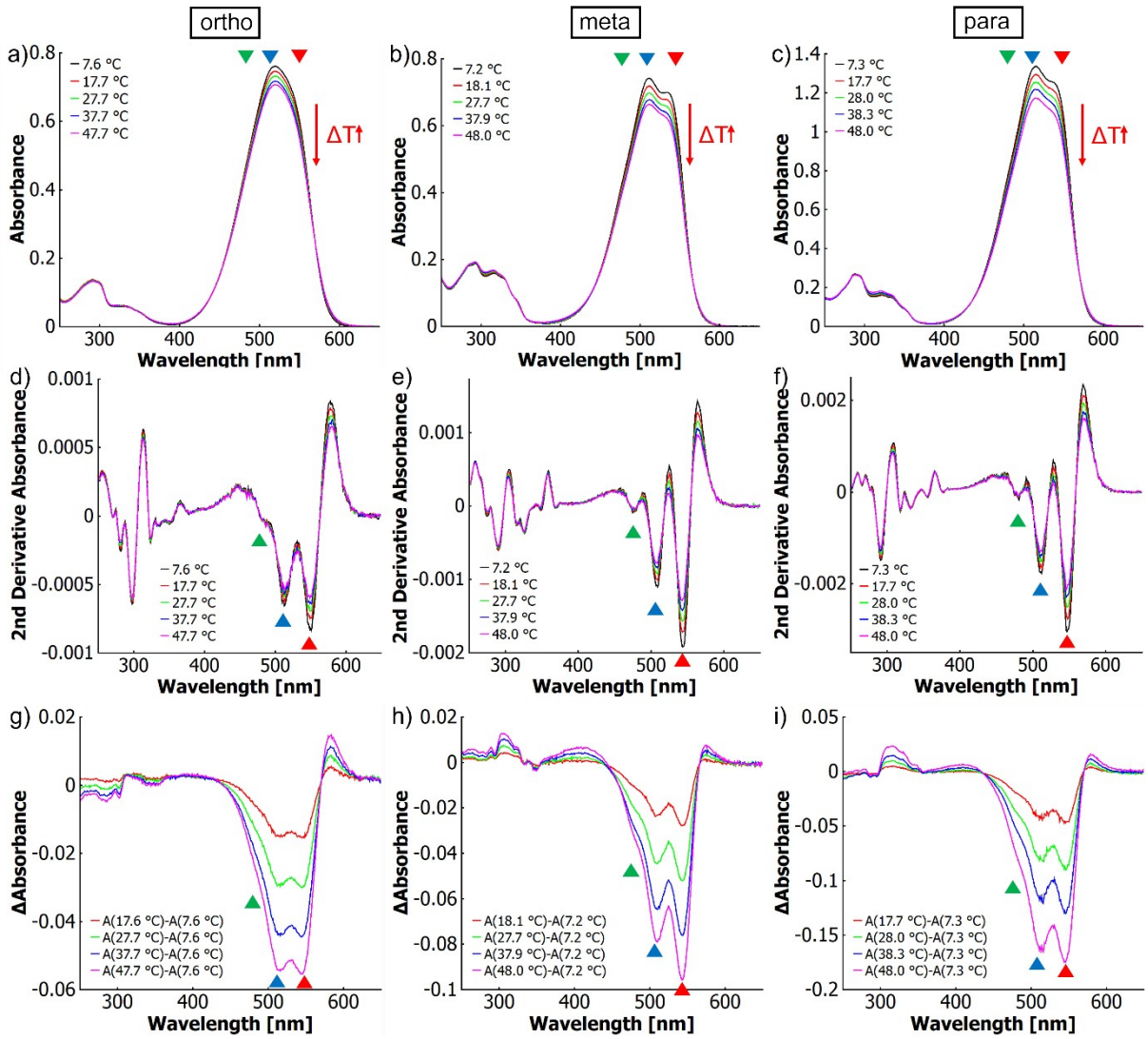


*Figure S 33: a)-c) UV-vis spectra, d)-f) derivative spectra and g)-i) difference spectra showing thermo-solvatochromism of completely protonated ortho-, meta- and para-methyl red esters of N-(2-hydroxyethyl)acrylamide ($1.4*10^{-5}$ mol $L^{-1}$) at different temperatures in ethanolic sulfuric acid (1 v/v%). Triangles mark the wavelength positions of vibronic sub-bands in the respective graphs (red: 0-0 transition; blue: 0-1 transition; green 0-2 transition).*

In the derivative spectra corresponding to the azonium ion in ethanolic solution (cf. ESI Figure S 33 d-f), three sub-bands can be identified for all isomers, with the $0\text{-}2_{azonium}$ sub-band being more pronounced for the meta- and para-isomers. The energy differences between the $0\text{-}0_{azonium}$ and the $0\text{-}1_{azonium}$ sub-band is in the energy range of the N-N stretching mode of the parent compound MR.[13,14] The energy difference between the $0\text{-}1_{azonium}$ and the $0\text{-}2_{azonium}$ sub-band is slightly lower, reflecting the anharmonicity of electronic potentials (cf. Table 3).

The vibronic fine structure is also visible in the difference spectra (cf. ESI Figure S 33 g-i), yet with considerable distinctions between the constitutional isomers. While the negative peaks of the ortho-isomer possess equal intensity at the positions of the $0\text{-}0_{azonium}$ and $0\text{-}1_{azonium}$ sub-bands, the negative peak corresponding to the $0\text{-}0_{azonium}$

sub-band is substantially stronger for the meta- and para-isomers. This leads to a significant temperature-induced variation of the band shape in the absorption spectra for the meta- and para-isomers, while the effect is of minor relevance for the ortho-isomer. Positive peaks can be observed at longer wavelengths above the 0-$0_{azonium}$ sub-band as well as around the absorption band of the ammonium ion (~310 nm). Apparently, the tautomeric equilibrium shifts slightly from the azonium ion to the ammonium form with rising temperature. Concomittantly to a reduced dye volume fraction due to the thermal expansion of the solvent, this tautomerism contributes to the observed decrease of the azonium ion absorbance (cf. ESI Figure S 33 a-c).

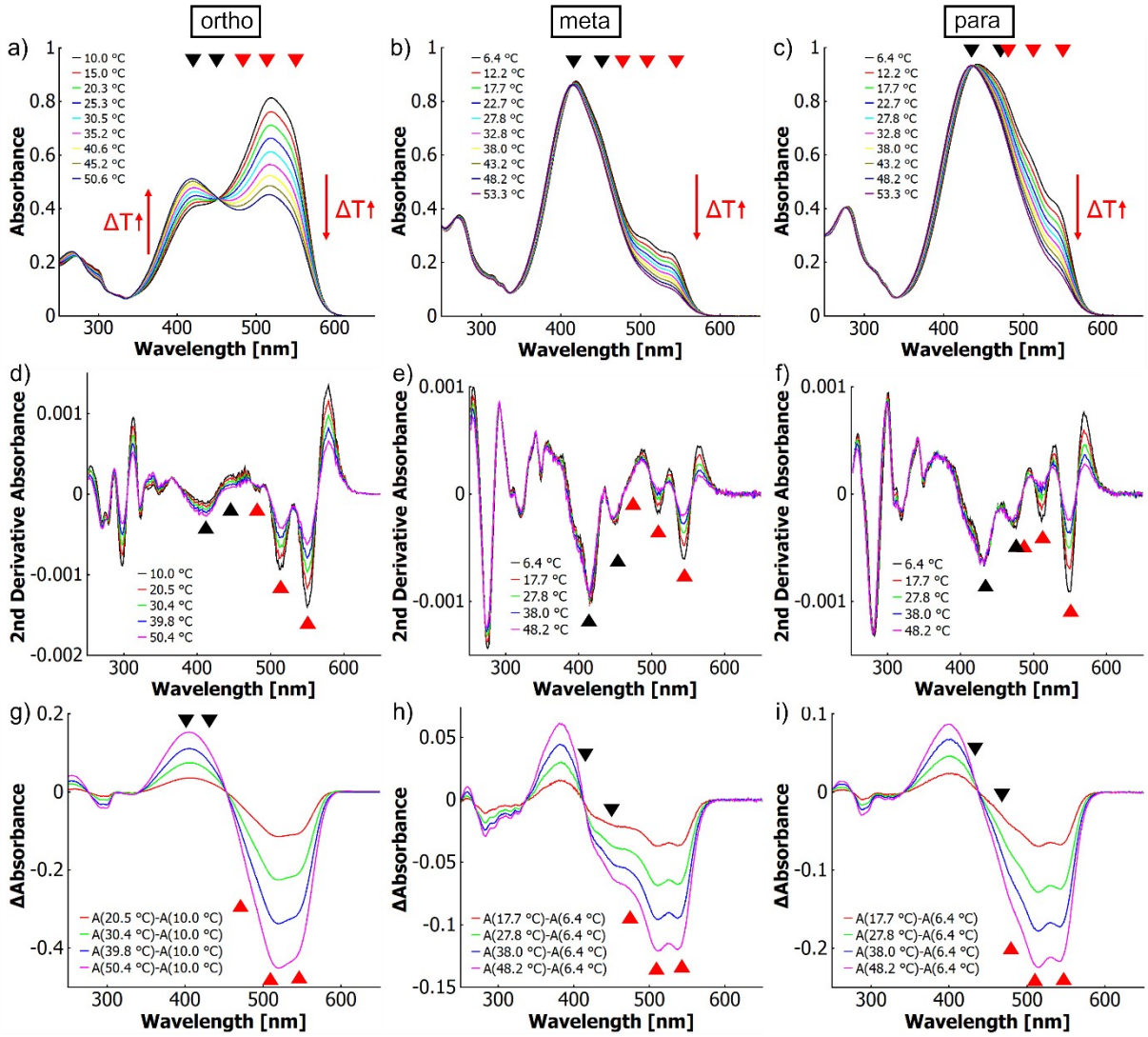


*Figure S 34: a)-c) UV-vis spectra, d)-f) derivative spectra and g)-i) difference spectra showing thermo-halochromism of ortho-, meta- and para-methyl red esters of N-(2-hydroxyethyl)acrylamide ($2.7*10^{-5}$ mol $L^{-1}$) at different temperatures in ethanolic trifluoroacetic acid (1 v/v%). Triangles mark the wavelength positions of vibronic sub-bands in the respective graphs (red: vibronic transitions of the azonium ion; black: vibronic transitions of the neutral species).*

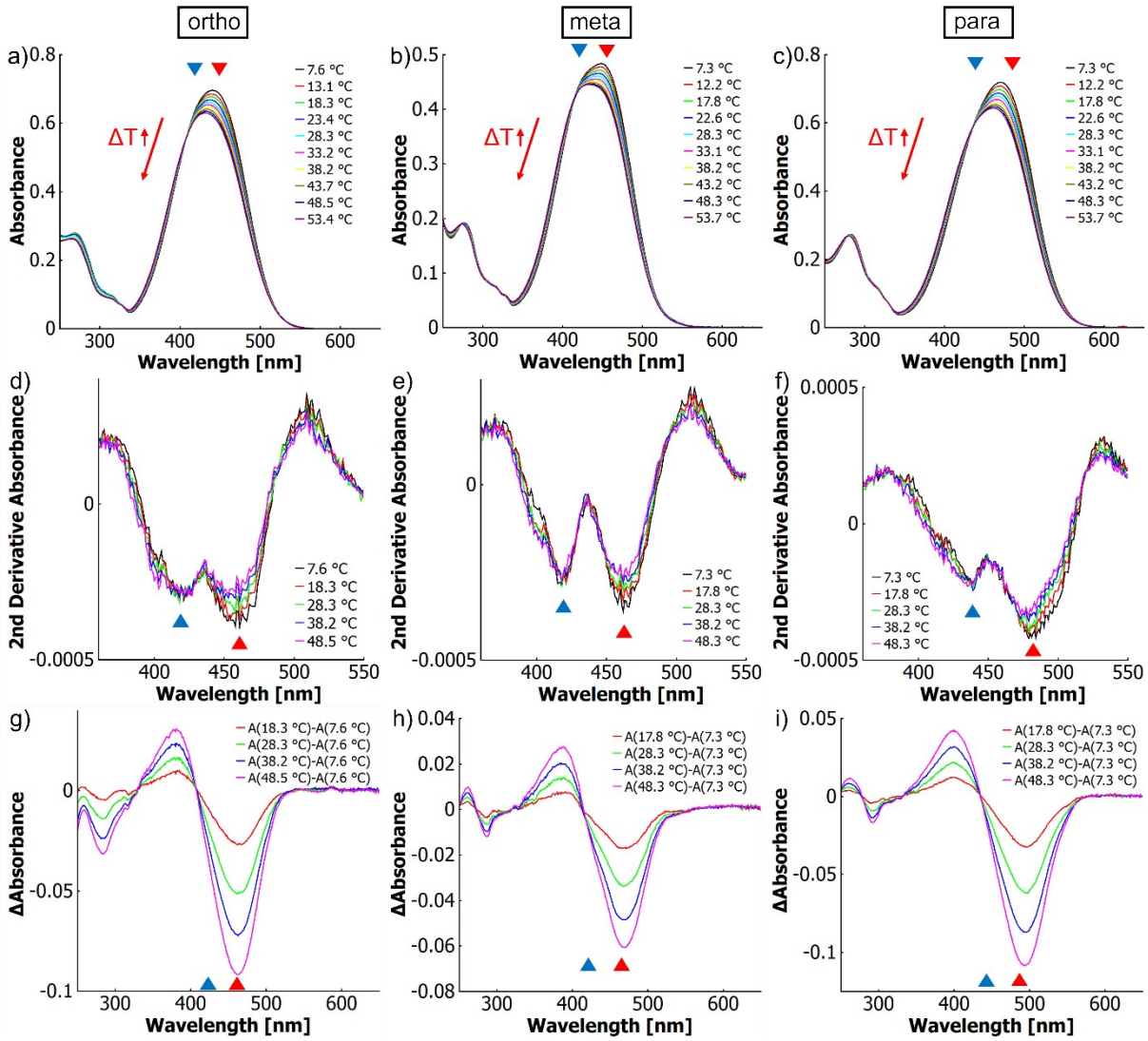


*Figure S 35: a)-c) UV-vis spectra, d)-f) derivative spectra and g)-i) difference spectra showing thermo-solvatochromism of ortho-, meta- and para-methyl red esters of N-(2-hydroxyethyl)acrylamide (2.7*10$^{-5}$ mol L$^{-1}$) at different temperatures in $H_2O$:EtOH ($X_{EtOH}$=0.31). Triangles mark the wavelength positions of vibronic sub-bands in the respective graphs (red: 0-0 transition; blue: 0-2 transition).*

As performed for the dyes in neat ethanol, derivative and difference spectroscopy were applied to the UV-vis spectra for the binary solvent mixture. As observed with vibronic thermochromism in neat ethanol, a variation of temperature also results in a change of the vibronic structure in the UV-vis spectra for thermo-solvatochromism occurring in the binary solvent mixture. However, the application of both techniques reveals intricate differences between the mechanisms of vibronic thermochromism and thermo-solvatochromism. For thermo-solvatochromism, the sub-bands in the derivative spectra are broadened and their energy difference is by about 450-500 cm$^{-1}$ higher than in the case of vibronic thermochromism (cf. ESI Figure S 32 d-f, Figure S 35 d-f, Table 2). The intensity ratio of the sub-bands is inverse for the two mechanisms. In thermo-solvatochromism, the lower energy sub-band is stronger than the high

energy sub-band, while in vibronic thermochromism the lower energy sub-band is weaker. The larger energy differences of 2100-2300 $cm^{-1}$ between the sub-bands in the binary solvent mixture do not match any specific vibration of the MR dye that would be responsible for the vibronic transition.[1,2] The mismatch between these energy differences and the vibrational modes found in Raman spectra suggests that either a combination of vibrations leads to the observed vibronic transition or that the 0-1 transition is forbidden and only the 0-2 transition is allowed. Assuming a considerable influence of the binary solvent mixture on the energy of the vibrational modes, as follows, the 0-2 transition would roughly agree with the N=N stretching mode in an anharmonic oscillator. In the parent compound MR, the 0-1 stretching mode equals to about 1400 $cm^{-1}$. This energy would be lower in the 1-2 mode, totaling to around 2600-2700 $cm^{-1}$ for the 0-2 transition, which approaches the range of the observed energy difference in derivative spectroscopy. However, as stated above, vibrational mode mixing[15,16] would be another likely scenario. In the binary solvent mixture, temperature has an unequal influence on the sub-band structure in the derivative spectra. Consequently, for all positional isomers, the higher energy sub-bands do not change in intensity, while the lower energy sub-bands decrease noticeably as signified by an increase in the second derivative. This is in contrast to the behaviour in neat ethanol, where both bands change equally upon temperature increase (cf. ESI Figure S 32 d-f, Figure S 35 d-f).

At the same time, there is only one symmetric negative band without any vibronic structure in the difference spectra for each of the configurational isomers (cf. ESI Figure S 35 g-i). The higher intensity of the 0-0 transition compared to the 0-x (x=1, 2) transition in the derivative spectra and the distinct decrease in only one sub-band are considered here to be features of thermo-solvatochromism. In contrast, the lower intensity of the 0-0 transition compared to the 0-1 transition and a vibronic component in the negative bands in the difference spectra can be considered a feature of vibronic thermochromism.

The azonium ions of all three configurational isomers in binary solvent mixtures of water and ethanol exhibit a vibronic structure in UV-vis, derivative, and difference spectra (cf. ESI Figure S 36). In the derivative spectra, there are three vibronic sub-bands with energy differences between them that correspond to N-N valence modes (assuming a single bond between the nitrogens in the quinoid structure of the azonium form).[1,2] The negative bands in the difference spectra show peaks at the positions of

the vibronic sub-bands as identified by derivative spectroscopy. The absorbance change upon temperature variation is more intense at the 0-0 sub-band than at the higher energy sub-bands in all isomers. The corresponding 0-1 sub-band changes are less intense to varying degrees in the three isomers. While the meta- and para-isomers exhibit similar changes for 0-0 and 0-1, the ortho-isomer shows a distinct difference between the changes of the 0-0 and the 0-1 sub-bands (compare red and blue triangles in ESI Figure S 36 g-i). Consequently, the vibronic structure is in all cases reduced at higher temperatures as the higher energy sub-bands are more populated. A slight increase in absorbance can be observed at the wavelength for the ammonium ion, meaning that the tautomeric equilibrium shifts slightly towards the ammonium ion at higher temperatures. In essence, the obtained results surprisingly reveal that the thermochromic behaviour of the azonium ions are quite similar both in the binary solvent mixture and in neat ethanol (cf. ESI Figure S 33, Figure S 36).

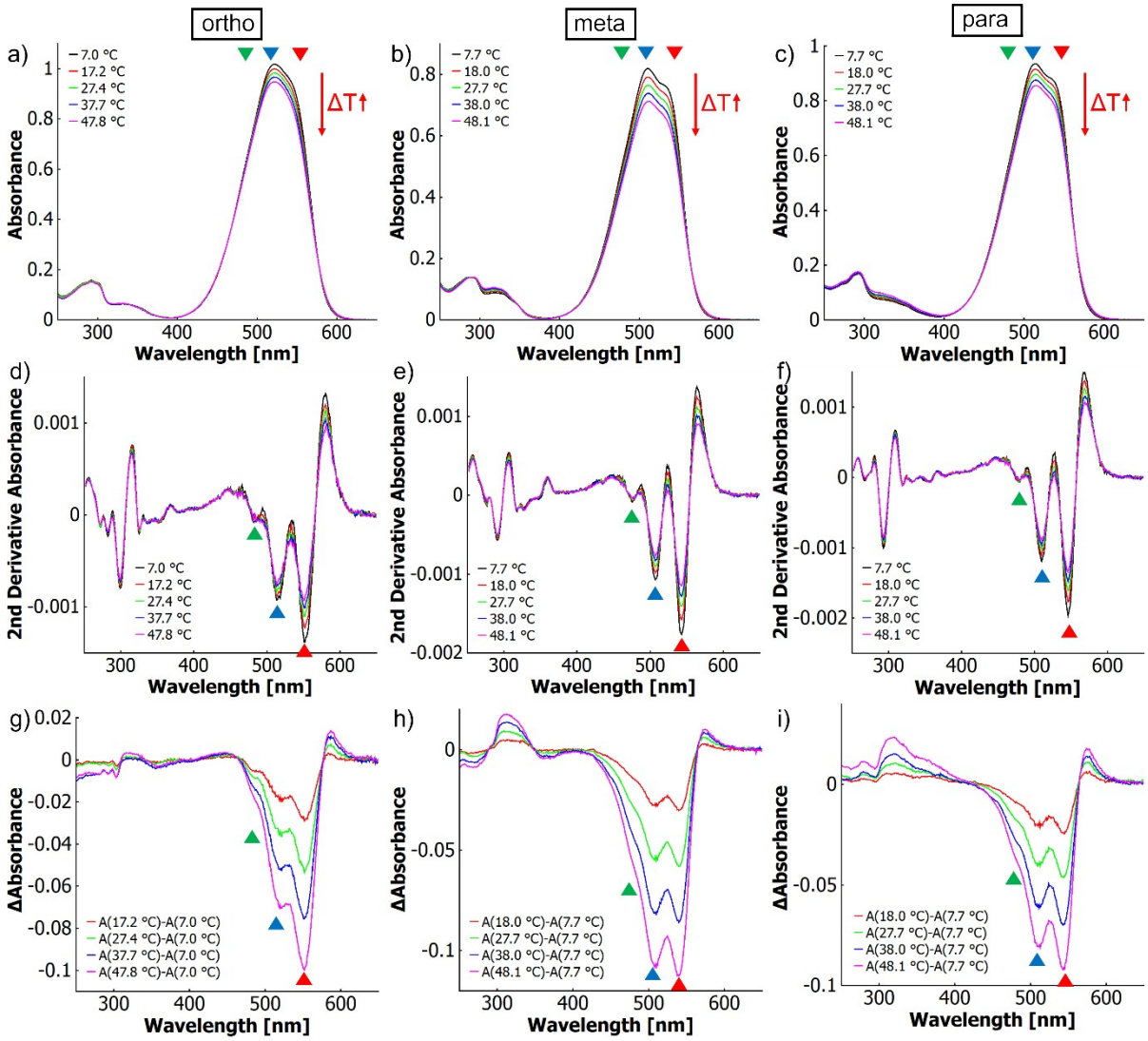

*Figure S 36: a)-c) UV-vis spectra, d)-f) derivative spectra and g)-i) difference spectra showing thermo-solvatochromism of completely protonated ortho-, meta- and para-methyl red esters of N-(2-hydroxyethyl)acrylamide ($1.4*10^{-5}$ mol $L^{-1}$) at different temperatures in $H_2O$:EtOH ($X_{EtOH}$=0.31) with hydrochloric acid (5 M). Triangles mark the wavelength positions of vibronic sub-bands in the respective graphs (red: 0-0 transition; blue: 0-1 transition; green 0-2 transition).*

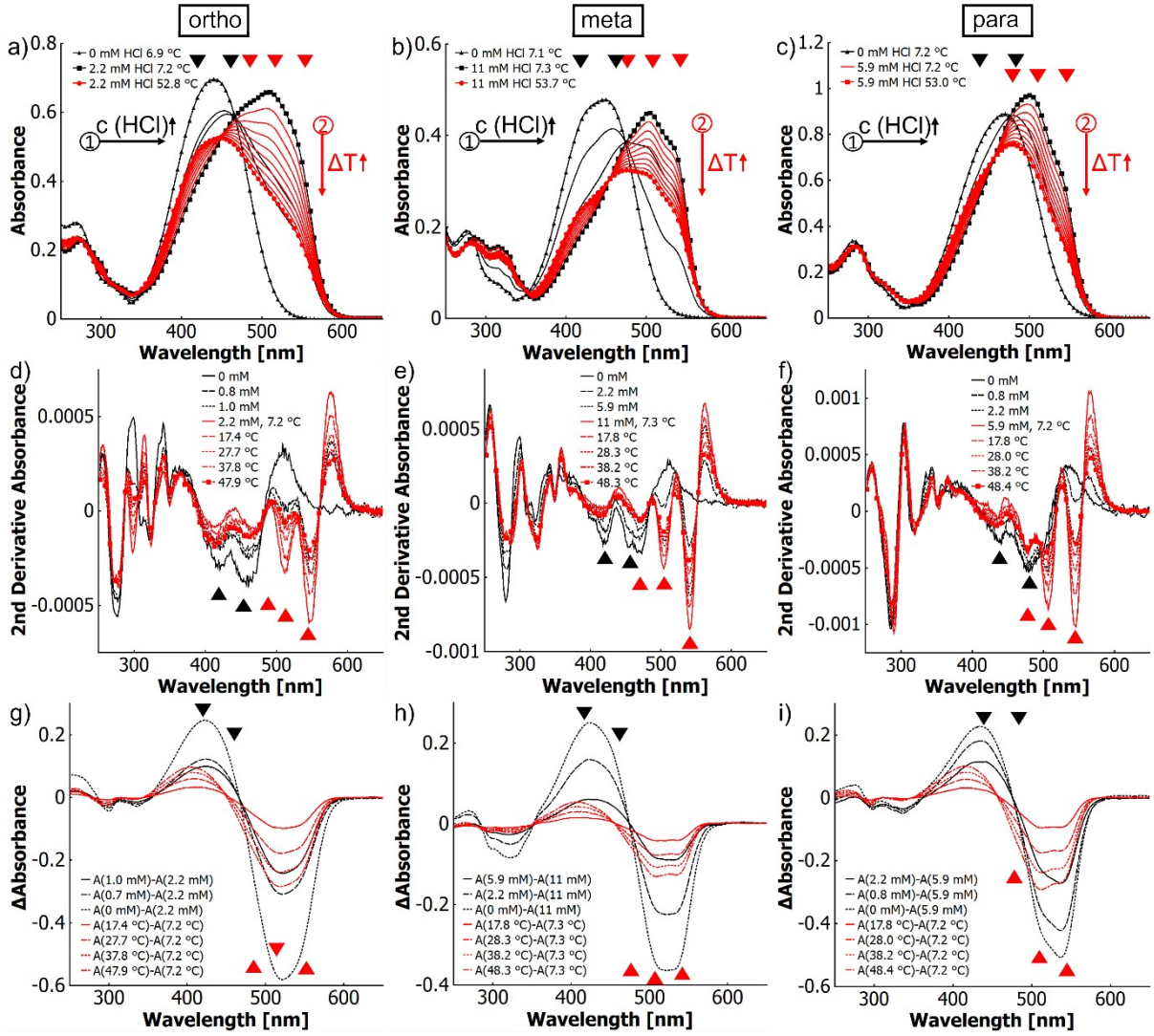


*Figure S 37: a)-c) UV-vis spectra, d)-f) derivative spectra and g)-i) difference spectra showing thermo-solvato-halochromism of ortho-, meta- and para-methyl red esters of N-(2-hydroxyethyl)acrylamide ($2.7*10^{-5}$ mol $L^{-1}$) in $H_2O$:EtOH ($X_{EtOH}$=0.31) after titration (black arrow 1) with hydrochloric acid at ~6-7 °C to ~50% protonation and at different temperatures (red arrow 2). The black graphs represent different concentrations of hydrochloric acid (provided as values in brackets in the legends) and the red graphs changes in temperature. Triangles mark the wavelength positions of vibronic sub-bands in the respective graphs (red: vibronic transitions of the azonium ion; black: vibronic transitions of the neutral species).*

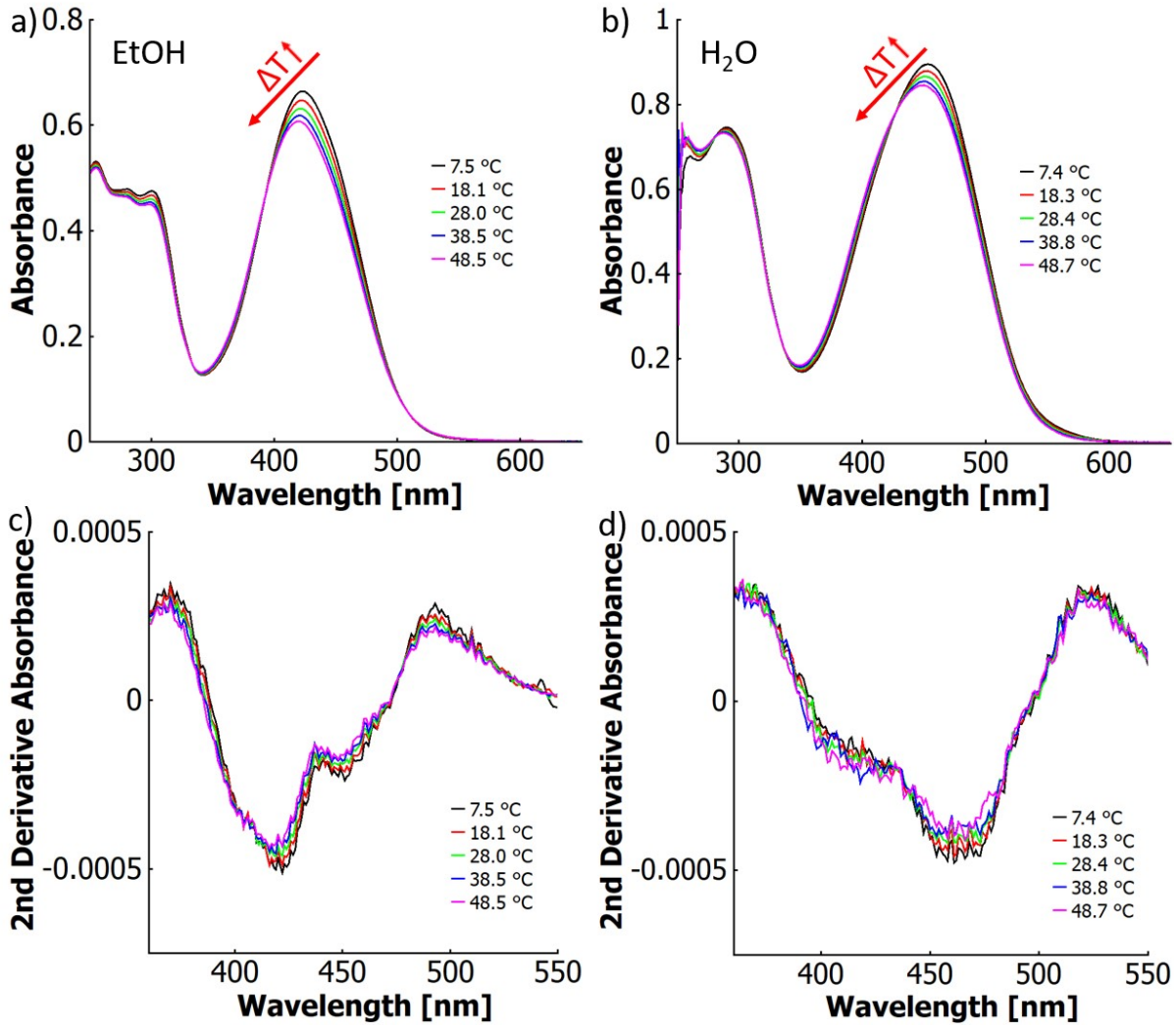


*Figure S 38: UV-vis spectra of a poly(HEAm-co-o-MREAm-co-BPAAm) copolymer (P1) a) 0.02 w% in ethanol and b) 0.03 w% in water, as well as their second derivatives in c) ethanol and d) water at different temperatures.*

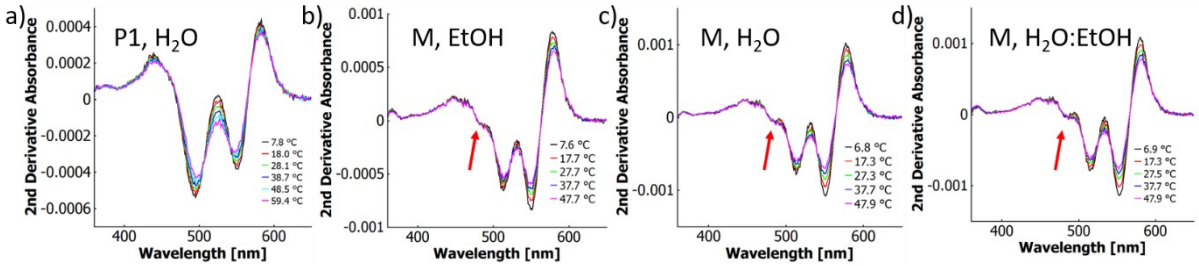


*Figure S 39: Smoothed (Savitzky-Golay, 25 points) 2nd derivative of the UV-vis spectra of a) the completely protonated copolymer (P1) poly(HEAm-co-o-MREAm-co-BPAAm) in aqueous HCl (1 M), and of the completely protonated dye monomer M o-MREAm ($1.4*10^{-5}$ mol/L) in b) ethanolic sulfuric acid (1 v/v%), c) aqueous HCl (5 M) and d) in $H_2O$:EtOH ($X_{EtOH}$=0.31) with 5M HCl. Red arrows indicate a third vibronic sub-band for the monomer.*

*Van't Hoff analysis graphs:*

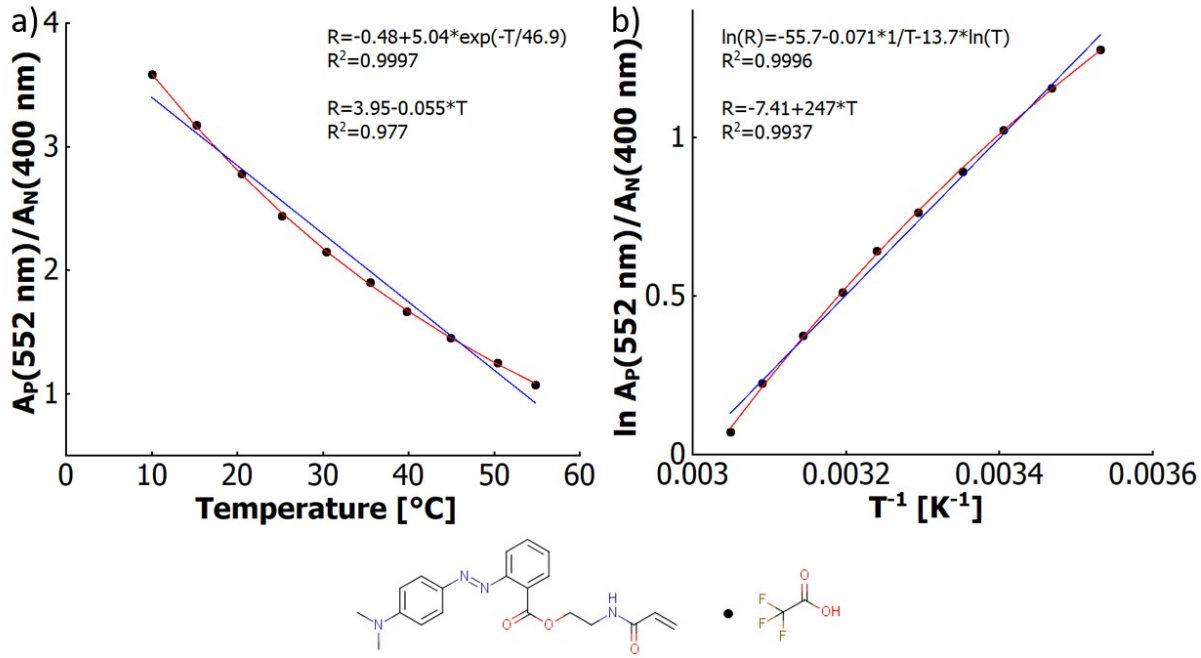


*Figure S 40: a) Ratio of the absorbance of the protonated species (552 nm) and the neutral species (400 nm) (R) vs temperature, analysed with a linear fit in comparison to an exponential decay fit and b) natural logarithm of R vs the inverse absolute temperature, analysed with a linear fit (blue) in comparison to a ln(R)=a-b*1/T+c*ln(T) fit (red) for a solution of ortho-methyl red ethyl acrylamide in EtOH ($2.7*10^{-5}$ mol/L) with trifluoroacetic acid (1v/v%).*

The non-linearity of the decrease in the ratio of absorbances of the protonated and neutral species (R) with temperature, as well as the non-linearity of the van't Hoff plot are shown in ESI Figure S 40. Linear fits and non-linear fits (exponential decay in the case of R and ln(R)=a-b*1/T+c*ln(T) for the van't Hoff plot) are both applied. In both plots, the non-linear fit has a higher coefficient of determination than the linear fit. While the $R^2$ is high in the linear fit as well, this seems to be a statistical error, as the data points deviate similarly from the fit on both of its sides. This has also been pointed out in the literature for different systems.[17,18]

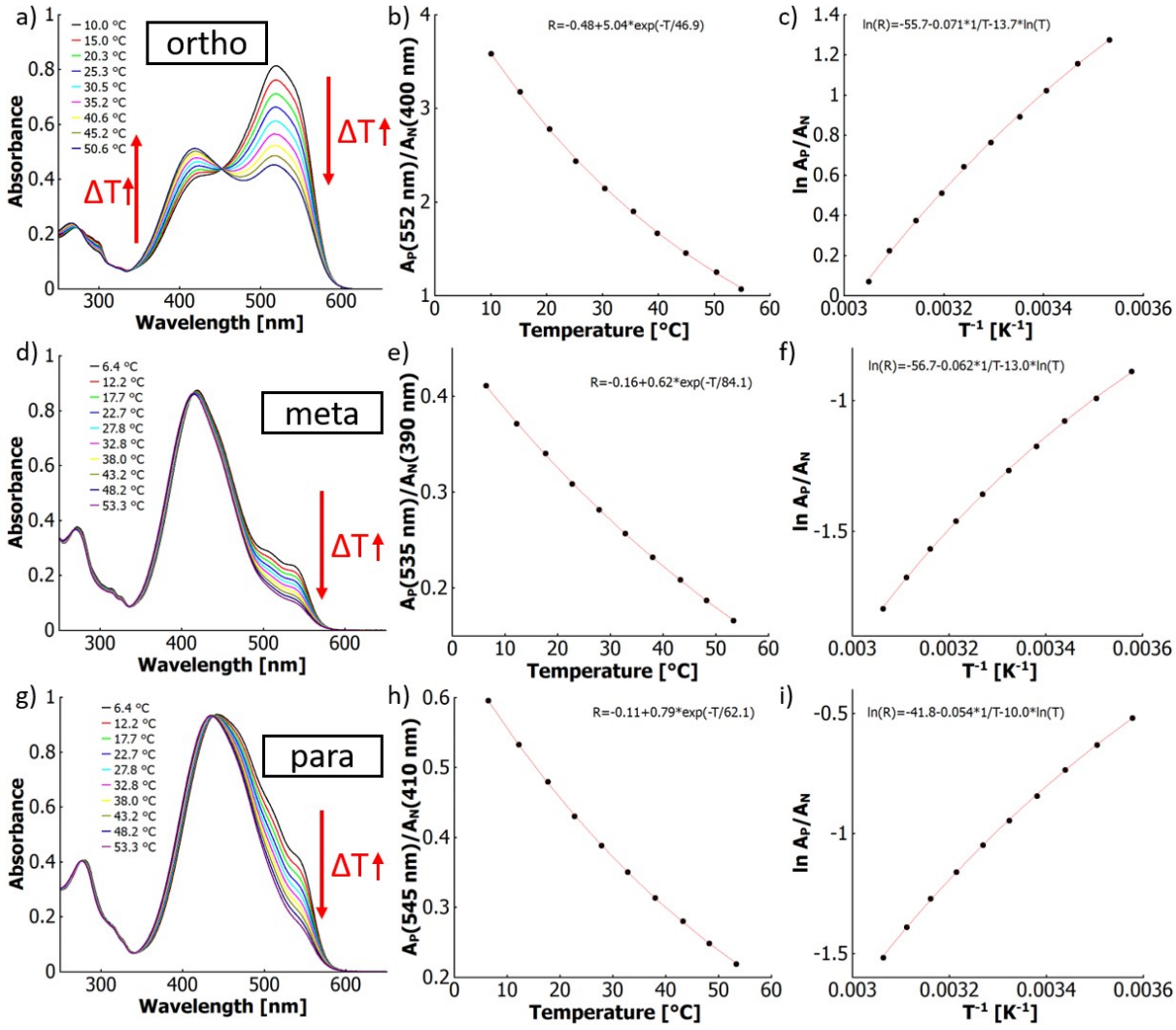


*Figure S 41: UV-vis spectra demonstrating thermo-halochromism of a) o-MREAm, d) m-MREAm and g) p-MREAm (all 2.7*10$^{-5}$ mol/L) in ethanolic trifluoroacetic acid (1 v/v%); ratio of the absorbance of the protonated species and the neutral species ("R" in the equation, wavelengths marked in the axis description) vs temperature, fitted with a first order exponential decay function for b) o-MREAm, e) m-MREAm and h) p-MREAm; natural logarithm of the ratio of the absorbance of the protonated species and the neutral species vs the inverse of the absolute temperature, fitted with a function ln(R)=a-b*1/T+c*ln(T) for c) o-MREAm, f) m-MREAm and i) p-MREAm.*

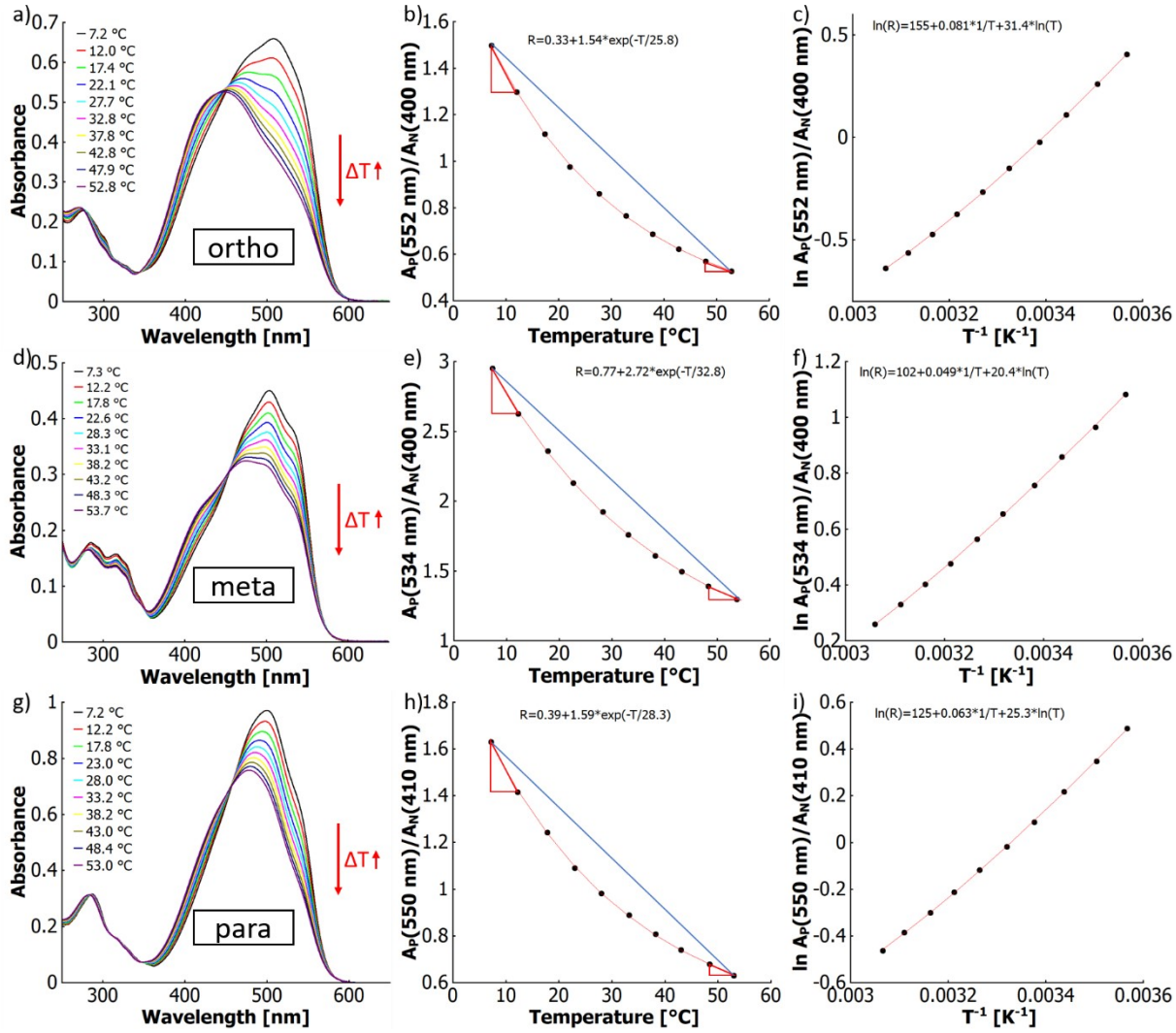


*Figure S 42: UV-vis spectra demonstrating thermo-halochromism of a) o-MREAm, d) m-MREAm and g) p-MREAm (all 2.7*10$^{-5}$ mol/L) in $H_2O$:EtOH ($X_{EtOH}$=0.31) with added hydrochloric acid: a) 2.2 mM, d) 11 mM and g) 5.9 mM; Ratio of the absorbance of the protonated species and the neutral species ("R" in the equation, wavelengths marked in the axis description) vs temperature, fitted with a first order exponential decay function for b) o-MREAm, e) m-MREAm and h) p-MREAm. The blue line along with the red slope triangles serve as a reference to display the non-linearity of the graphs; Natural logarithm of the ratio of the absorbance of the protonated species and the neutral species vs the inverse of the absolute temperature, fitted with a function ln(R)=a-b*1/T+c*ln(T) for c) o-MREAm, f) m-MREAm and i) p-MREAm.*

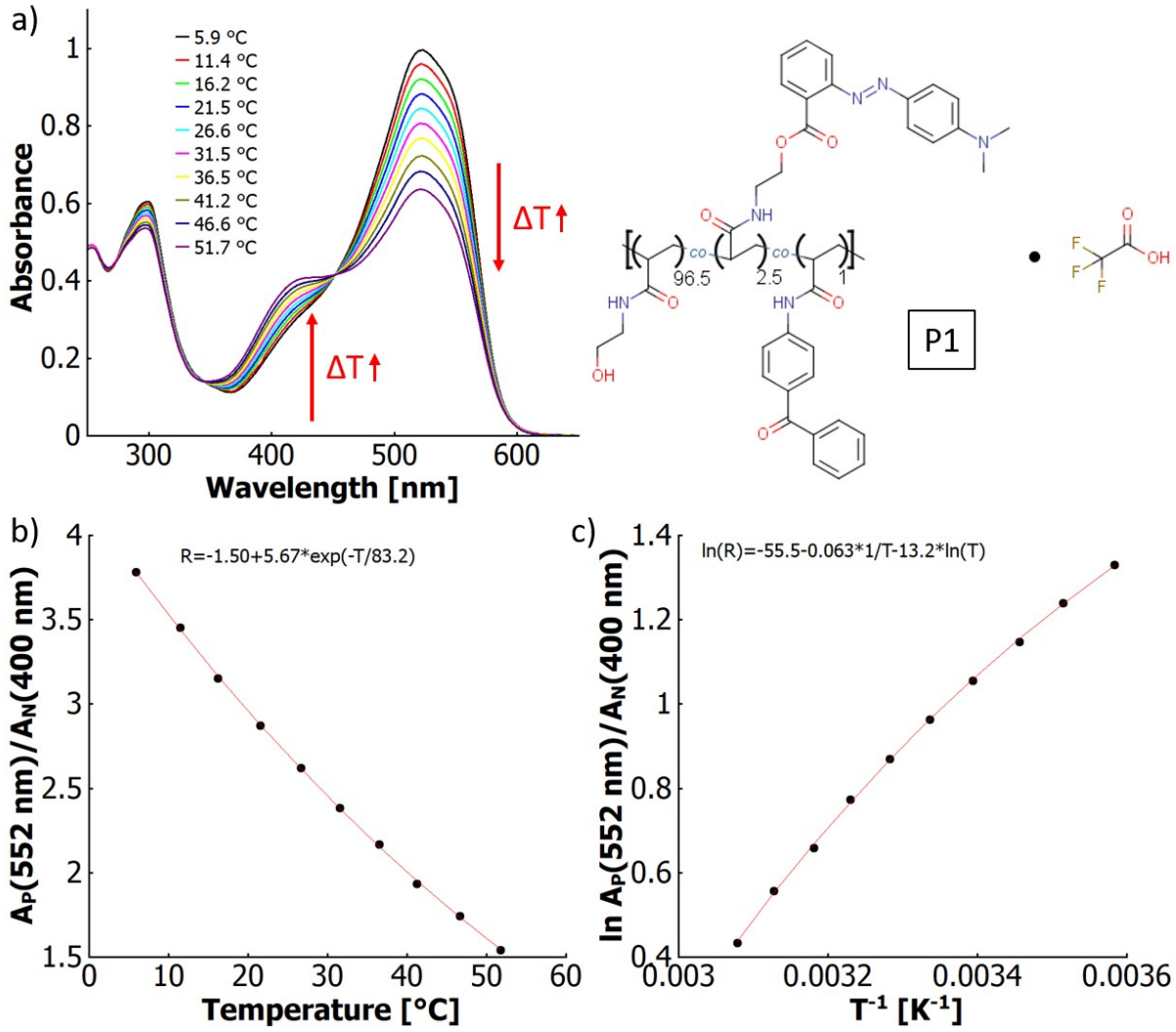


*Figure S 43: a) UV-vis spectra of a poly(HEAm-co-o-MREAm-co-BPAAm) copolymer (P1) 0.02 w% in ethanolic trifluoroacetic acid (1 v/v%) at different temperatures with structure of the copolymer, direction of shifts in absorbance upon heating marked with red arrows; b) absorbance ratio of the protonated (552 nm) and the neutral species (400 nm) vs temperature, fitted with an exponential decay function; c) van't Hoff plot of the logarithmic absorbance ratio vs the inverse temperature, fitted with a function ln(R)=a-b*1/T+c*ln(T).*

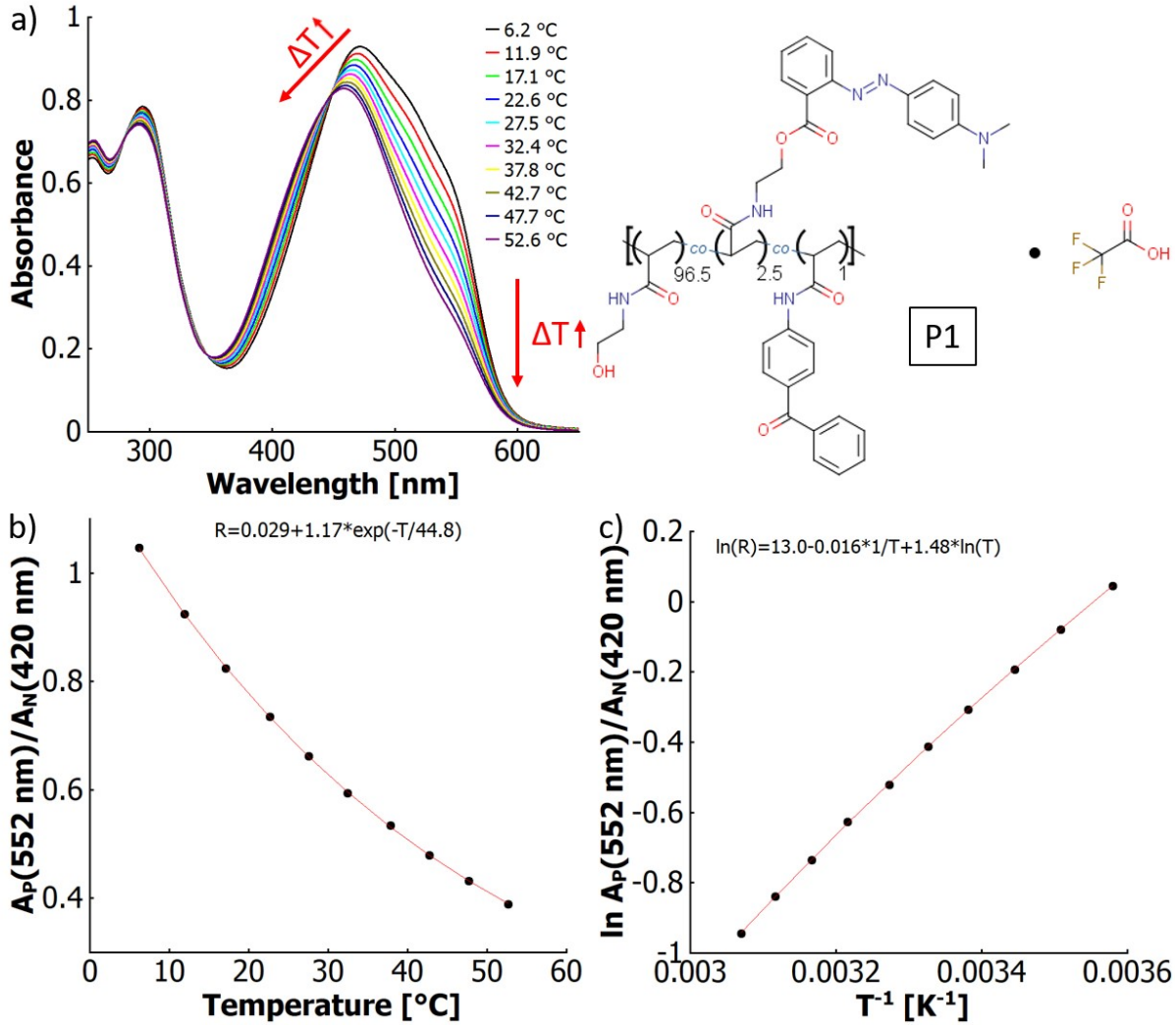


*Figure S 44: a) UV-vis spectra of a poly(HEAm-co-o-MREAm-co-BPAAm) copolymer (P1) 0.03 w% in aqueous trifluoroacetic acid (0.001 v/v%) at different temperatures with structure of the copolymer, direction of shifts in absorbance upon heating marked with red arrows; b) absorbance ratio of the protonated (552 nm) and the neutral species (420 nm) vs temperature, fitted with an exponential decay function; c) van't Hoff plot of the logarithmic absorbance ratio vs the inverse temperature, fitted with a function ln(R)=a-b*1/T+c*ln(T).*

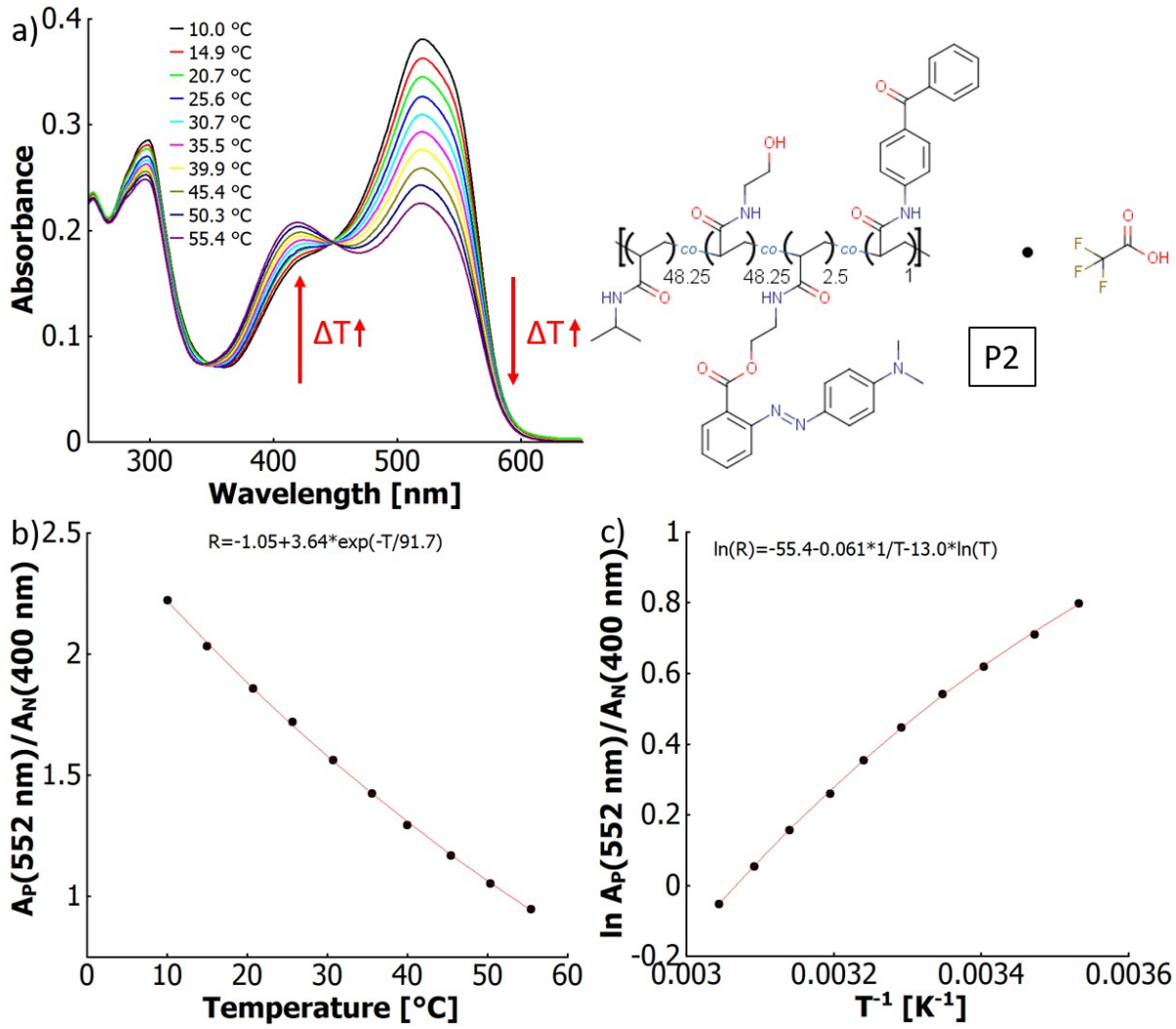


*Figure S 45: a) UV-vis spectra of a poly(NiPAAm-co-HEAm-co-o-MREAm-co-BPAAm) copolymer (P2) 0.02 w% in ethanolic trifluoroacetic acid (1 v/v%) at different temperatures with structure of the copolymer, direction of shifts in absorbance upon heating marked with red arrows; b) absorbance ratio of the protonated (552 nm) and the neutral species (400 nm) vs temperature, fitted with an exponential decay function; c) van't Hoff plot of the logarithmic absorbance ratio vs the inverse temperature, fitted with a function ln(R)=a-b*1/T+c*ln(T).*

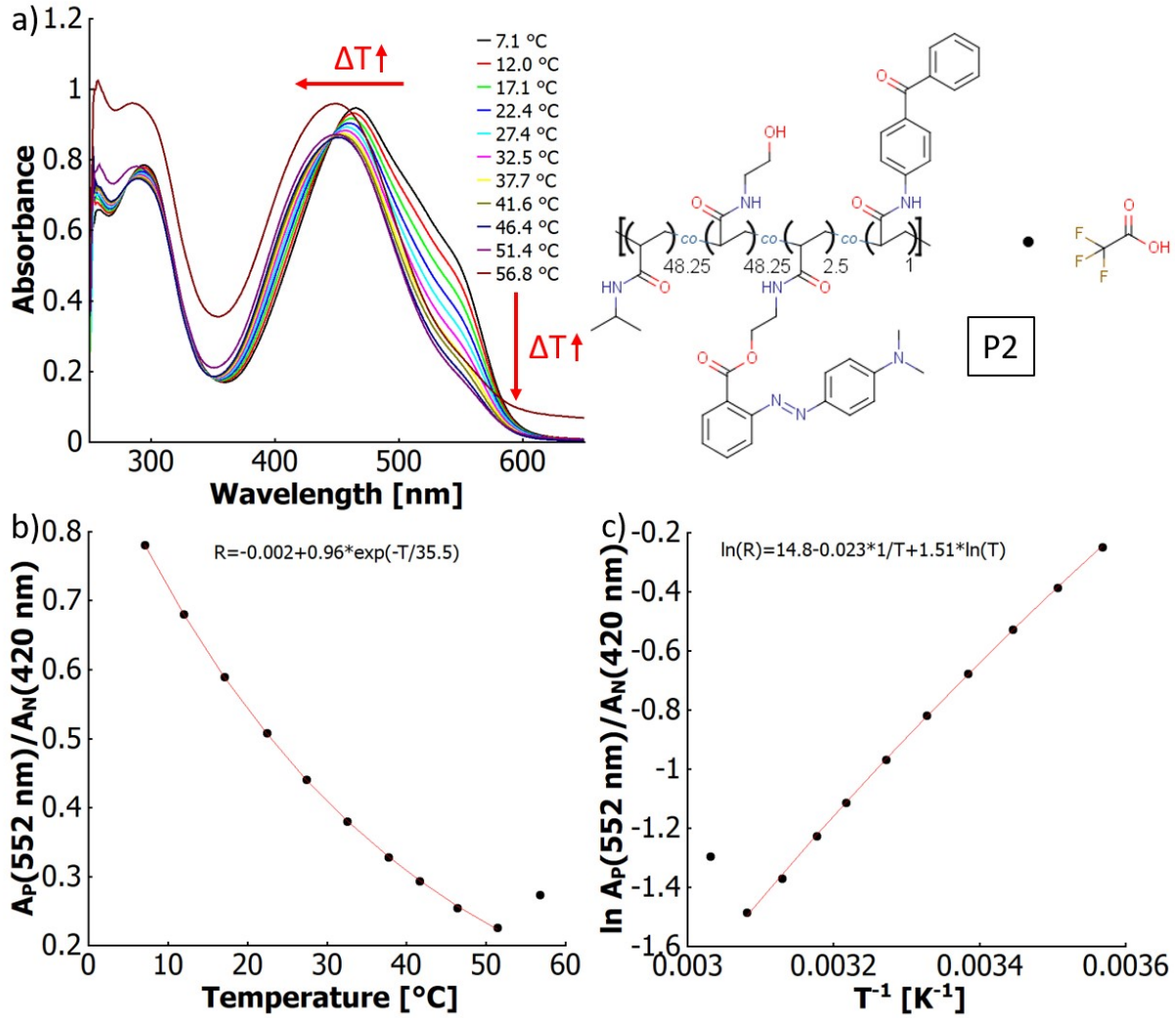


*Figure S 46: a) UV-vis spectra of a poly(NiPAAm-co-HEAm-co-o-MREAm-co-BPAAm) copolymer (P2) 0.03 w% in aqueous trifluoroacetic acid (0.001 v/v%) at different temperatures with structure of the copolymer, direction of shifts in absorbance upon heating marked with red arrows; b) absorbance ratio of the protonated (552 nm) and the neutral species (420 nm) vs temperature, fitted with an exponential decay function; c) van't Hoff plot of the logarithmic absorbance ratio vs the inverse temperature, fitted with a function ln(R)=a-b*1/T+c*ln(T).*

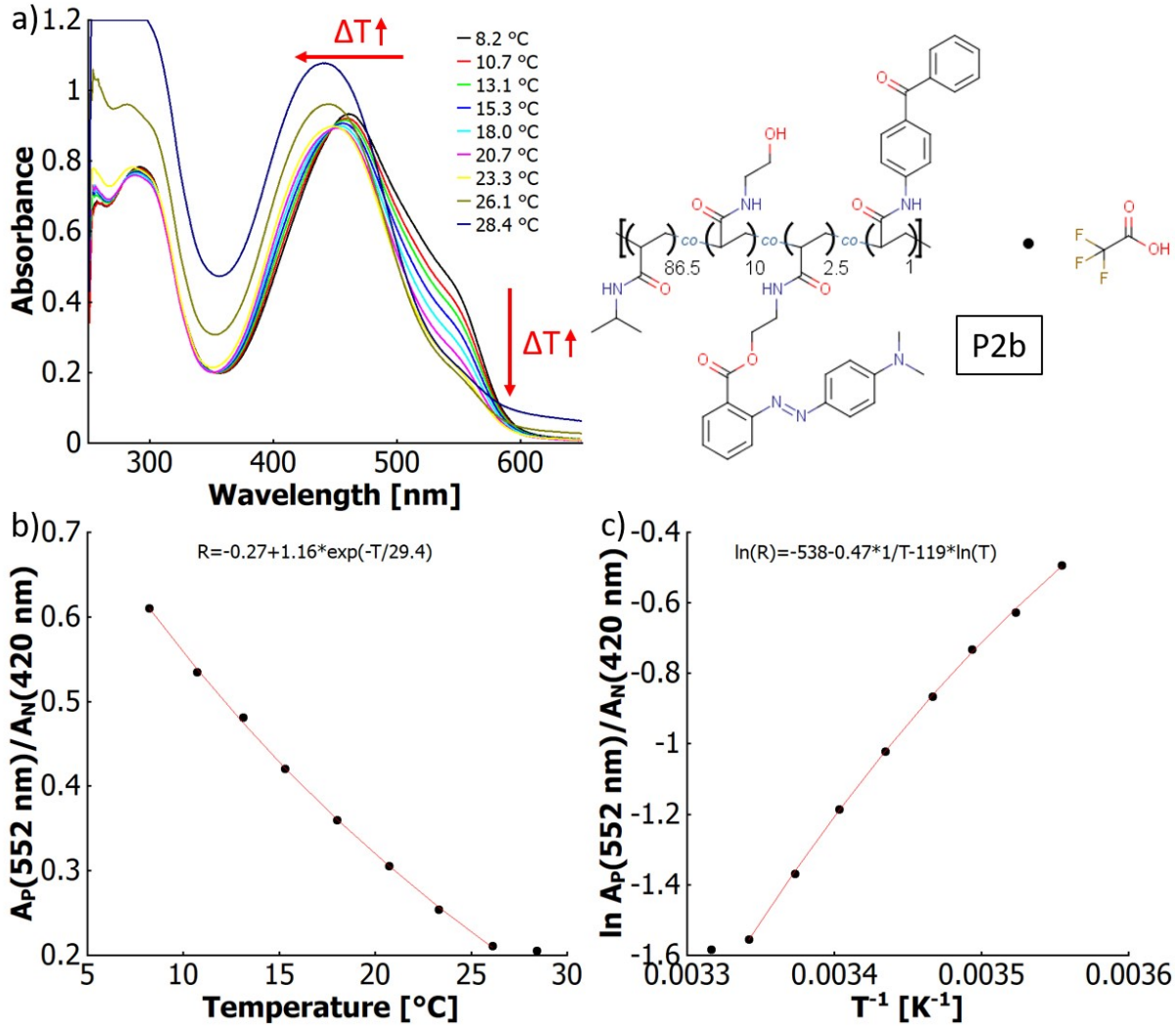


*Figure S 47: a) UV-vis spectra of a poly(NiPAAm-co-HEAm-co-o-MREAm-co-BPAAm) copolymer (P2b) 0.03 w% in aqueous trifluoroacetic acid (0.001 v/v%) at different temperatures with structure of the copolymer, direction of shifts in absorbance upon heating marked with red arrows; b) absorbance ratio of the protonated (552 nm) and the neutral species (420 nm) vs temperature, fitted with an exponential decay function; c) van't Hoff plot of the logarithmic absorbance ratio vs the inverse temperature, fitted with a function ln(R)=a-b*1/T+c*ln(T).*

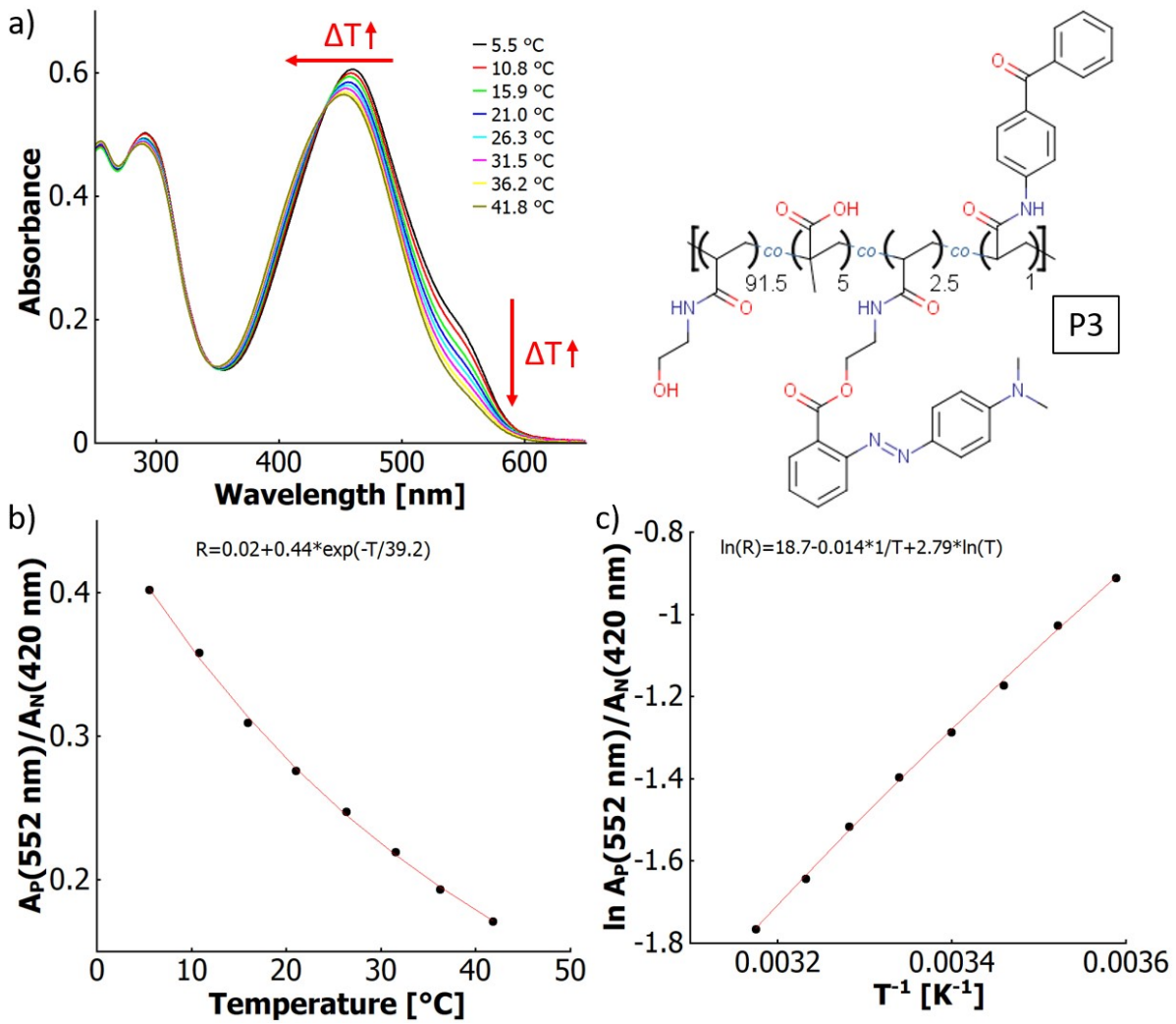


*Figure S 48: a) UV-vis spectra of a poly(HEAm-co-MAA-co-o-MREAm-co-BPAAm) copolymer (P3) 0.02 w% in water at different temperatures with structure of the copolymer, direction of shifts in absorbance upon heating marked with red arrows; b) absorbance ratio of the protonated (552 nm) and the neutral species (420 nm) vs temperature, fitted with an exponential decay function; c) van't Hoff plot of the logarithmic absorbance ratio vs the inverse temperature, fitted with a function ln(R)=a-b*1/T+c*ln(T).*

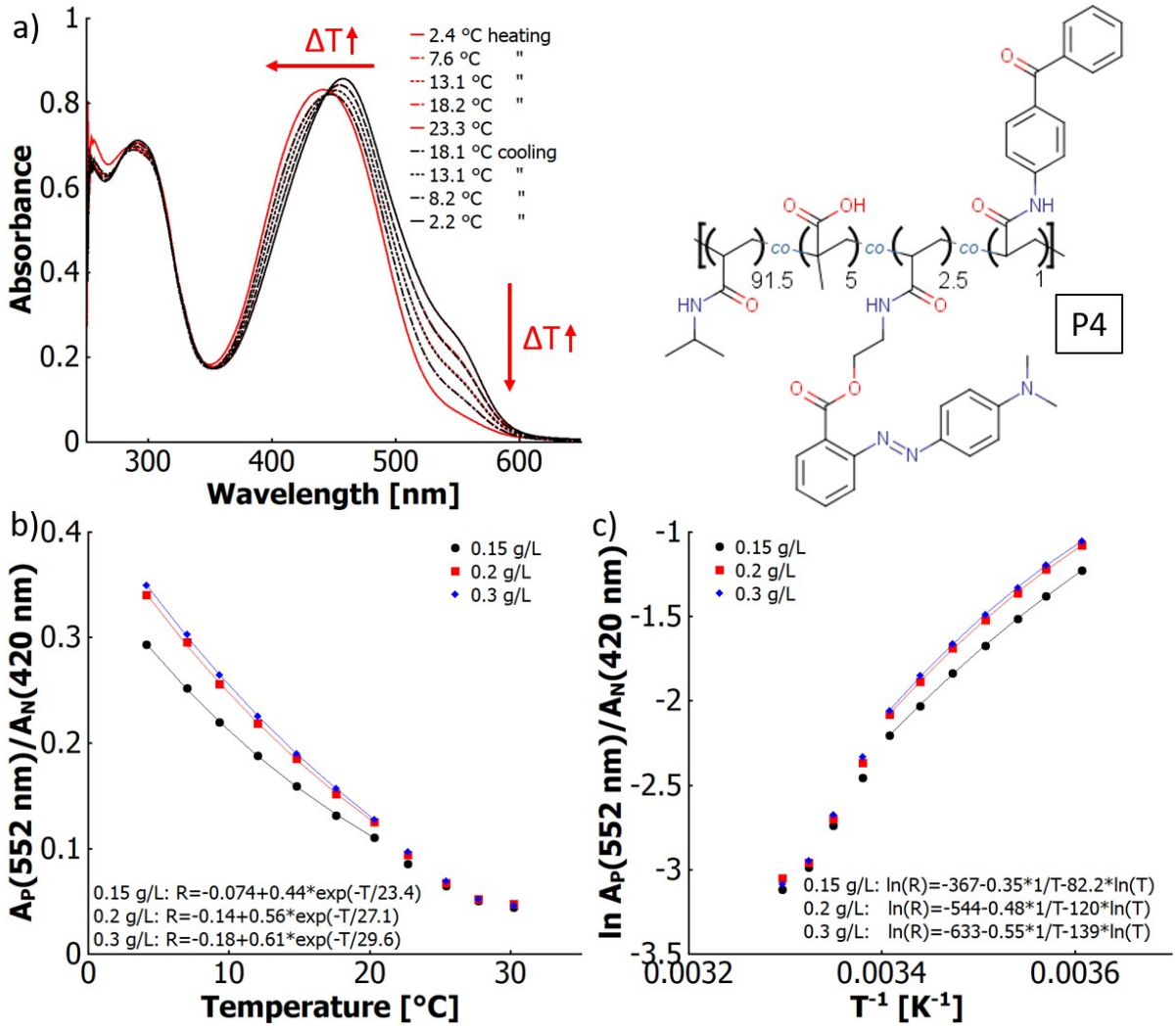


*Figure S 49: a) UV-vis spectra of a poly(NiPAAm-co-MAA-co-o-MREAm-co-BPAAm) copolymer (P4) 0.03 w% in water at different temperatures with structure of the copolymer, direction of shifts in absorbance upon heating marked with red arrows; b) absorbance ratio of the protonated (552 nm) and the neutral species (420 nm) vs temperature, fitted with an exponential decay function; c) van't Hoff plot of the logarithmic absorbance ratio vs the inverse temperature, fitted with a function ln(R)=a-b*1/T+c*ln(T).*

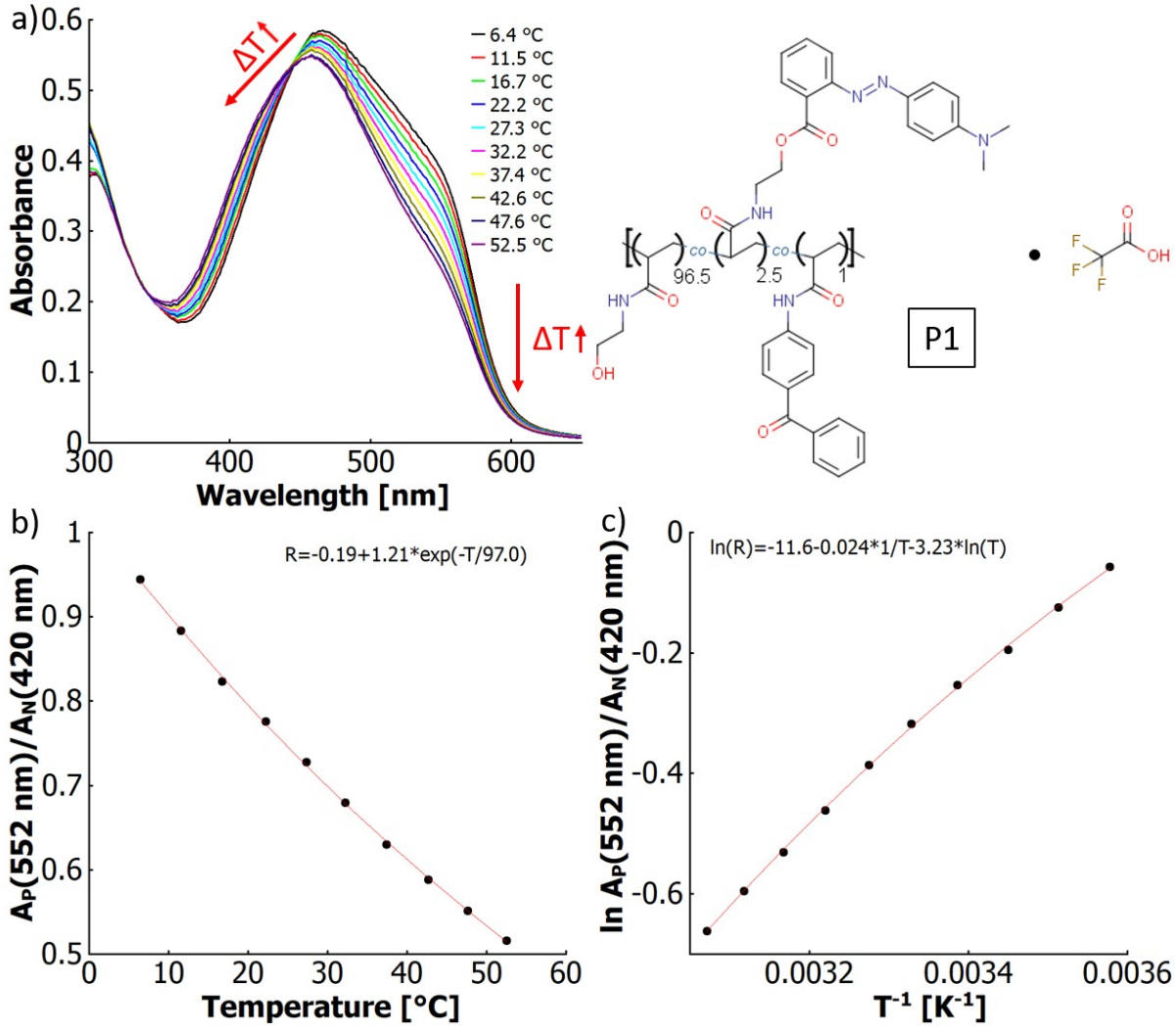


*Figure S 50: a) UV-vis spectra of a photocrosslinked poly(HEAm-co-o-MREAm-co-BPAAm) P1 film swollen in aqueous TFA (0.01 v%), at different temperatures with the structure of the copolymer before crosslinking; b) absorbance ratio R of the protonated (552 nm) and the neutral species (420 nm) vs temperature, fitted with an exponential decay function; c) van't Hoff plot of the logarithmic absorbance ratio vs the inverse temperature, fitted with a function ln(R)=a-b*1/T+c*ln(T). The absorbance was baseline corrected by subtracting the absorbance at 750 nm.*

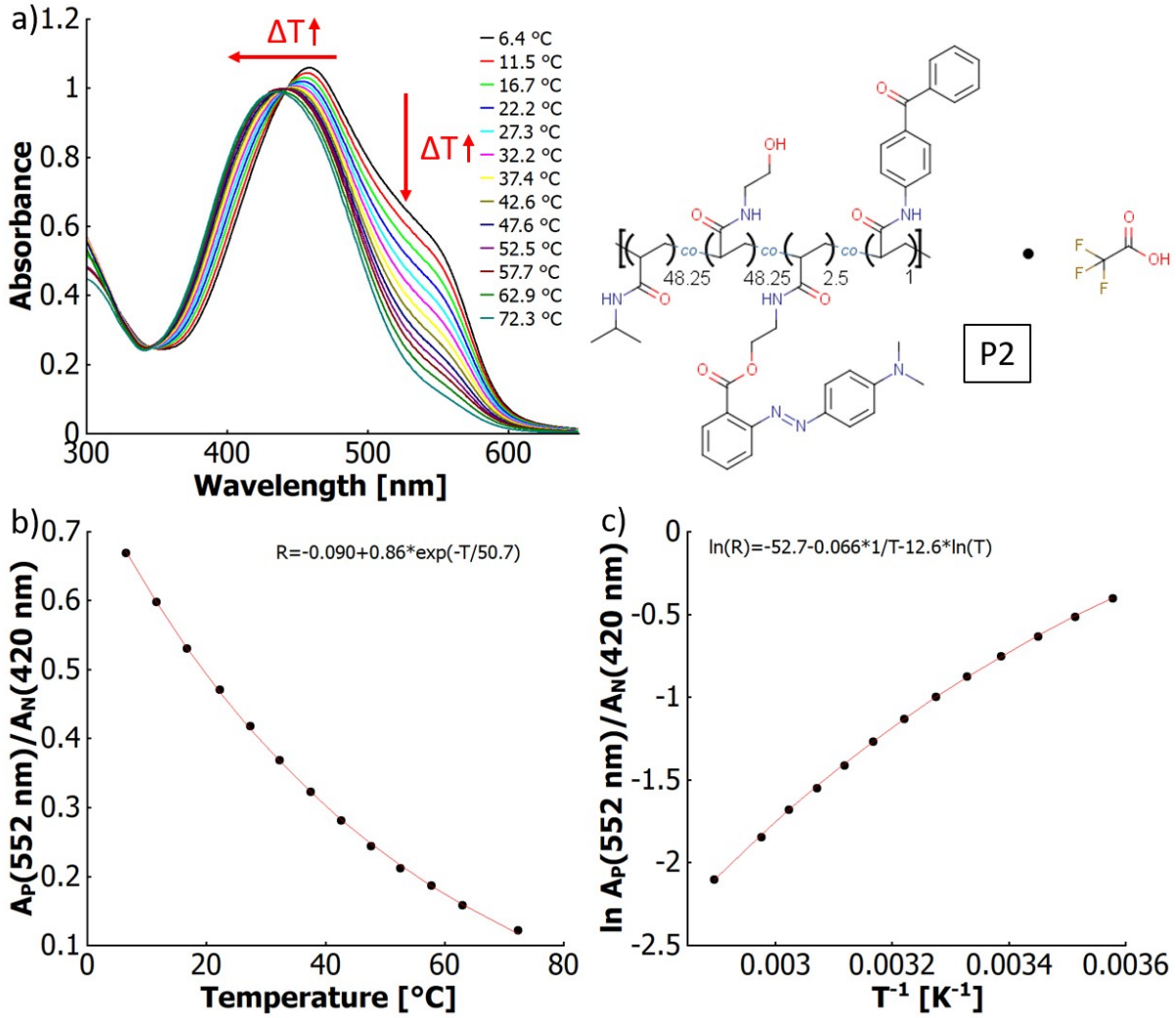


*Figure S 51: a) UV-vis spectra of a photocrosslinked poly(NiPAAm-co-HEAm-co-o-MREAm-co-BPAAm) P2 film swollen in aqueous TFA (0.01 v%), at different temperatures with the structure of the copolymer before crosslinking; b) absorbance ratio R of the protonated (552 nm) and the neutral species (420 nm) vs temperature, fitted with an exponential decay function; c) van't Hoff plot of the logarithmic absorbance ratio vs the inverse temperature, fitted with a function ln(R)=a-b*1/T+c*ln(T). The absorbance was baseline corrected by subtracting the absorbance at 750 nm.*

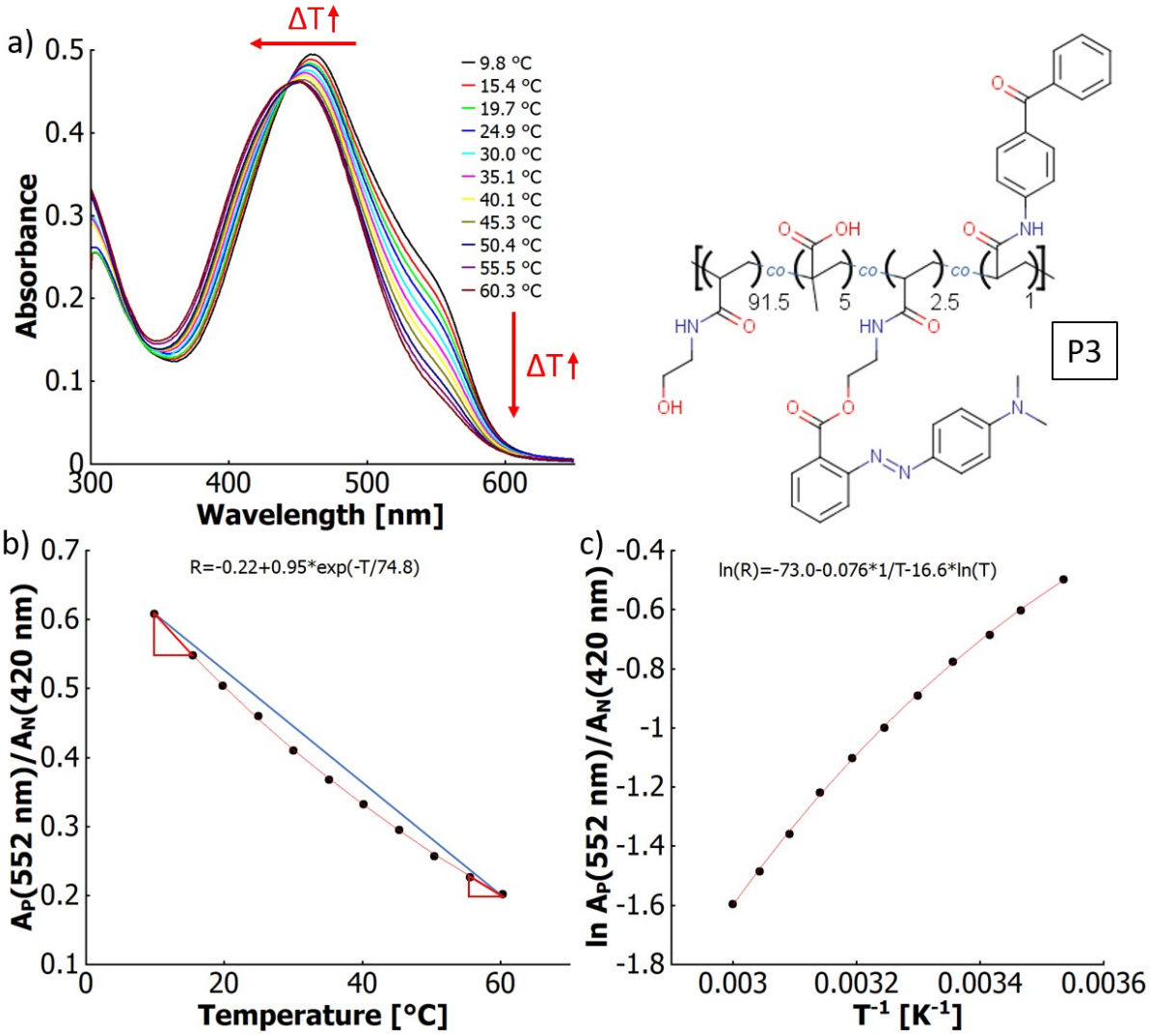


*Figure S 52: a) UV-vis spectra of a photocrosslinked poly(HEAm-co-MAA-co-o-MREAm-co-BPAAm) P3 film swollen in water, at different temperatures with the structure of the copolymer before crosslinking; b) absorbance ratio R of the protonated (552 nm) and the neutral species (420 nm) vs temperature, fitted with an exponential decay function. The blue line along with the red slope triangles serve as a reference to display the non-linearity of the graphs; c) van't Hoff plot of the logarithmic absorbance ratio vs the inverse temperature, fitted with a function ln(R)=a-b*1/T+c*ln(T).*

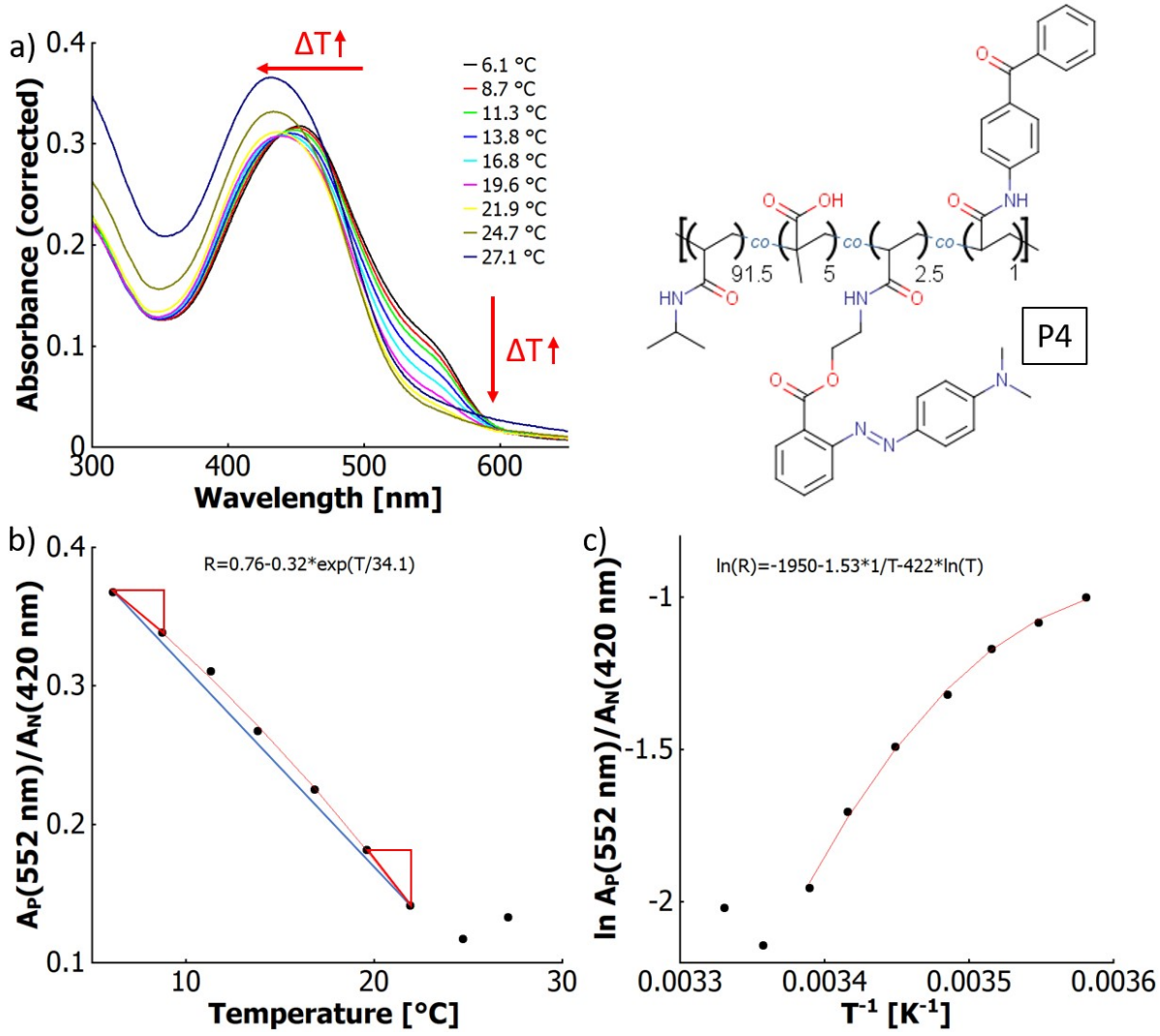


*Figure S 53: a) UV-vis spectra of a photocrosslinked poly(NiPAAm-co-MAA-co-o-MREAm-co-BPAAm) P4 film swollen in water, at different temperatures with the structure of the copolymer before crosslinking; b) absorbance ratio R of the protonated (552 nm) and the neutral species (420 nm) vs temperature, fitted with an exponential decay function. The blue line along with the red slope triangles serve as a reference to display the non-linearity of the graphs; c) van't Hoff plot of the logarithmic absorbance ratio vs the inverse temperature, fitted with a function ln(R)=a-b*1/T+c*ln(T). The absorbance was baseline corrected by subtracting the absorbance at 750 nm.*

## *Photocrosslinking:*

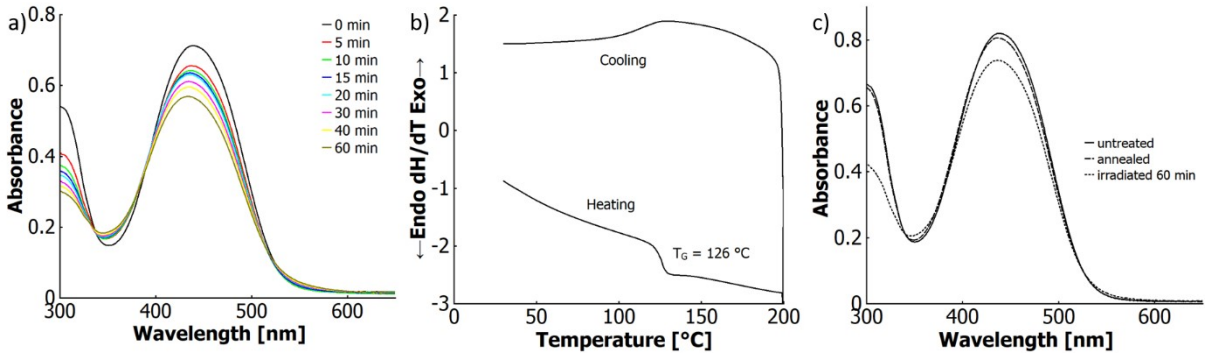


*Figure S 54: a) UV-vis spectra of poly(HEAm-co-MREAm-co-BPAAm) P1 after successive irradiation intervals at 302 nm (additive exposure time provided, overall energy dose 20.3 J/cm²); b) DSC curves of P1 with heating and cooling rates of 10 K/min; c) UV-vis spectra of P1 after dropcasting, annealing, and photocrosslinking after annealing.*

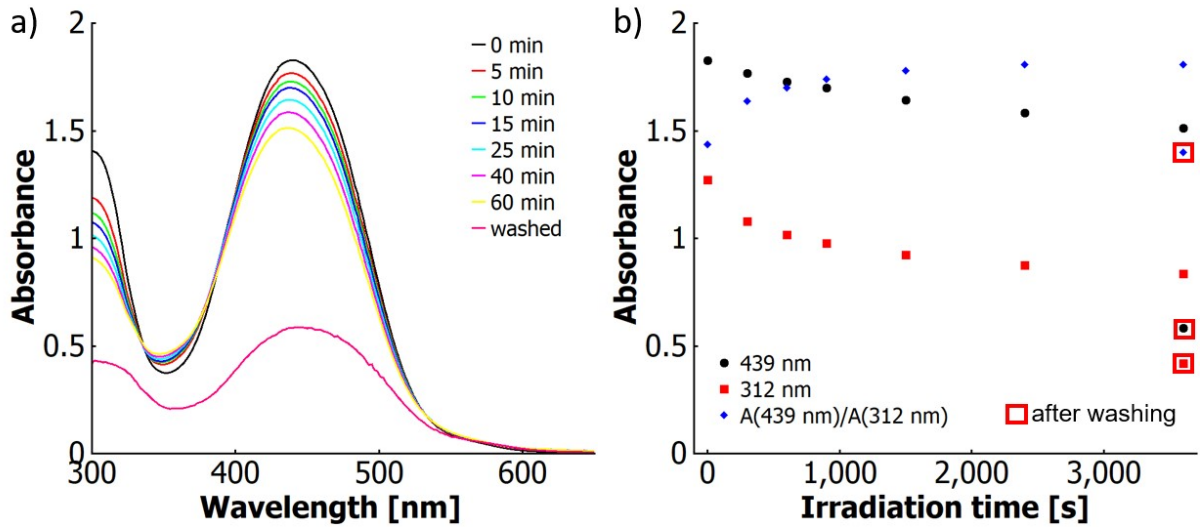


*Figure S 55: a) UV-vis spectra of poly(HEAm-co-MAA-co-MREAm-co-BPAAm) P3 after successive irradiation intervals at 302 nm (additive exposure time provided, overall energy dose 20.3 J/cm²); b) absorbances at different wavelengths (characteristic for benzophenone 312 nm, azobenzene 439 nm) and ratio of the absorbances of the azobenzene and benzophenone vs irradiation time at 302 nm.*

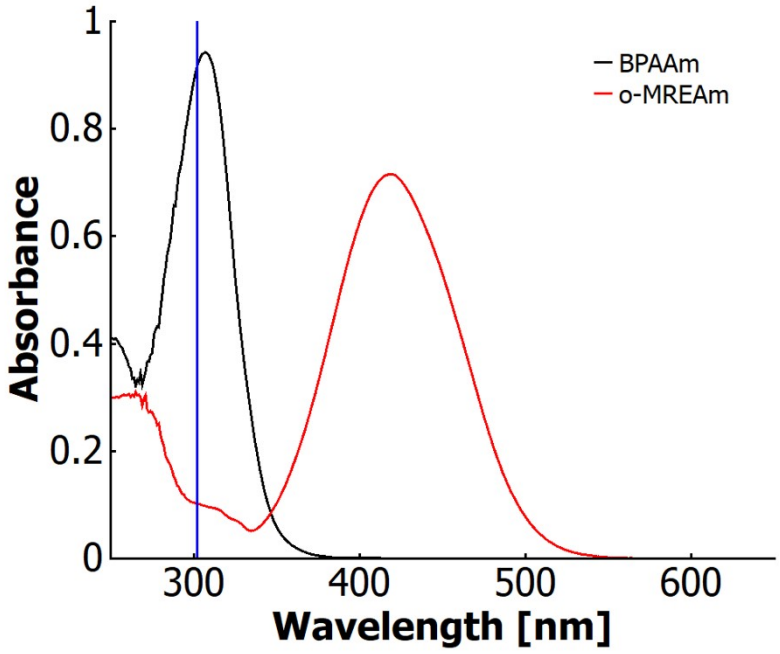


*Figure S 56: Absorbance spectra in ethanolic solution at room temperature of an ortho-methyl red ester of N-(2-hydroxyethyl)acrylamide ($2.7*10^{-5}$ mol $L^{-1}$) (red spectrum) and 4-benzophenone acrylamide ($4.0*10^{-5}$ mol $L^{-1}$) (black spectrum). The vertical blue line indicates the wavelength at which copolymers containing both units were irradiated at.*

## References

1 J. Jia, M. Sarker, M. G. Steinmetz, R. Shukla and R. Rathore, Photochemical elimination of leaving groups from zwitterionic intermediates generated via electrocyclic ring closure of alpha,beta-unsaturated anilides, The Journal of organic chemistry, 2008, 73, 8867–8879.

2 M. Gianneli, R. F. Roskamp, U. Jonas, B. Loppinet, G. Fytas and W. Knoll, Dynamics of swollen gel layers anchored to solid surfaces, Soft matter, 2008, 4, 1443–1447.
3 H. A. Staab and A. Mannschreck, Synthese von Carbonsäureestern nach der Imidazolidmethode, Chem. Ber., 1962, 95, 1284–1297.
4 D. E. Bergbreiter, P. L. Osburn and C. Li, Soluble Polymer-Supported Catalysts Containing Azo Dyes, Org. Lett., 2002, 4, 737–740.
5 H. A. Staab, M. Lüking and F. H. Dürr, Darstellung von Imidazoliden. Synthese von Amiden, Hydraziden und Hydroxamsäuren nach der Imidazolidmethode, Chem. Ber., 1962, 95, 1275–1283.
6 J. Gao, Y. He, F. Liu, X. Zhang, Z. Wang and X. Wang, Azobenzene-Containing Supramolecular Side-Chain Polymer Films for Laser-Induced Surface Relief Gratings, Chem. Mater., 2007, 19, 3877–3881.
7 K. M. Tawarah and H. M. Abu-Shamleh, A spectrophotometric study of the acid-base equilibria of o-methyl red in aqueous solutions, Dyes and Pigments, 1991, 17, 203–215.
8 E. Sawicki, Physical Properties of Aminoazobenzene Dyes. V. The C ϵ /A ϵ Ratio, J. Org. Chem., 1957, 22, 621–625.
9 G. Seu, Spectrophotometric study of the prototropic equilibrium of methyl red in organic solvents, Dyes and Pigments, 1995, 29, 227–240.
10 S. J. Khouri, I. A. Abdel-Rahim, E. M. Alshamaileh and A. M. Altwaiq, Equilibrium and Structural Study of m-Methyl Red in Aqueous Solutions: Distribution Diagram Construction, J Solution Chem, 2013, 42, 1844–1853.
11 K. Tawarah, The tautomeric and acid-base equilibria of p-methyl red in aqueous solutions, Dyes and Pigments, 1992, 20, 261–270.
12 A. Savitzky and M. J. E. Golay, Smoothing and Differentiation of Data by Simplified Least Squares Procedures, Anal. Chem., 1964, 36, 1627–1639.
13 S. Bell, A. Bisset and T. J. Dines, Ab initio and density functional study of the resonance Raman spectra of Methyl Red, Ethyl Red and their protonated derivatives, *J. Raman Spectrosc.*, 1998, **29**, 447–462.
14 S.-K. Park, C.-K. Lee, K.-C. Min and N.-S. Lee, Fourier Transform Raman Studies of Methyl Red Adsorbed on γ-Alumina and Silica-Alumina, *Bulletin of the Korean Chemical Society*, 2004, **25**, 1817–1821.

15 A. M. Mebel, M. Hayashi, K. K. Liang and S. H. Lin, Ab Initio Calculations of Vibronic Spectra and Dynamics for Small Polyatomic Molecules: Role of Duschinsky Effect, *J. Phys. Chem. A*, 1999, **103**, 10674–10690.

16 A. Baiardi, J. Bloino and V. Barone, General Time Dependent Approach to Vibronic Spectroscopy Including Franck-Condon, Herzberg-Teller, and Duschinsky Effects, *Journal of chemical theory and computation*, 2013, **9**, 4097–4115.

17 A. Zhukov and R. Karlsson, Statistical aspects of van't Hoff analysis: a simulation study, Journal of molecular recognition:JMR, 2007, 20, 379–385.

18 H. Naghibi, A. Tamura and J. M. Sturtevant, Significant discrepancies between van't Hoff and calorimetric enthalpies, Proceedings of the National Academy of Sciences of the United States of America, 1995, 92, 5597–5599.